

5-13-2016

Fuzzy Control of Flexible Multibody Spacecraft: A Linear Matrix Inequality Approach

Chokri Sendi
Santa Clara University

Follow this and additional works at: http://scholarcommons.scu.edu/eng_phd_theses



Part of the [Mechanical Engineering Commons](#)

Recommended Citation

Sendi, Chokri, "Fuzzy Control of Flexible Multibody Spacecraft: A Linear Matrix Inequality Approach" (2016). *Engineering Ph.D. Theses*. Paper 1.

This Dissertation is brought to you for free and open access by the Student Scholarship at Scholar Commons. It has been accepted for inclusion in Engineering Ph.D. Theses by an authorized administrator of Scholar Commons. For more information, please contact rsccroggin@scu.edu.

Santa Clara University

Department of Mechanical Engineering

Date: May 13, 2016

I HEREBY RECOMMEND THAT THE THESIS PREPARED UNDER MY
SUPERVISION BY

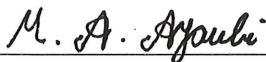
Chokri Sendi

ENTITLED

**Fuzzy Control of Flexible Multibody Spacecraft:
A Linear Matrix Inequality Approach**

BE ACCEPTED IN PARTIAL FULFILLMENT OF THE REQUIREMENTS FOR
THE DEGREE OF

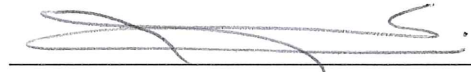
DOCTOR OF PHILOSOPHY IN MECHANICAL ENGINEERING



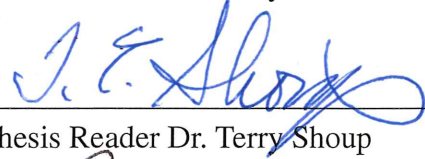
Thesis Advisor
Dr. Mohammad A. Ayoubi



Chairman of Department
Dr. Drazen Fabris



Thesis Reader Dr. Maryam Khanbaghi



Thesis Reader Dr. Terry Shoup



Thesis Reader Dr. Sean Swei



Thesis Reader Dr. Drazen Fabris

**Fuzzy Control of Flexible Multibody Spacecraft:
A Linear Matrix Inequality Approach**

By

Chokri Sendi

Dissertation

Submitted in Partial Fulfillment of the Requirements
for the Degree of Doctor of Philosophy
in Mechanical Engineering
in the School of Engineering at
Santa Clara University, 2016

Santa Clara, California

This thesis is dedicated to my mother and to the loving memory of my father. You will always be remembered.

Acknowledgments

I would like to express my sincere gratitude to my advisor Professor Mohammad Ayoubi for his support of my Ph.D. study and related research, for his patience, motivation, and knowledge. His guidance helped me in all the time of research and writing of this thesis.

The members of my dissertation committee, Dr. Drazen Fabris, Dr. Maryam Khanbaghi, Dr. Terry Shoup and Dr. Sean Swei, have generously given their time and expertise to better my work. I thank them for their contribution and their good-natured support.

I must acknowledge as well the help and contribution of Dr. Stephen Chiappari and Heidi Williams for taking the time to review some of the published articles, their feedback was extremely valuable.

I am grateful for the opportunity and support provided to me by the department of mechanical engineering through out the time it took me to complete this research and write the dissertation.

I must acknowledge as well the many friends and teachers who assisted, advised, and supported my research and writing efforts over the years.

Fuzzy Control of Flexible Multibody Spacecraft: A Linear Matrix Inequality Approach

Chokri Sendi

Department of Mechanical Engineering
Santa Clara University
Santa Clara, California
2016

ABSTRACT

To reduce the cost of lifting to orbit, modern spacecraft and structures used in space applications are designed from light material as flexible multibody system. Moreover The unprecedented requirements for rapid retargeting, precision pointing and tracking capability have made these multibody highly flexible spacecraft vulnerable to dynamic excitation caused by the slewing/pointing maneuver, vibration and external disturbances. As a result, this will degrade the performance of the spacecraft including the pointing accuracy. Thus the aspect of modeling and control become extremely important for the safe and effective operation. Despite the numerous research, the development of high performance, nonlinear control laws for attitude stability, rapid slewing and precision pointing remain the primary objective of scientists and engineers. The aim of the work presented in this thesis is to investigate the stability, performance, and robustness of a class of fuzzy control system called Takagi-Sugeno (T-S) applied to a flexible multi-body spacecraft, and to show the advantage and the simplicity in implementing the T-S fuzzy controller over other baseline nonlinear controllers.

Table of Contents

1	Introduction	1
2	Mathematical Model	4
2.1	Introduction	4
2.2	Equations of Motion	5
2.3	Open Loop Response	12
2.4	Reduced Model and Control Problems	16
3	Takagi-Sugeno Fuzzy Control	19
3.1	Introduction	19
3.2	The Takagi Sugeno (T-S) Model	19
3.3	Parallel Distributed Compensator (PDC)	21
3.4	Fuzzy Observer	22
3.5	T-S Fuzzy Model Validation	22
4	Full-State Feedback Fuzzy Control with Actuator Norm Constraint	26
4.1	Introduction	26
4.2	Linear Matrix Inequality approach	26
4.2.1	Stability Conditions	26
4.2.2	Stable Closed-Loop System	27
4.2.3	Stable Closed-Loop with Fuzzy Observer	28
4.2.4	Disturbance Rejection	30
4.2.5	Constraints On the Control Input	34
4.2.6	Constraints on Initial Condition	35
4.3	Numerical Simulation	36

5	Robust-Optimal Fuzzy Control With Individual Actuator Constraint	41
5.1	Introduction	41
5.2	Takagi-Sugeno (T-S) Fuzzy Model for Uncertain Systems with Disturbance	42
5.3	Robust Stability Condition	44
5.4	Optimal Fuzzy Control	49
5.5	Fuzzy Controller Design	54
5.6	Numerical Simulation	59
5.6.1	Sliding Mode Control Law	60
5.6.2	Simulation for Nominal System	61
5.6.3	Simulation for System With Uncertainty	64
5.6.4	Higher Frequency Modes and Controller Performance	66
6	Robust Model-Reference Fuzzy Control	70
6.1	Introduction	70
6.2	Takagi-Sugeno (T-S) Fuzzy Modeling	70
6.3	Parallel Distributed Compensation (PDC) Control and H_∞ Performance	71
6.4	Output Feedback LMI Tracking Control	72
6.5	Numerical Simulation	83
6.5.1	Adaptive Control Law	84
6.5.2	Simulation for Nominal System	85
6.5.3	Simulation for System With Uncertainty	89
7	Conclusions and Future Work	93
7.1	Conclusions	93
7.2	Future Work	95
A		96
A.1	Nomenclature	96
A.2	Fuzzy Model Parameters, Controller and Observer gains	98
A.2.1	Fuzzy Model Parameters:	98
A.2.2	Full State Feedback Fuzzy Controller Gains:	100

A.2.3	Robust-Optimal Fuzzy Controller and Observer Gains:	101
A.2.4	Robust Model-Reference Fuzzy Controller and Observer Gains: . . .	104

List of Figures

2.1	Model of the flexible spacecraft.	5
2.2	Angular position, velocity, and acceleration of the antenna.	13
2.3	Elastic displacement δ_y of the antenna	14
2.4	Angular position of the rigid platform θ_x	15
2.5	Position of the platform center-of-gravity R_y	15
2.6	Position of the platform center-of-gravity R_z	16
2.7	Elastic displacement δ_y of the antenna for different admissible functions	17
2.8	Angular position of the rigid platform θ_x for different admissible functions	17
2.9	Frequency of the flexible antenna for different admissible functions	18
2.10	Frequency of the flexible antenna with uncertainty for different admissible functions	18
3.1	Fuzzy Membership Function	23
3.2	Position of the platform center-of-gravity R_z for nonlinear and fuzzy model.	24
3.3	Position of the platform center-of-gravity R_y for the nonlinear and fuzzy model.	24
3.4	Angular position of the rigid platform θ_x for the nonlinear and fuzzy model.	25
3.5	Elastic displacement of the antenna in the y -direction for the nonlinear and fuzzy model.	25
4.1	Elastic displacement of the antenna in the y direction for different input control upper bounds, μ	37
4.2	Angular position of the rigid platform for different input control upper bound, μ	37
4.3	Position of the platform center of gravity in the inertial frame with input constraint upper bound of $\mu = 5$ lbf.	38
4.4	Angular position of the rigid platform with input constraint upper bound of $\mu = 5$ lbf.	38
4.5	Actuator forces on the platform with input constraint upper bound of $\mu = 5$ lbf.	39

4.6	Actuator moments on the platform with input constraint upper bound of $\mu = 5$ lbf.	39
4.7	Actuator forces on the tip of antenna in the x and y directions with input constraint upper bound of $\mu = 5$ lbf.	40
5.1	Schematic diagram of the system.	60
5.2	Elastic displacement δ_y of the antenna in the y direction.	62
5.3	Angular position of the rigid platform θ_x	62
5.4	Position of the platform center-of-gravity R_z	63
5.5	Actuator moment M_y on the rigid platform.	63
5.6	Actuator force f_{2x} on the antenna tip in the x -direction.	64
5.7	Elastic displacement of the antenna δ_y in the y -direction for a system with uncertainties.	65
5.8	Angular position of the rigid platform θ_x for a system with uncertainties.	65
5.9	Position of the platform center-of-gravity R_z for a system with uncertainties.	66
5.10	Elastic displacement of the antenna δ_y in the y -direction for higher frequency mode.	67
5.11	Angular position of the rigid platform θ_x for a system with higher frequency mode.	67
5.12	Position of the platform center-of-gravity R_z for a system with higher frequency mode.	68
5.13	Position of the platform center-of-gravity R_z for a system with higher frequency mode.	68
6.1	Schematic diagram of the system.	83
6.2	Elastic displacement δ_y of the antenna tip in the y direction.	85
6.3	Angular position of the rigid platform θ_x	86
6.4	Angular position of the rigid platform θ_y	86
6.5	Angular position of the rigid platform θ_z	87
6.6	Position of the rigid platform center-of-gravity R_x	87
6.7	Position of the rigid platform center-of-gravity R_y	88
6.8	Position of the rigid platform center-of-gravity R_z	88
6.9	Actuator force F_y on the rigid platform center-of-gravity.	89

6.10	Actuator force F_z on the rigid platform center-of-gravity.	89
6.11	Actuator moment M_x on the rigid platform center-of-gravity.	90
6.12	Actuator force on the tip of the elastic antenna in the x direction.	90
6.13	Elastic displacement δ_y of the antenna tip in the y -direction for a system with uncertainties	91
6.14	Angular position θ_x of the rigid platform for a system with uncertainties. . . .	92
6.15	Position of the platform center-of-gravity R_z for a system with uncertainties. .	92

List of Tables

2.1 Parameters of the Flexible Spacecraft 14

6.1 Parameter of the Flexible Spacecraft with uncertainties 91

CHAPTER 1

Introduction

The problem of dynamics and control of flexible structure remains a big challenge despite the huge amount of literature accumulated over the years. Indeed, flexible spacecraft dynamics tend to differ from rigid body dynamics in several important ways. First, flexible dynamics are higher order than rigid body dynamics. The full set of dynamics for a rigid body system involves only twelve states. Additional actuator dynamics need to be added. A flexible spacecraft model have an infinite number of states unless the model is truncated and even though, the number of states still large. This will increase the complexity of the control problem. Hence, design techniques that work well for tenth order systems may have difficulty handling systems with ten times that many states. The second important difference between rigid body and flexible body dynamics is that often the mathematical models developed to predict the flexible dynamics differ from the physical system. The physical model is highly influenced by the mechanical property such as mass distribution, material stiffness and damping. As a result, the controller design based on mathematical models must be made robust to withstand the discrepancies between the mathematical model and physical system. The third difference between these dynamics is that rigid body dynamics can often be treated as decoupled, whereas flexible body dynamics are most often highly coupled. As a result, control problems that can often be treated as a series of SISO problems when dealing with rigid body systems become MIMO problems when dealing with flexible systems. The fourth difference between these dynamics is the goal of the systems designed to control them. Rigid body control usually involves commanding the rigid degrees of freedom to follow desired trajectories. By contrast,

the goal of flexible spacecraft controllers is either to perform the desired rigid body control without exciting flexible modes, or to provide active damping for structural modes that are excited.

Over the last forty years, the amount of literature accumulated on the subject of spacecraft dynamics and control is very rich. For instance, Hughes [1] derived the equations of motion for a chain of flexible multi-body systems using the Newton-Euler approach. Using the Lagrangian approach, Modi and Ibrahim [2] presented the general equations of motion for a large spacecraft with deployable flexible members, taking into consideration the gravitational effect, the shifting center of mass, the variable moments of inertia and transverse oscillation. Meirovich et al. [3] developed the equations of motions for a flexible spacecraft with retargeting flexible antennas using the Lagrangian approach by mean of quasi-coordinates. Modern techniques like finite element analysis (FEA) are also being used.

Most of the literature on flexible spacecraft control is concerned mainly with two problems: attitude stability and vibration suppression. To mention a few, Meirovitch et al. [3, 5] provided a procedure for vibration control using a method of assumed mode. Juang and Junkins [6] used the eigenvalues assignment technique to improve the control robustness. Agrawal and Bang [7] developed a closed-loop switching function to provide a good attitude performance in the presence of a modeling error and disturbances. Other techniques such as proportional–integral (PI) control [4], optimal control [8], output-feedback [9], and model reference adaptive control [10], [11] have been proposed.

In the past few years, there has been a growing interest to investigate and implement fuzzy controllers for nonlinear systems. These types of nonlinear controllers are especially useful in the presence of incomplete knowledge of the plant or actuator dynamics. A number of researchers have considered the Takagi-Sugeno (T-S) fuzzy model-based control for attitude stabilization of rigid spacecraft and aircraft. For instance, Park et al. [12], [13] proposed an optimal T-S fuzzy controller based on the inverse optimal approach with input constraints.

Zhang et al. introduced a T-S fuzzy model with output-feedback [14], decay rate [15], and H_∞ control for a rigid spacecraft [16]. Butler et al. [17] introduced a T-S fuzzy model-based PDC flight control for controlling a damaged rigid aircraft. Hong and Nam [18] proposed a stable fuzzy control design with a pole placement constraint. The application of a fuzzy controller to a flexible spacecraft is relatively new [19, 23].

The aim of this research is to investigate the stability, performance, and robustness of a class of fuzzy control system called Takagi-Sugeno (T-S) applied to a flexible multi-body spacecraft. First, the effect of disturbances will be investigated and a control law based on T-S model with disturbance rejection and full state feedback law will be implemented. Next, to accommodate uncertainties in the state estimation and actuators, a new fuzzy model is adopted. Moreover, for practical implementation, the output feedback control law with upper bound constraints on the actuators amplitude is considered. Then, we compare the results with a nonlinear sliding mode controller. To improve the performance and the stability of the controller, we investigate the use of a reference model based controller, and compare the results with an adaptive control law designed specifically for this system.

CHAPTER 2

Mathematical Model

2.1 Introduction

The problem of modeling and control of flexible spacecraft has been a subject of considerable research in recent years. These spacecraft would consist of a rigid platform and several flexible appendages, such as long beams, solar panels, antennas etc. Flexibility of various components of the spacecraft introduces many unforeseen complexities in the process of system modeling and controller design. To ensure satisfactory performance, it is essential to take into account the distributed nature of the flexible members.

The most natural model for a flexible spacecraft could be given by a hybrid system, i.e. a combination of a finite dimensional model for the rigid parts, and an infinite dimensional model for the elastic parts. Since infinite dimensional model is not practical, the commonly used approach for modeling the dynamics of the elastic parts is to approximate by considering some finite number of modes. A wide list of contributions in this area can be found in the literature [24, 26]. Techniques of finite dimensional control theory have also been utilized in designing stabilizing regulators [27, 30]. However, the number of modes of a flexible structure is actually infinite, and for a given accuracy the number of modes that should be included in the model is also not known a priori. Another problem associated with the controller designed on the basis of this reduced order model is the lack of control on the unmodeled modes, which is usually known as control spillover. Hybrid models for some simple flexible structures have been discussed previously [31, 35]. In this chapter, the dynamics of a flexible spacecraft,

consisting of a rigid platform and a beam, developed by Meirovitch [3] will be introduced and used for control and analysis through out the remaining chapters.

2.2 Equations of Motion

Consider a flexible spacecraft in the inertial frame G . The spacecraft consists of a rigid platform, in frame B , and one flexible antenna in frame A , as shown in Fig. (2.1). The

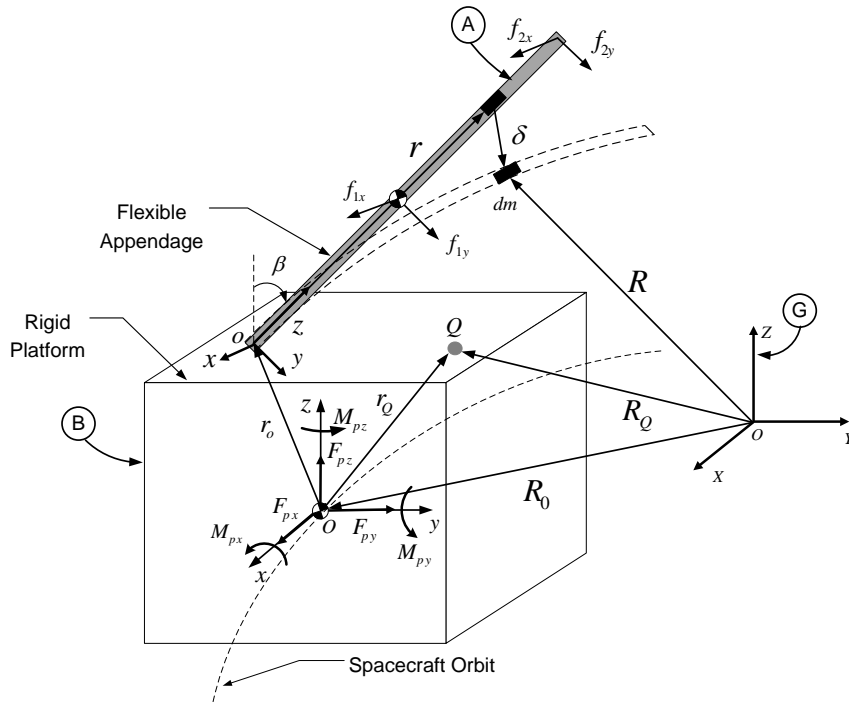


Fig. 2.1: Model of the flexible spacecraft.

position vector of a point on the platform and on the flexible antenna can be written in matrix form as

$$R_Q = R_0 + r_Q \quad (2.1)$$

and

$$R = R_0 + r_o + r + \delta \quad (2.2)$$

where $R_0 \in \mathbb{R}^{3 \times 1}$ is the position vector from the origin of the frame G to the center of the body frame B , $r_Q \in \mathbb{R}^{3 \times 1}$ is the position vector of a point on the platform with respect to the body frame B , $r_o \in \mathbb{R}^{3 \times 1}$ is the position vector from the frame B to the point where the antenna is attached to the platform, $r \in \mathbb{R}^{3 \times 1}$ is the position of an undeformed point on the antenna with respect to the frame A , and $\delta \in \mathbb{R}^{3 \times 1}$ is the position vector with respect to the undeformed antenna expressed in the frame A . The absolute velocity vector of point Q on the platform and the differential element with mass dm on the elastic antenna can be expressed, respectively as:

$$V_Q = V_0 + {}^G\omega^B \times r_Q \quad (2.3)$$

and

$$V = v + {}^A C^B (V_0 + {}^G\omega^B \times r_o) + ({}^A C^B {}^G\omega^B + {}^B\omega^A) \times (r + \delta) \quad (2.4)$$

where ${}^A C^B$ is the rotation matrix from the B frame to the A frame, $v = \dot{\delta}$ is the velocity vector of a point on the antenna with respect to the frame A , ${}^G\omega^B$ is the angular velocity of the platform with respect to frame G , and ${}^B\omega^A$ is the angular velocity of the flexible antenna with respect to frame B . It should be noted that

$${}^G\omega^B = H\dot{\theta} \quad (2.5)$$

where for the (3-1-3) Euler angle sequence, is given by

$$H = \begin{bmatrix} c\theta_y c\theta_z & s\theta_z & 0 \\ -c\theta_y s\theta_z & c\theta_z & 0 \\ s\theta_y & 0 & 1 \end{bmatrix} \quad (2.6)$$

and the symbols s and c in Eq. (2.6) denote sine and cosine functions, respectively.

Using the Lagrange equations in terms of quasi-coordinates, $\theta = [\theta_x, \theta_y, \theta_z]^T$, we obtain a set

of hybrid ordinary and partial differential equations as follows

$$\frac{d}{dt} \left(\frac{\partial \mathcal{L}}{\partial V_0} \right) + {}^G \tilde{\omega}^B \left(\frac{\partial \mathcal{L}}{\partial V_0} \right) - {}^B C^G \left(\frac{\partial \mathcal{L}}{\partial R_0} \right) = F_p \quad (2.7)$$

$$\frac{d}{dt} \left(\frac{\partial \hat{\mathcal{L}}}{\partial \omega} \right) + \tilde{V}_0 \left(\frac{\partial \mathcal{L}}{\partial V_0} \right) + {}^G \tilde{\omega}^B \left(\frac{\partial \mathcal{L}}{\partial \omega} \right) - (H^T)^{-1} \frac{\partial \mathcal{L}}{\partial \theta} = M_p \quad (2.8)$$

$$\frac{\partial}{\partial t} \left(\frac{\partial \hat{\mathcal{L}}_a}{\partial v} \right) - \frac{\partial \hat{\mathcal{T}}_a}{\partial \delta} - \mathcal{L} \delta = \hat{U} \quad (2.9)$$

where $\mathcal{L} = \mathcal{T} - \mathcal{V}$ is the Lagrangian, \mathcal{T} is the kinetic energy, \mathcal{V} is the potential energy. $\hat{\mathcal{L}}_a$ is the Lagrangian density, $\hat{\mathcal{T}}_a$ is the kinetic energy density for the antenna, and \mathcal{L} is a matrix of differential operators. The vectors $F_p \in \mathbb{R}^{3 \times 1}$ and $M_p \in \mathbb{R}^{3 \times 1}$ are external forces and moments acting on the rigid platform, \hat{U} is the nonconservative force density associated with the antenna and, ${}^G \tilde{\omega}^B$ is a skew symmetric matrix giving by

$${}^G \tilde{\omega}^B = \begin{bmatrix} 0 & -\omega_z & \omega_y \\ \omega_z & 0 & -\omega_x \\ -\omega_y & \omega_x & 0 \end{bmatrix} \quad (2.10)$$

The kinetic energy and the potential energy of the system can be determined from the following equations

$$\mathcal{T} = \frac{1}{2} \int_{m_p} V_Q^T V_Q dm_p + \frac{1}{2} \int_m V^T V dm \quad (2.11)$$

and

$$\mathcal{V} = \frac{1}{2} [\delta, \delta] \quad (2.12)$$

where $[\cdot, \cdot]$ represents an energy inner product [3]. Note that all the quantities in Eq. (2.7) and Eq. (2.8) are expressed in the B frame while the quantities in Eq. (2.9) are expressed in the

A frame. By using the following equation

$$\delta(r, t) = \Phi(r)q(t) \quad (2.13)$$

where $\Phi(r) \in \mathbb{R}^{3 \times n}$ is a matrix of admissible functions and $q(t) \in \mathbb{R}^{n \times 1}$ is a vector of generalized coordinates, we can replace the partial differential equation Eq. (2.9) by the ordinary differential equation.

$$\frac{d}{dt} \left(\frac{\partial \mathcal{L}}{\partial \dot{q}} \right) - \frac{\partial \mathcal{L}}{\partial q} = Q \quad (2.14)$$

where

$$Q = \int_D \Phi^T \hat{U} dD \quad (2.15)$$

The Kinetic and potential energy are as follows:

$$\begin{aligned} \mathcal{T} = & \frac{1}{2} \int_{m_p} V_Q^T V_Q dm_p + \frac{1}{2} \int_m V^T V dm = \frac{1}{2} m_t V_0^T V_0 + V_0^T \tilde{S}_t^T G \omega^B + \\ & \frac{1}{2} G \omega^{B^T} \mathbb{I}_t G \omega^B + \frac{1}{2} B \omega^{A^T} \mathbb{I} B \omega^A + V_0^T A C^{B^T} \tilde{S}^T B \omega^A + \\ & G \omega^{B^T} (\tilde{r}_o A C^{B^T} \tilde{S}^T + A C^{B^T} \mathbb{I}) B \omega^A + \frac{1}{2} \dot{q}^T M_e \dot{q} - \frac{1}{2} q^T \bar{H} (B \omega^A) q + \\ & V_0^T A C^{B^T} \bar{\Phi} \dot{q} + V_0^T A C^{B^T} B \tilde{\omega}^A \bar{\Phi} q + G \omega^{B^T} \tilde{r}_o A C^{B^T} \bar{\Phi} \dot{q} + \\ & G \omega^{B^T} \tilde{r}_o A C^{B^T} B \tilde{\omega}^A \bar{\Phi} q + \dot{q}^T \bar{\Phi}^T A C^{B^T} G \omega^A + \dot{q}^T \bar{\Phi}^T B \omega^A + \dot{q}^T \tilde{H} (B \omega^A) q + \\ & G \omega^{B^T} B C^A J (B \omega^A) q + B \omega^{A^T} \left[\int_m \tilde{r} B \tilde{\omega}^A \Phi dm \right] q \end{aligned} \quad (2.16)$$

and

$$\mathcal{V} = \frac{1}{2} [\delta, \delta] = \frac{1}{2} q^T [\Phi, \Phi] q = \frac{1}{2} q^T k_e q \quad (2.17)$$

where $k_e = [\Phi, \Phi]$ is the stiffness matrix of the antenna. It should be noted that Eqs. (2.16–

2.17) are derived assuming small elastic motion, hence the terms of order higher than two have been neglected.

The various quantities in Eqs. (2.16–2.17) are as follows:

$$m_t = m_p + m \quad (2.18)$$

$$\mathbb{I}_t = \mathbb{I}_p + (m\tilde{r}_o \tilde{r}_o^T + {}^B C^{AT} \mathbb{I} {}^B C^A + \tilde{r}_o^T {}^B C^{AT} \tilde{S} {}^B C^A + {}^B C^{AT} \tilde{S}^T {}^A C^B \tilde{r}_o) \quad (2.19)$$

$$\tilde{S}_t = m\tilde{r}_o + {}^B C^{AT} \tilde{S} {}^B C^A \quad (2.20)$$

$$S = \int_m r \, dm \quad (2.21)$$

$$\mathbb{I}_p = \int_{m_p} \tilde{r}_Q \tilde{r}_Q^T \, dm_p \quad (2.22)$$

$$\mathbb{I} = \int_m \tilde{r} \tilde{r}^T \, dm \quad (2.23)$$

$$M_e = \int_m \Phi^T \Phi \, dm \quad (2.24)$$

$$\bar{\Phi} = \int_m \Phi \, dm \quad (2.25)$$

$$\tilde{\Phi} = \int_m \tilde{r} \Phi dm \quad (2.26)$$

$$\tilde{H}^{(B\omega^A)} = \int_m \Phi^T \tilde{\omega}^A \Phi dm \quad (2.27)$$

$$\bar{H}^{(B\omega^A)} = \int_m \Phi^T ({}^B \tilde{\omega}^A)^2 \Phi dm \quad (2.28)$$

$$\bar{J}^{(B\omega^A)} = \int_m [\tilde{r}^B \tilde{\omega}^A + \widetilde{r^B \omega^A}] \Phi dm \quad (2.29)$$

It can be shown [3] that the mathematical model of the flexible spacecraft represented by Eqs. (2.7–2.9) can be written as:

$$\dot{x} = A(t)x(t) + B(t)u(t) + D(t)d(t) \quad (2.30)$$

where

$$A(t) = \begin{bmatrix} 0 & I \\ -M^{-1}(t)K(t) & -M^{-1}(t)G(t) \end{bmatrix} \quad (2.31)$$

and

$$B(t) = \begin{bmatrix} 0 \\ M^{-1}(t)B^*(t) \end{bmatrix} \quad (2.32)$$

and

$$D(t) = \begin{bmatrix} 0 \\ M^{-1}(t) \end{bmatrix} \quad (2.33)$$

where I is identity matrix, $M(t)$ is the mass matrix, $K(t)$ is the stiffness matrix, $B^*(t)$ is

a matrix that relates the discrete force vectors to the modal vectors, and $d(t)$ is the inertial disturbance vector.

The state vector, $x \in \mathbb{R}^{n \times 1}$ and the control vector $u \in \mathbb{R}^{m \times 1}$ are defined as

$$x = [R_0^T \ \theta^T \ q^T \ V_0^T \ G \omega^{B^T} \ \dot{q}^T]^T \quad (2.34)$$

and

$$u = [F_p^T \ M_p^T \ f_1^T \ f_2^T]^T \quad (2.35)$$

where $f_1 \in \mathbb{R}^{3 \times 1}$, $f_2 \in \mathbb{R}^{3 \times 1}$ represent the actuator force vector at the middle and tip of the antenna.

The various quantities in Eqs. (2.30–2.33) are as follow:

$$M(t) = \begin{bmatrix} m_t & \tilde{S}_t^T & {}^B C^A \bar{\Phi} \\ \tilde{S}_t & \mathbb{I}_t & {}^B C^A \tilde{\Phi} + \tilde{r}_o {}^B C^A \bar{\Phi} \\ \bar{\Phi}^T {}^A C^B & \tilde{\Phi}^T {}^A C^B + \bar{\Phi}^T {}^A C^B \tilde{r}_o^T & M_e \end{bmatrix} \quad (2.36)$$

$$K(t) = \begin{bmatrix} 0 & 0 & {}^B C^A ({}^B \tilde{\omega}^A + {}^B \tilde{\omega}^{A^2}) \bar{\Phi} \\ 0 & 0 & \tilde{r}_o {}^B C^A ({}^B \tilde{\omega}^{A^2} + {}^B \tilde{\omega}^A) \bar{\Phi} + {}^B C^A [{}^B \tilde{\omega}^A J({}^B \omega^A) + J({}^B \dot{\omega}^A)] \\ 0 & 0 & K_e + \bar{H}({}^B \omega^A) + \tilde{H}({}^B \tilde{\omega}^A) \end{bmatrix} \quad (2.37)$$

$$G(t) = \begin{bmatrix} 0 & 2 {}^A C^B (\tilde{S} \widetilde{{}^B \omega^A}) {}^A C^B & 2 {}^B C^A {}^B \tilde{\omega}^A \bar{\Phi} \\ 0 & G_{22} & G_{23} \\ 0 & [\tilde{\Phi}^T {}^B \tilde{\omega}^{A^T} - J^T({}^B \omega^A)] {}^A C^B & 2 \tilde{H}({}^B \omega^A) \end{bmatrix} \quad (2.38)$$

where

$$G_{22} = {}^B C^A (2 {}^B \tilde{\omega}^A \mathbb{I} - \text{trace}(\mathbb{I}) {}^B \tilde{\omega}^A) {}^A C^B + 2 \tilde{r}_o {}^B C^A (\widetilde{{}^S B \dot{\omega}^A}) {}^B C^A \quad (2.39)$$

and

$$G_{23} = 2 \tilde{r}_o {}^B C^A {}^B \tilde{\omega}^A \tilde{\Phi} + {}^B C^A {}^B \tilde{\omega}^A \tilde{\Phi} + {}^B C^A {}^T J({}^B \omega^A) \quad (2.40)$$

moreover

$$B^*(t) = \begin{bmatrix} I & b \\ 0 & c \end{bmatrix} \quad (2.41)$$

where

$$b = \begin{bmatrix} {}^B C^A & {}^B C^A \\ \tilde{r}_o {}^B C^A + {}^B C^A \tilde{r}_1 & \tilde{r}_o {}^B C^A + {}^B C^A \tilde{r}_2 \end{bmatrix} \quad (2.42)$$

and

$$c = \begin{bmatrix} \Phi^T(r_1) & \Phi^T(r_2) \end{bmatrix} \quad (2.43)$$

finally

$$d(t) = \begin{bmatrix} {}^B C^A (\tilde{S} {}^B \dot{\omega}^A + {}^B \tilde{\omega}^A \tilde{S} {}^B \tilde{\omega}^A) \\ \tilde{r}_o {}^B C^A (\tilde{S} {}^B \dot{\omega}^A + {}^B \tilde{\omega}^A \tilde{S} {}^B \tilde{\omega}^A) - {}^B C^A (\mathbb{I} {}^B \dot{\omega}^A + {}^B \tilde{\omega}^A \mathbb{I} {}^B \tilde{\omega}^A) \\ -\tilde{\Phi}^T {}^B \dot{\omega}^A + \int_m \Phi^T {}^B \tilde{\omega}^A \tilde{r} {}^B \tilde{\omega}^A dm \end{bmatrix} \quad (2.44)$$

2.3 Open Loop Response

The maneuver consist of retargeting the antenna relative to the platform through a 45° angle about the $x - axis$, such that it points to a given direction in the inertial frame. The angular velocity of the antenna is ${}^B \omega^A = [\dot{\beta}_x \ 0 \ 0]^T$. Ideally, the maneuver should not cause elastic

deformation, and this likely to require a long maneuver time. For a minimum time maneuver, the acceleration of the antenna is bang-bang as seen in Fig. (2.2).

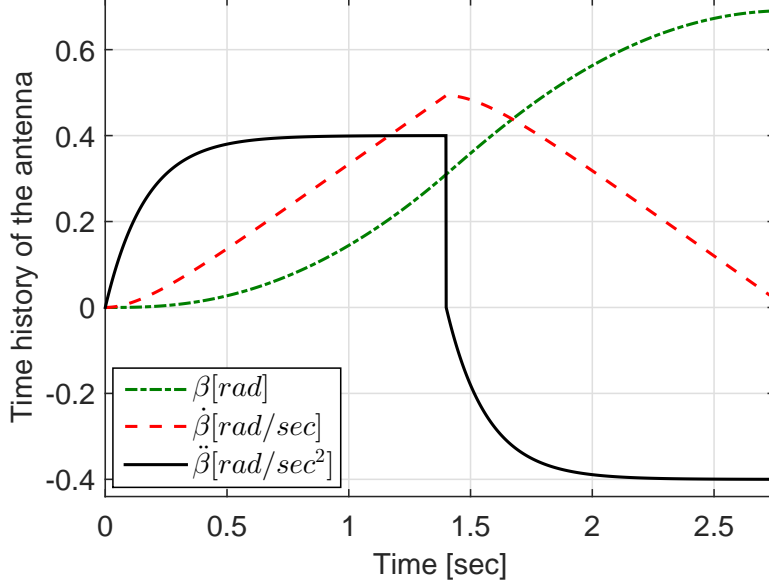


Fig. 2.2: Angular position, velocity, and acceleration of the antenna.

The elastic motion consist of bending vibration in the x and y directions assuming no vibration in the z direction. The vibration is represented by identical admissible functions in each direction in the form of

$$\phi_{xi} = \phi_{yi} = -[\cos(\zeta_i z) - \cosh(\zeta_i z)] + \xi_i[\sin(\zeta_i z) - \sinh(\zeta_i z)] \quad i = 1, 2, \dots, n \quad (2.45)$$

The vectors $\xi \in \mathbb{R}^{1 \times n}$ and $\zeta_i \in \mathbb{R}^{1 \times n}$ depend upon the adopted number of admissible functions. The matrix of admissible functions for a one-beam antenna is in the form of

$$\Phi(r) = \begin{bmatrix} \phi_x & 0 \\ 0 & \phi_y \\ 0 & 0 \end{bmatrix} \quad (2.46)$$

To examine the response of the open-loop system, we use the nominal values of the spacecraft parameters which are listed in the following table. For the purpose of simulation, we assume that the platform and the elastic antenna inertia matrix are diagonal.

Table 2.1: Parameters of the Flexible Spacecraft

Parameters	Values
ξ	[0.7341, 1.0185, 0.9992, 1, 1]
ζ	[1.8750, 4.6940, 7.9000, 10.9950, 14.1370]
l	1.5 m
r_o	[0 0 0.12] ^T m
m	2.2 kg
m_p	228 kg
S	[0 0 1.7] ^T kg · m
$\tilde{\Phi}$	[0.569 0.091 0.032 0.017 0.010] m · l
$\bar{\Phi}$	[0.783 0.434 0.254 0.182 0.141] m
\mathbb{I}_p	diag[17.7 65 80] kg · m ²
\mathbb{I}	diag[1.7 1.7 0] kg · m ²

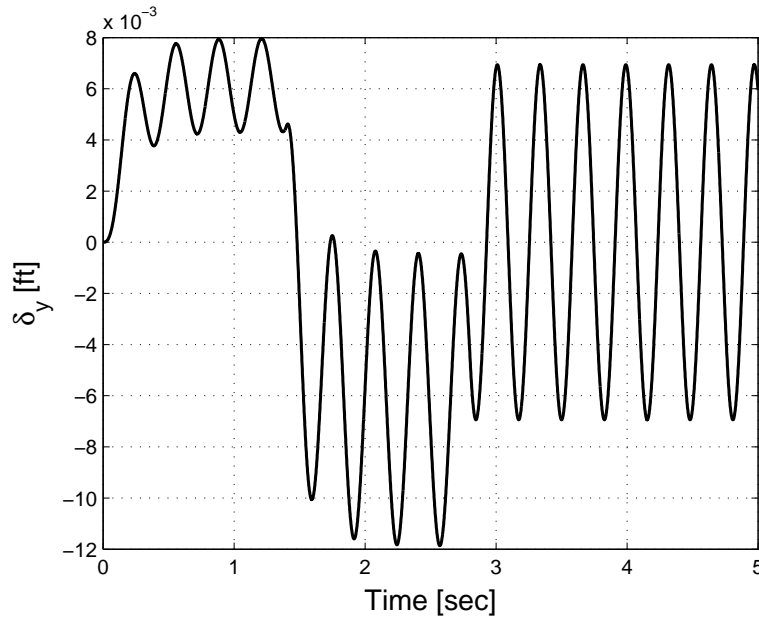


Fig. 2.3: Elastic displacement δ_y of the antenna

The system is characterized by two factors that distinguish it from most commonly encountered systems. It is time varying and it is subjected to persistence disturbances, both factors

arise from the retargetting of the maneuver of the antenna.

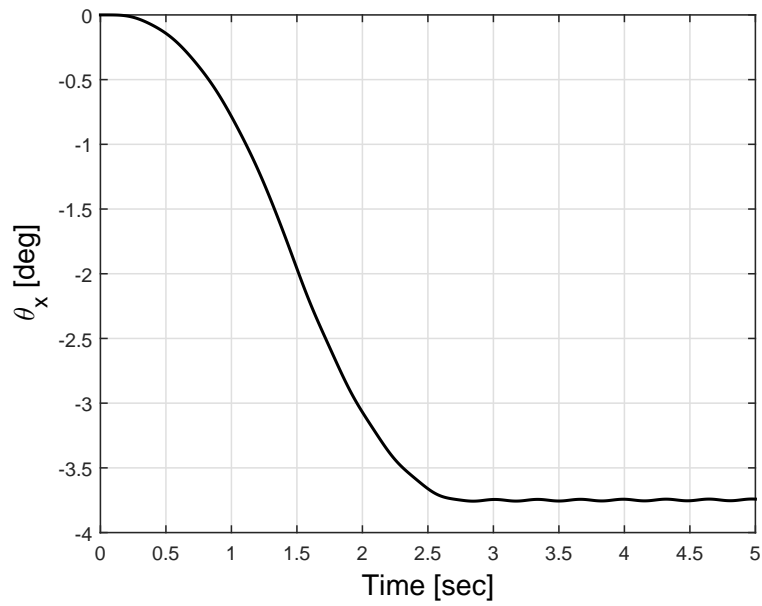


Fig. 2.4: Angular position of the rigid platform θ_x

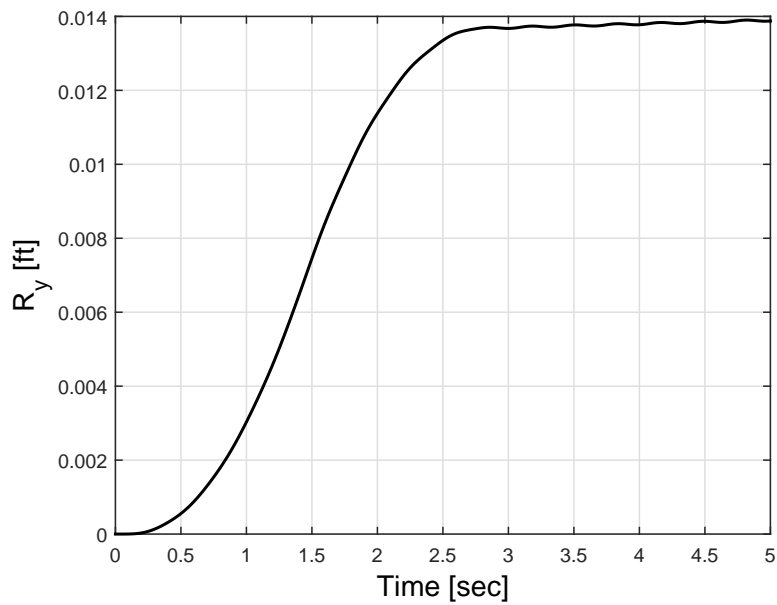


Fig. 2.5: Position of the platform center-of-gravity R_y

The open-loop response of the rigid platform rotation and translation as well as the elastic deformation of the antenna is shown in Figs. (2.3–2.6).

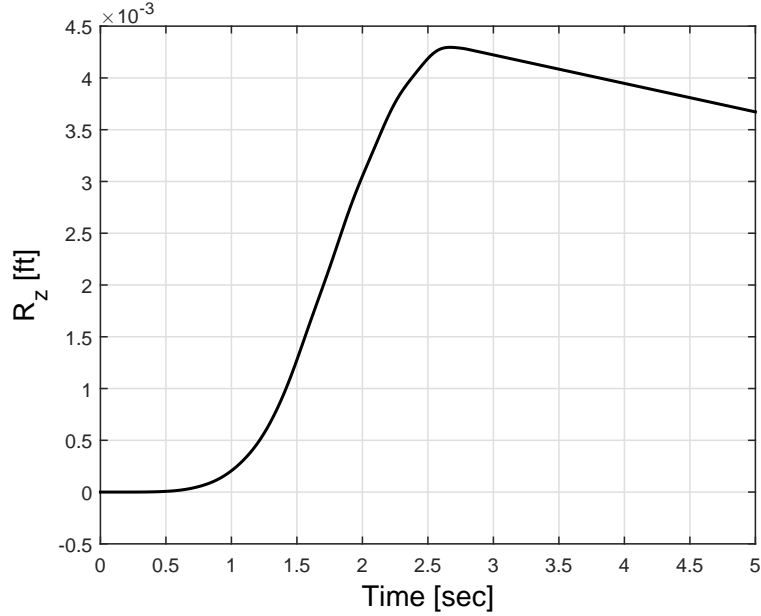


Fig. 2.6: Position of the platform center-of-gravity R_z

2.4 Reduced Model and Control Problems

In general, structure used in space applications are lightly damped, hence they are more susceptible to vibration and dynamic excitation. As mentioned earlier the controller is designed based on the reduced model of the flexible structure and the control of only a small number of modes is considered. It was demonstrated by Balas et al. [36], that even for a simple loop flexible beam, control spillover can cause closed-loop instability and increase the response time due to unmodeled higher frequencies. The open-loop response for different admissible functions is shown in Figs. (2.7–2.8), it can be seen that with five admissible functions we can reach a relatively accurate model.

For the specific maneuver shown in Fig. (2.2), the fast fourier analysis (FFT) reveals that for the nominal model without uncertainties, the antenna will vibrate with two dominant frequencies, the first one is around 1 Hz and the second is about 15 Hz as seen in Fig. (2.9) However, By adding 15% uncertainty in flexural rigidity of the the antenna, the second dominant fre-

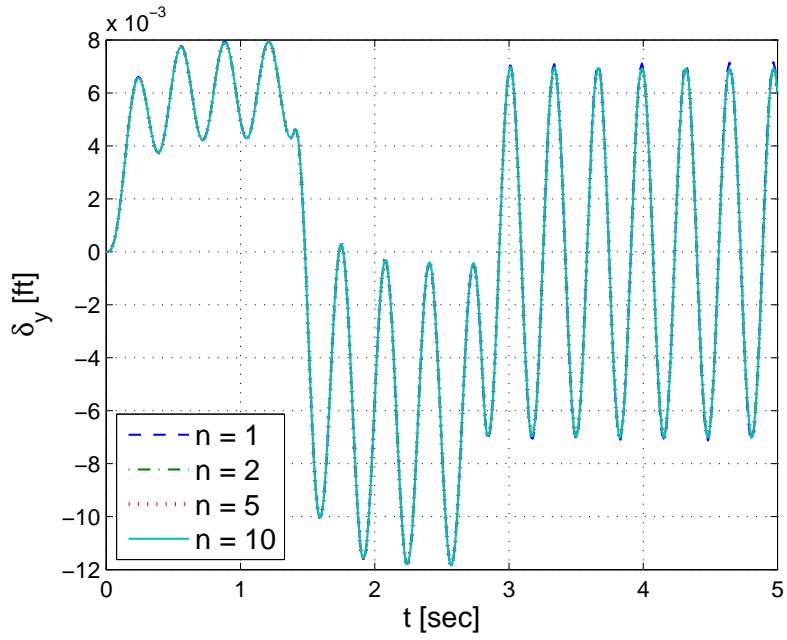


Fig. 2.7: Elastic displacement δ_y of the antenna for different admissible functions

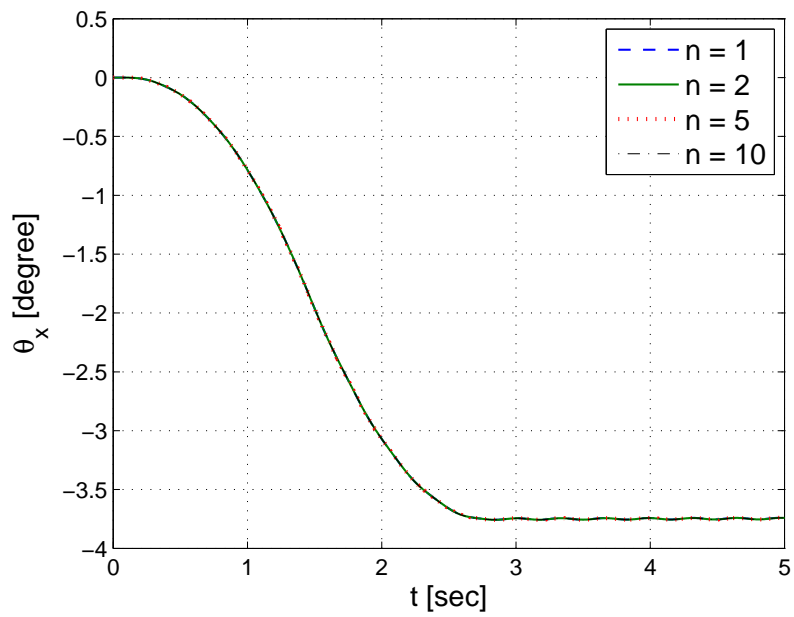


Fig. 2.8: Angular position of the rigid platform θ_x for different admissible functions

quency will increase up to 32 Hz as seen in Fig. (2.10)

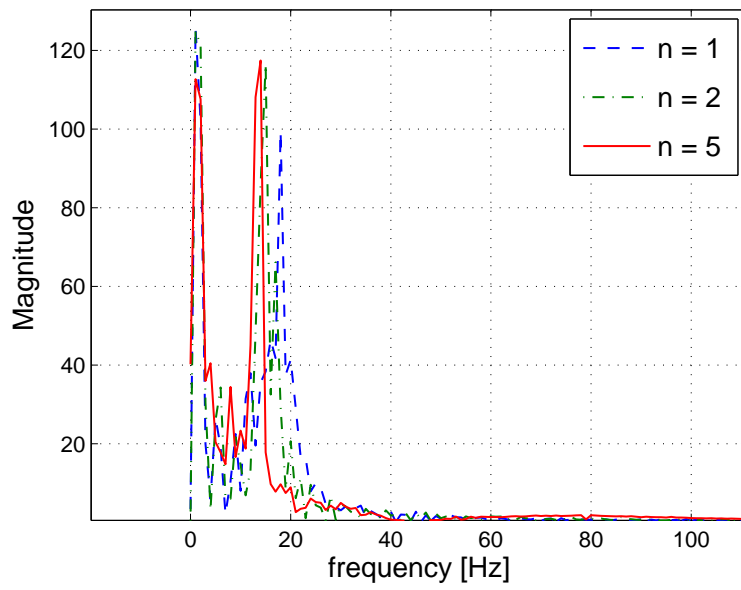


Fig. 2.9: Frequency of the flexible antenna for different admissible functions

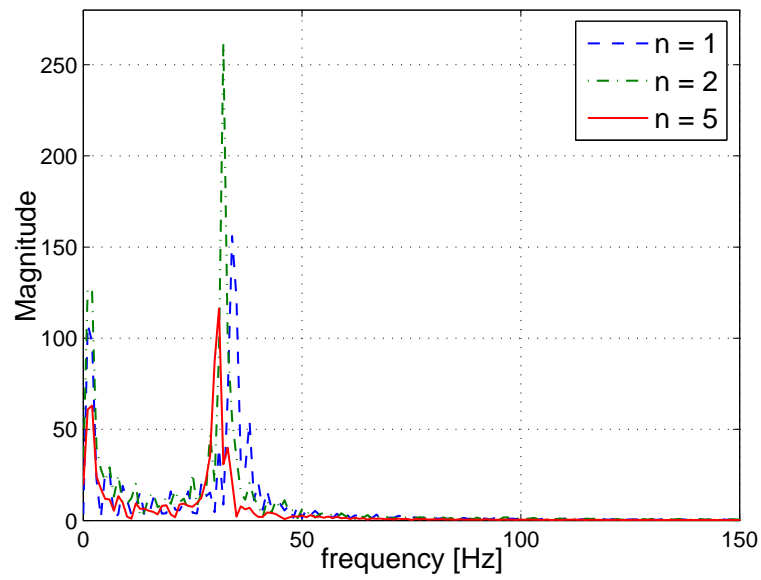


Fig. 2.10: Frequency of the flexible antenna with uncertainty for different admissible functions

CHAPTER 3

Takagi-Sugeno Fuzzy Control

3.1 Introduction

The Takagi-Sugeno (T-S) fuzzy model [37] has become very popular in recent years. One of the reasons is that the stability and performance characteristics of the system represented by the T-S model can be analyzed using a Lyapunov function approach [38, 43]. A further and significant step has also been taken to utilize Lyapunov-function based control techniques to the control synthesis problem for the T-S model. The parallel distributed compensation (PDC) [39] [40] is one such control design framework that has been proposed and developed over the last few years. It has also been shown that within the framework of the T-S fuzzy model and PDC control design, design conditions for stability and performance of a system can be stated in terms of the feasibility of a set of linear matrix inequalities (LMIs) [39] [40]. The gains of the controller can be determined automatically using LMI formulation.

3.2 The Takagi Sugeno (T-S) Model

The fuzzy model proposed by Takagi and Sugeno [44] is described by the fuzzy IF-THEN rules which represent local linear input-output relations of a nonlinear system. The main feature of a T-S fuzzy model is to express the local dynamics of each fuzzy implication by a linear system model. The i^{th} rule of the T-S fuzzy models for a dynamic system are of the following forms.

Model Rule i:

IF $z_1(t)$ is about $\mu_{i1}[z_1(t)]$, and \dots , $z_p(t)$ is about $\mu_{ip}[z_p(t)]$ THEN

$$\begin{cases} \dot{x}(t) = A_i x(t) + B_i u(t) \\ y(t) = C_i x(t) \end{cases} \quad (i = 1, 2, \dots, r) \quad (3.1)$$

where $A_i \in \mathbb{R}^{n \times n}$ is the nominal system matrix, $B_i \in \mathbb{R}^{n \times m}$ is the nominal control matrix and $C_i \in \mathbb{R}^{s \times n}$ is the output matrix, $x(t) \in \mathbb{R}^{n \times 1}$ is the state vector, $u(t) \in \mathbb{R}^{m \times 1}$ is the control input, and $y(t) \in \mathbb{R}^{s \times 1}$ represents the output vector. The variable $z_p(t)$ is a vector of measurable parameters, in general, these parameters may be functions of the state variable, external disturbances, time and uncertainties. We will use r to represent the number of IF-THEN rules, and μ_{ip} to represent the membership functions of the fuzzy sets.

The firing strength of each rule can be determined using a T - norm product

$$w_i[z(t)] = \prod_{j=1}^p \mu_{ij}[z(t)], \quad (i = 1, 2, \dots, r) \quad (3.2)$$

and the fuzzy basis functions are determined from

$$h_i[z(t)] = \frac{w_i[z(t)]}{\sum_{i=1}^r w_i[z(t)]}, \quad (i = 1, 2, \dots, r) \quad (3.3)$$

After combining all the rules for the T-S models, the overall system can be approximated as

$$\Sigma_{TS} : \begin{cases} \dot{x}(t) = \sum_{i=1}^r h_i[z(t)] \{A_i x(t) + B_i u(t)\} \\ y(t) = \sum_{i=1}^r h_i[z(t)] C_i x(t) \end{cases} \quad (3.4)$$

If the parameter $z_p(t)$ is independent of the state vector or control input of the system, as is the case of the maneuver of the flexible spacecraft, then in this case, Eq. (3.4) will describe

a time-varying linear system. It should be noted that the fuzzy model described by Eq. (3.4) can be modified to accommodate external disturbances and uncertainties as we will explain in Chapters 4, 5 and 6.

3.3 Parallel Distributed Compensator (PDC)

The Parallel Distributed Compensation (PDC) theory introduced by Wang et al. [39] provides a procedure to design a fuzzy controller from a given T-S fuzzy model. The feedback control law for each model rule is designed from the corresponding rule of a T-S fuzzy model. Therefore, each control rule has the same premise variables as the T-S model, i.e., “IF” statement but different consequent, i.e., “THEN” statement. The general structure of each control rule is as follows

Control Rule i:

IF $z_1(t)$ is about $\mu_{i1}[z_1(t)]$, and \dots , $z_p(t)$ is about $\mu_{ip}[z_p(t)]$, THEN

$$u(t) = -K_i x(t), \quad (i = 1, 2, \dots, r) \quad (3.5)$$

where $K_i \in \mathbb{R}^{m \times n}$ represents the state feedback gain, The overall control law with fuzzy basis functions become

$$u(t) = - \sum_{i=1}^r h_i(z) K_i x(t) \quad (3.6)$$

The feedback control law described by Eq. (3.6) has a simple structure, and it can be modified to include a reference model as it will be seen in Chapter 6.

3.4 Fuzzy Observer

In practice, all of the states are not fully measurable, and thus it is necessary to design a fuzzy observer in order to implement the fuzzy controller Eq. (3.6). It is known for a linear system that if the pairs $A_i, C_i, (i = 1, 2, \dots, r)$ are observable, the fuzzy system Eq. (3.1) is called locally observable. It is also known [45] that stabilizing state feedback and an observer yield a stabilizing output feedback controller, this is known as the separation principle. The observer has the following structure [45][46]

$$\Sigma_{Observer} : \begin{cases} \dot{\hat{x}}(t) = \sum_{i=1}^r h_i[z(t)] \{A_i \hat{x}(t) + B_i u(t) + L_i [y(t) - \hat{y}(t)]\} \\ \hat{y}(t) = \sum_{i=1}^r h_i[z(t)] C_i \hat{x}(t) \end{cases} \quad (3.7)$$

where $L_i \in \mathbb{R}^{n \times s}$ is the observer gain, $y(t)$ is the measurable output, and $\hat{y}(t)$ is the estimated output vector. The fuzzy observer is required to satisfy $e(t) = x(t) - \hat{x}(t) \rightarrow 0$ as $t \rightarrow \infty$. This condition guarantees that the steady state error between $x(t)$ and $\hat{x}(t)$ converge to zero. In the presence of the fuzzy observer Eq. (3.7), the PDC fuzzy controller Eq. (3.6) takes on the following form

$$u(t) = - \sum_{i=1}^r h_i[z(t)] K_i \hat{x}(t), \quad (i = 1, 2, \dots, r) \quad (3.8)$$

3.5 T-S Fuzzy Model Validation

In this section, first we present the open-loop response of the T-S fuzzy model for the flexible spacecraft described by Eq. (3.1), then in the following chapters we examine and compare the stability, performance and robustness of the proposed controller with a baseline controller.

We choose two rules to fuzzify the input variable $\beta(t)$ as shown in Fig. (3.1). The matrices

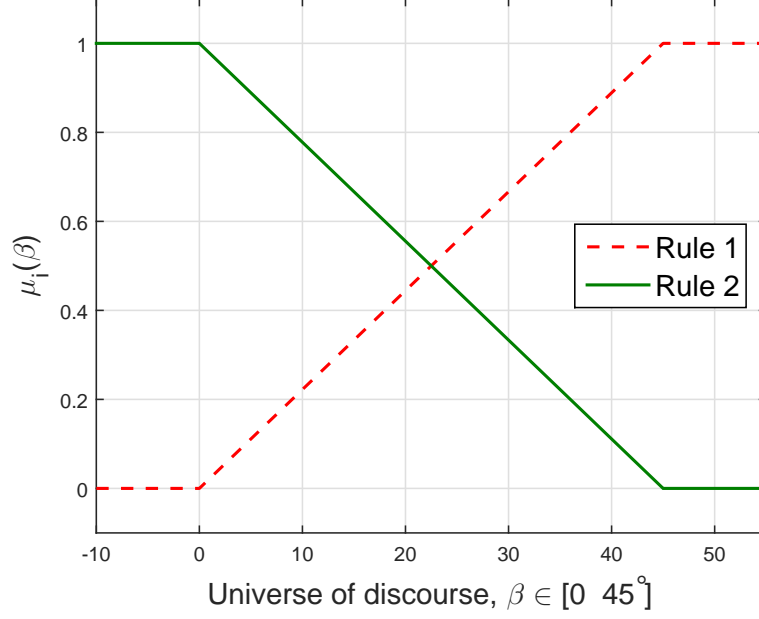


Fig. 3.1: Fuzzy Membership Function

A_i , and B_i , ($i = 1, 2$) are derived by local approximation in the fuzzy partition space of β at points $\beta = 0^\circ$ and $\beta = 45^\circ$. We validate the T-S fuzzy model by comparing the open-loop response of the T-S fuzzy model with the nonlinear model Eqs. (2.7–2.9) for the input shown in Fig. (2.2). For the sake of brevity, only the results for R_z , R_y , θ_x , and U_y are shown in Figs. (3.2–3.5).

We notice that the maximum relative error in approximating the T-S fuzzy model to the nonlinear model is on the order of 10^{-2} for the position R_y to 10^{-4} for the elastic deflection of the antenna. We consider that with two rules, the approximation of the fuzzy model is satisfactory. It should be noted that with more rules, the approximation of the nonlinear model with the fuzzy model tend to be more accurate but the computational cost is high.

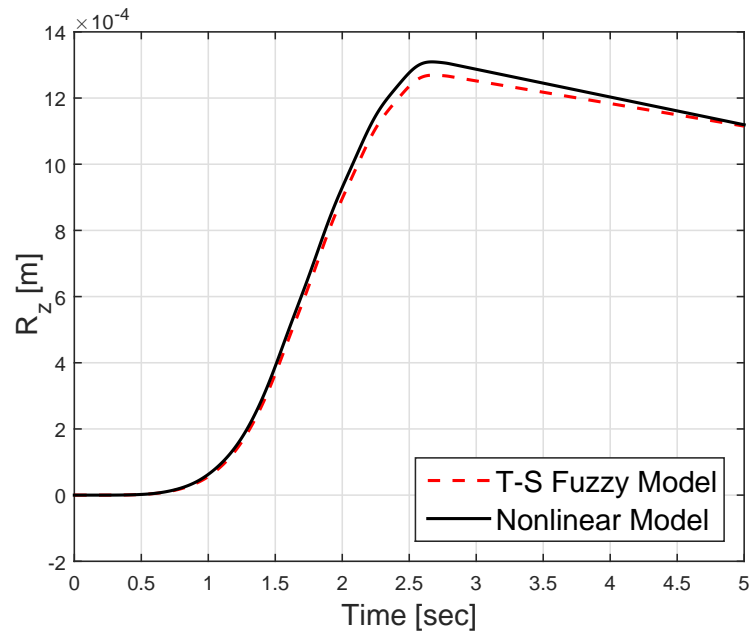


Fig. 3.2: Position of the platform center-of-gravity R_z for nonlinear and fuzzy model.

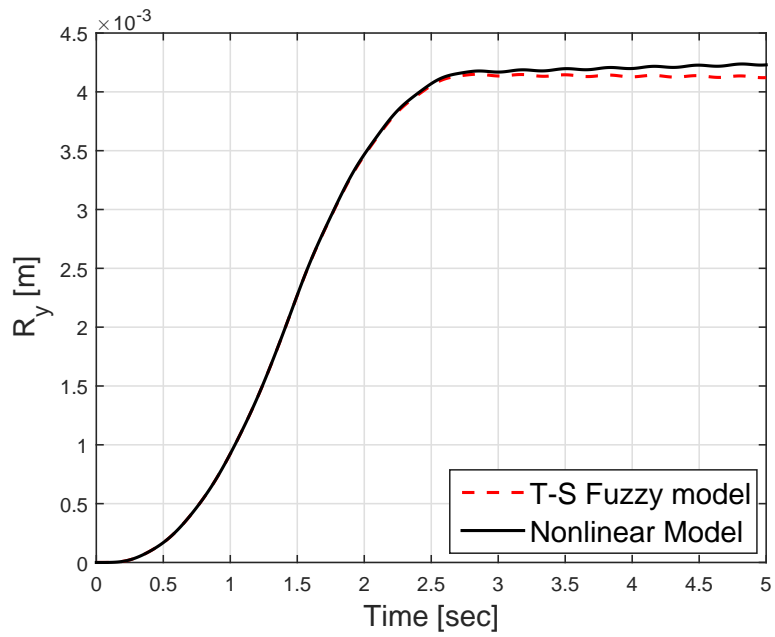


Fig. 3.3: Position of the platform center-of-gravity R_y for the nonlinear and fuzzy model.

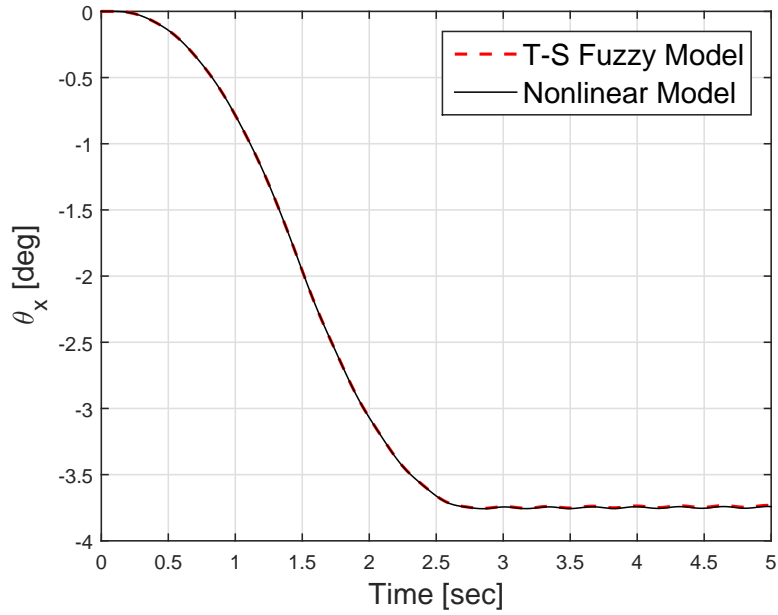


Fig. 3.4: Angular position of the rigid platform θ_x for the nonlinear and fuzzy model.

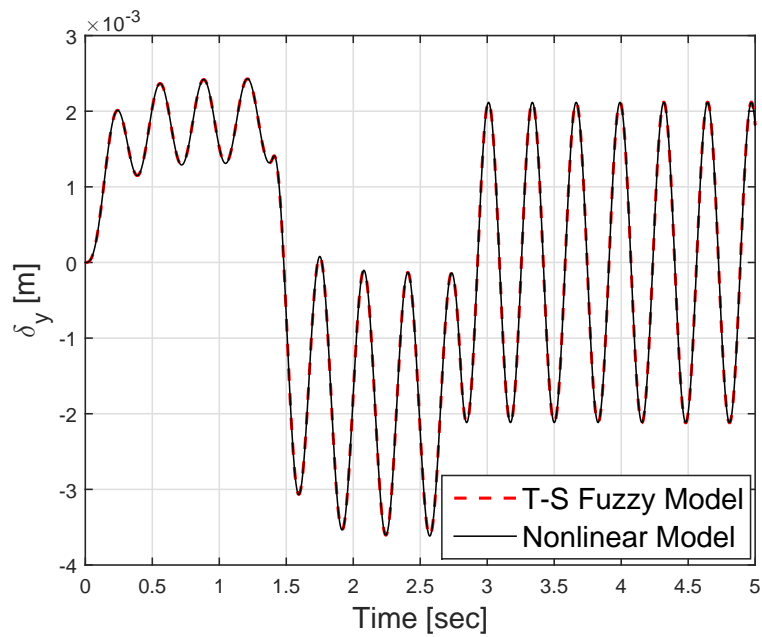


Fig. 3.5: Elastic displacement of the antenna in the y -direction for the nonlinear and fuzzy model.

CHAPTER 4

Full-State Feedback Fuzzy Control with Actuator Norm Constraint

4.1 Introduction

In this chapter, we presents a robust full state feedback fuzzy control law with actuator norm constraints based on Takagi-Sugeno (T-S) fuzzy model for attitude stabilization and vibration suppression of a flexible spacecraft made of a rigid platform and a flexible antenna. First, the linear matrix inequality conditions are derived then the parallel distributed compensator technique is applied to the spacecraft. The controller produces an asymptotically stable closed-loop system which is robust to external disturbances and has a simple structure which make it easy to implement. Numerical simulation is provided for performance evaluation of the proposed controller design.

4.2 Linear Matrix Inequality approach

4.2.1 Stability Conditions

Using Lyapunov stability theory, the stability of a continuous fuzzy system Eq. (3.4) with a control input $u(t) = 0$ is stated in the following theorem

Theorem 4.2.1. *The equilibrium of the continuous fuzzy system Eq. (3.4) is globally asymptotically stable if there exists a common positive definite matrix P for all subsystems such that*

$$A_i^T P + P A_i < 0 \quad (i = 1, 2, \dots, r) \quad (4.1)$$

4.2.2 Stable Closed-Loop System

Now we consider the closed-loop system with $u(t) \neq 0$. Using the the parallel distributer compensator given by:

$$u(t) = - \sum_{i=1}^r h_i(z) K_i x(t) \quad (4.2)$$

and the fuzzy system given by the following Eq. (3.4)

$$\dot{x}(t) = \sum_{i=1}^r h_i[z(t)] \{ A_i x(t) + B_i u(t) \} \quad (4.3)$$

we obtain the following

$$\dot{x}(t) = \sum_{i=1}^r \sum_{j=1}^r h_i[z(t)] h_j[z(t)] \{ A_i - B_i K_j \} x(t) \quad (4.4)$$

let

$$G_{ij} = A_i - B_i K_j \quad (4.5)$$

Equation (4.4) becomes

$$\dot{x}(t) = \sum_{i=1}^r h_i[z(t)] h_j[z(t)] G_{ii} x(t) + 2 \sum_{i=1}^r \sum_{j=1}^r h_i[z(t)] h_j[z(t)] \left\{ \frac{G_{ij} + G_{ji}}{2} \right\} x(t) \quad (4.6)$$

using the stability condition stated in theorem 4.2.1, we can derive the stability condition for a continuous system described by Eq. (4.6)

Theorem 4.2.2 ([38]). *The equilibrium of the continuous fuzzy control system described by Eq. (4.6) is globally asymptotically stable if there exists a common positive definite matrix P*

such that

$$\begin{cases} G_{ii}^T P + P G_{ii} < 0 \\ \left(\frac{G_{ij} + G_{ji}}{2} \right)^T P + P \left(\frac{G_{ij} + G_{ji}}{2} \right) \leq 0 \end{cases} \quad (i, j = 1, 2, \dots, r, i \neq j \mid h_i \cap h_j \neq \emptyset) \quad (4.7)$$

The purpose of the fuzzy control design problem is to determine K_i , ($i = 1, 2, \dots, r$) which satisfy the conditions of theorem 4.2.2 with a common positive definite matrix P .

Multiplying the inequality in theorem 4.2.2 on the left and right by P^{-1} and let $X = P^{-1}$ we get

$$\begin{cases} -X A_i^T - A_i X + X K_i^T B_i^T + B_i K_i X > 0 \\ -X A_i^T - A_i X - X A_j^T - A_j X + X K_j^T B_i^T + B_i K_j X + X K_i^T B_j^T + B_j K_i X \geq 0 \end{cases} \quad (4.8)$$

let $M_i = K_i X$, substituting into Eq. (4.8) yields the following stability condition

$$\begin{cases} -X A_i^T - A_i X + M_i^T B_i^T + B_i M_i > 0 \\ -X A_i^T - A_i X - X A_j^T - A_j X + M_j^T B_i^T + B_i M_j + M_i^T B_j^T + B_j M_i \geq 0 \end{cases}$$

$\forall i, j = 1, 2, \dots, r, i \neq j \mid h_i \cap h_j \neq \emptyset$

4.2.3 Stable Closed-Loop with Fuzzy Observer

It was shown by Xiao et al. [46] that the fuzzy controller and the fuzzy observer can be independently designed to be stable. Moreover, if the premise variable is independent of the states as in the case that is being studied in this dissertation, and using the condition

$e(t) = x(t) - \hat{x}(t)$ with Eq. (3.8) we get the following:

$$\begin{cases} \dot{x}(t) = \sum_{i=1}^r \sum_{j=1}^r h_i[z(t)]h_j[z(t)] \left\{ (A_i - B_iK_j)x(t) + B_iK_j e(t) \right\} \\ \dot{e}(t) = \sum_{i=1}^r \sum_{j=1}^r h_i[z(t)]h_j[z(t)] \left\{ A_i - L_iC_j \right\} e(t) \end{cases} \quad (4.9)$$

Let $x_a(t) = [x(t) \ e(t)]^T$ and

$$G_{ij} = \begin{bmatrix} A_i - B_iK_j & B_iK_j \\ 0 & A_i - L_iC_j \end{bmatrix} \quad (4.10)$$

Using the same procedure as in the previous section, we get the following theorem:

Theorem 4.2.3. *The equilibrium of the augmented system Eq. (4.9) is globally asymptotically stable if there exists a common positive definite matrix P such that*

$$\begin{cases} G_{ii}^T P + P G_{ii} < 0 \\ \left(\frac{G_{ij} + G_{ji}}{2} \right)^T P + P \left(\frac{G_{ij} + G_{ji}}{2} \right) \leq 0 \end{cases} \quad (i \neq j \mid h_i \cap h_j \neq \emptyset) \quad (4.11)$$

let $M_i = K_i P_1$ and $N = P_2 L_i$, substituting into Eq. (4.11) yields the following stability condition

$$\begin{cases} P_1 > 0, P_2 > 0 \\ P_1 A_i^T - M_i^T B_i^T + A_i P_1 - B_i M_i < 0 \\ P_1 A_i^T - M_j^T B_j^T + A_i P_1 - B_i M_j + P_1 A_j^T - M_i^T B_j^T + A_j P_1 - B_j M_i < 0 \\ A_i^T P_2 - C_i^T N_i^T + P_2 A_i - N_i C_i < 0 \\ A_i^T P_2 - C_j^T N_i^T + P_2 A_i - N_i C_j + A_j^T P_2 - C_i^T N_j^T + P_2 A_j - N_j C_i < 0 \end{cases} \quad (4.12)$$

If a feasible solution exist, the matrices $P_1, P_2, M_i,$ and N_i can be found by convex optimiza-

tion techniques. The feedback gains and the observer gains can be calculated respectively as

$$K_i = M_i P_1^{-1} \quad (4.13)$$

and

$$L_i = P_2^{-1} N_i \quad (4.14)$$

4.2.4 Disturbance Rejection

A successfully designed control system should always be able to maintain stability and performance levels in spite of uncertainties in system dynamics and/or in the working environment to a certain degree. The robustness issue was not that prominently considered until late 1970s and early 1980s with the pioneering work by Zames [47] and Zames and Francis [48] on the theory, now known as the H_∞ control theory. The H_∞ control theory provides a systematic design procedures of robust controllers for linear systems.

Consider the following fuzzy system with disturbance:

$$\Sigma_{TS} : \begin{cases} \dot{x}(t) = \sum_{i=1}^r h_i[z(t)] \{ A_i x(t) + B_i u(t) + E_i v(t) \} \\ y(t) = \sum_{i=1}^r h_i[z(t)] C_i x(t) \end{cases} \quad (4.15)$$

where $v(t)$ is the deterministic disturbance due to spacecraft configuration change. We assume that all the states are available. The disturbance rejection can be realized by:

Minimize: γ

Subject To:

$$\sup_{\|v(t)\|_2 \neq 0} \frac{\|y(t)\|_2}{\|v(t)\|_2} \leq \gamma \quad (4.16)$$

Theorem 4.2.4. *The feedback gains K_i that stabilize the fuzzy model Eq. (4.15) and minimize γ , can be obtained by solving the following LMIs:*

$$\min_{M_1, \dots, M_r} \gamma^2 \quad (4.17)$$

subject to :

$$X > 0 \quad (4.18)$$

$$\left[\begin{array}{ccc} \left(\begin{array}{c} -\frac{1}{2}(XA_i^T - M_j B_i^T + \\ A_i X - B_i M_j + \\ XA_j^T - M_i^T B_j^T + \\ A_j X - B_j M_i) \end{array} \right) & -\frac{1}{2}(E_i + E_j) & \frac{1}{2}X(C_i + C_j)^T \\ -\frac{1}{2}(E_i + E_j)^T & \gamma^2 I & 0 \\ \frac{1}{2}(C_i + C_j)X & 0 & I \end{array} \right] \geq 0 \quad (4.19)$$

where $M_i = K_i X$ and $X = P_1^{-1}$, $\forall i, j = 1, 2, \dots, r, i \neq j \mid h_i \cap .h_j \neq \emptyset$

Proof. Consider the quadratic Lyapunov function $V[x(t)] = x^T(t)P_1x(t)$, where $P_1 > 0$ and $\gamma \geq 0$ such that $\forall t$.

$$\dot{V}[x(t)] + y^T(t)y(t) - \gamma^2 v^T(t)v(t) \leq 0 \quad (4.20)$$

integrating Eq. (4.20), we get

$$\int_0^{t_f} \{\dot{V}[x(t)] + y^T(t)y(t) - \gamma^2 v^T(t)v(t)\} dt \leq 0 \quad (4.21)$$

assuming the initial condition $x(0) = 0$ we have

$$V[x(t_f)] + \int_0^{t_f} \{y^T(t)y(t) - \gamma^2 v^T(t)v(t)\} dt \leq 0 \quad (4.22)$$

and since $V[x(t_f)] \geq 0$, this implies

$$\frac{\|y(t)\|_2}{\|v(t)\|_2} \leq \gamma \quad (4.23)$$

using Eq. (4.20) we have

$$\dot{x}^T(t)P_1x(t) + x^T(t)P_1\dot{x}(t) + \sum_{i=1}^r \sum_{j=1}^r h_i[z(t)]h_j[z(t)]x^T(t)C_i^T C_j x(t) - \gamma^2 v^T(t)v(t) \quad (4.24)$$

$$\begin{aligned} &= \sum_{i=1}^r \sum_{j=1}^r h_i[z(t)]h_j[z(t)]x^T(t)(A_i - B_i K_j)^T P x(t) + \sum_{i=1}^r \sum_{j=1}^r h_i[z(t)]h_j[z(t)]x^T(t) \\ &P(A_i - B_i K_j)x(t) + \sum_{i=1}^r \sum_{j=1}^r h_i[z(t)]h_j[z(t)]x^T(t)C_i^T C_j x(t) - \gamma^2 v^T(t)v(t) \\ &+ \sum_{i=1}^r h_i[z(t)]v^T(t)E_i^T P x(t) + \sum_{i=1}^r h_i[z(t)]x^T(t)P E_i v(t) \end{aligned} \quad (4.25)$$

$$= \sum_{i=1}^r \sum_{j=1}^r h_i[z(t)]h_j[z(t)][x^T(t) \ v^T(t)] \begin{bmatrix} \begin{pmatrix} (A_i - B_i K_j)^T P_1 \\ + P_1(A_i - B_i K_j) \\ + C_i^T C_j \\ E_i^T P_1 \end{pmatrix} & P_1 E_i \\ & -\gamma^2 I \end{bmatrix} \begin{bmatrix} x(t) \\ v(t) \end{bmatrix} \leq 0 \quad (4.26)$$

Equation (4.26) can be written as

$$\left[\begin{array}{c} \left(\begin{array}{c} -\sum_{i=1}^r \sum_{j=1}^r h_i[z(t)]h_j[z(t)]\{(A_i - B_iK_j)^T P_1 \\ +P_1(A_i - B_iK_j) + C_i^T C_j\} \end{array} \right) \\ -P_1 \sum_{i=1}^r h_i[z(t)]E_i \\ -\sum_{i=1}^r h_i[z(t)]E_i^T P_1 \\ -\gamma^2 I \end{array} \right] \geq 0 \quad (4.27)$$

$$\Rightarrow \left[\begin{array}{c} \left(\begin{array}{c} -\sum_{i=1}^r \sum_{j=1}^r h_i[z(t)]h_j[z(t)]\{(A_i - B_iK_j)^T P_1 \\ +P_1(A_i - B_iK_j)\} \\ -\sum_{i=1}^r h_i[z(t)]E_i^T P_1 \end{array} \right) \\ -P_1 \sum_{i=1}^r h_i[z(t)]E_i \\ -\gamma^2 I \end{array} \right] \quad (4.28)$$

$$- \left[\begin{array}{cc} \sum_{i=1}^r \sum_{j=1}^r h_i[z(t)]h_j[z(t)]C_i^T C_j & 0 \\ 0 & 0 \end{array} \right] \geq 0$$

$$\Rightarrow \left[\begin{array}{c} \left(\begin{array}{c} -\sum_{i=1}^r \sum_{j=1}^r h_i[z(t)]h_j[z(t)]\{(A_i - B_iK_j)^T P_1 \\ +P_1(A_i - B_iK_j)\} \\ -\sum_{i=1}^r h_i[z(t)]E_i^T P_1 \end{array} \right) \\ -P_1 \sum_{i=1}^r h_i[z(t)]E_i \\ -\gamma^2 I \end{array} \right] \quad (4.29)$$

$$- \left[\begin{array}{c} \sum_{i=1}^r h_i[z(t)]C_i^T \\ 0 \end{array} \right] \left[\begin{array}{cc} \sum_{i=1}^r h_i[z(t)]C_i & 0 \end{array} \right] \geq 0$$

$$\Rightarrow \sum_{i=1}^r \sum_{j=1}^r h_i[z(t)]h_j[z(t)] \begin{bmatrix} \left(\begin{array}{c} -\frac{1}{2}\{(A_i - B_i K_j)^T P_1 + \\ P_1(A_i - B_i K_j) + \\ (A_j - B_j K_i)^T P_1 + \\ P_1(A_j - B_j K_i)\} \end{array} \right) & -\frac{1}{2}P_1(E_i + E_j) & \frac{1}{2}(C_i + C_j)^T \\ -\frac{1}{2}(E_i + E_j)^T P_1 & -\gamma^2 I & 0 \\ \frac{1}{2}(C_i + C_j) & 0 & I \end{bmatrix} \geq 0 \quad (4.30)$$

multiplying both side by the block diagonal $[X \ I \ I]$, where $X = P_1^{-1}$, we obtain Eq. (4.19). \square

4.2.5 Constraints On the Control Input

Theorem 4.2.5. *Assume that the initial condition $x(0)$ is known, the constraint $\|u(t)\|_2 \leq \mu$ is satisfied $\forall t \geq 0$ if the LMIs*

$$\begin{bmatrix} 1 & x(0)^T \\ x(0) & X \end{bmatrix} \geq 0 \quad (i = 1, 2, \dots, r) \quad (4.31)$$

$$\begin{bmatrix} X & M_i^T \\ M_i & \mu^2 I \end{bmatrix} \geq 0 \quad (i = 1, 2, \dots, r) \quad (4.32)$$

Proof. using $\|u(t)\|_2 \leq \mu$, we have

$$u^T(t)u(t) = \sum_{i=1}^r \sum_{j=1}^r h_i[z(t)]h_j[z(t)]x^T(t)K_i^T K_j x(t) \leq \mu^2$$

hence

$$\frac{1}{\mu^2} = \sum_{i=1}^r \sum_{j=1}^r h_i[z(t)]h_j[z(t)]x^T(t)K_i^T K_j x(t) \leq 1$$

since $x^T(t)X^{-1}x(t) < x^T(0)X^{-1}x(0) \leq 1, \forall t > 0$ if

$$\frac{1}{\mu^2} = \sum_{i=1}^r \sum_{j=1}^r h_i[z(t)]h_j[z(t)]x^T(t)K_i^T K_j x(t) \leq x^T(t)X^{-1}x(t)$$

therefore

$$\begin{aligned} & \sum_{i=1}^r \sum_{j=1}^r h_i[z(t)]h_j[z(t)]x^T(t)\left[\frac{1}{\mu^2}K_i^T K_j - X^{-1}\right]x(t) \leq 0 \\ &= \frac{1}{2} \sum_{i=1}^r \sum_{j=1}^r h_i[z(t)]h_j[z(t)]x^T(t)\left[\frac{1}{\mu^2}K_i^T K_j + \frac{1}{\mu^2}K_j^T K_i - 2X^{-1}\right]x(t) \\ &= \frac{1}{2} \sum_{i=1}^r \sum_{j=1}^r h_i[z(t)]h_j[z(t)]x^T(t)\left[\frac{1}{\mu^2}(K_i^T K_i + K_j^T K_j) - \frac{1}{\mu^2}(K_i^T - K_j)(K_i^T - K_j) - 2X^{-1}\right]x(t) \\ &\leq \frac{1}{2} \sum_{i=1}^r \sum_{j=1}^r h_i[z(t)]h_j[z(t)]x^T(t)\left[\frac{1}{\mu^2}(K_i^T K_i + K_j^T K_j) - 2X^{-1}\right]x(t) \\ &= \sum_{i=1}^r h_i[z(t)]x^T(t)\left[\frac{1}{\mu^2}K_i^T K_i - X^{-1}\right]x(t) \end{aligned}$$

if

$$\frac{1}{\mu^2}K_i^T K_i - X^{-1} \leq 0 \quad (4.33)$$

using the Schur complement and let $M_i = K_i X$, we get Eq. (4.32) \square

4.2.6 Constraints on Initial Condition

Theorem 4.2.6. *Assume that the initial condition is unknown but bounded $\|x(0)\| \leq \phi$, then*

$$x^T(0)X^{-1}x(0) \leq 1 \quad (4.34)$$

if

$$\phi^2 I \leq X \quad (4.35)$$

Proof. using Eq. (4.35), we write

$$X^{-1} \leq \frac{1}{\phi^2} I \quad (4.36)$$

therefore

$$x^T(0)X^{-1}x(0) \leq \frac{1}{\phi^2}x^T(0)x(0) \leq 1 \quad (4.37)$$

□

4.3 Numerical Simulation

The developed controller has been applied to the flexible spacecraft model Fig. (2.1). The parameters of the spacecraft are listed in Table. 2.1. We neglect the axial deflection, in the z -direction, in the beam and choose five admissible functions to approximate the deflections of the appendage in the x and y directions in terms of the generalized coordinates.

The spacecraft has twelve actuators, six on the platform for controlling the position and attitude along three axes and four actuators in the middle and tip of the appendage in the x and y directions. The time history of the tip of the appendage in the y -direction and the first Euler angle are shown in Figs. (4.1,4.2), respectively. The plots show the open-loop as well as the closed-loop responses with three different input constraint upper bounds, μ . It can be seen that by increasing μ , i.e. the actuator force, one may cause the controller do a better job in vibration suppression and attitude stabilization.

The components of the position vector of the platform are in Fig. (4.3). It can be seen from the plot that the position vector stabilizes around $(0, 0, 0)$ after about 25 seconds. Figure (4.4) shows the time history of attitude parameters, Euler angles, when $\mu = 5$ lbf. The platform

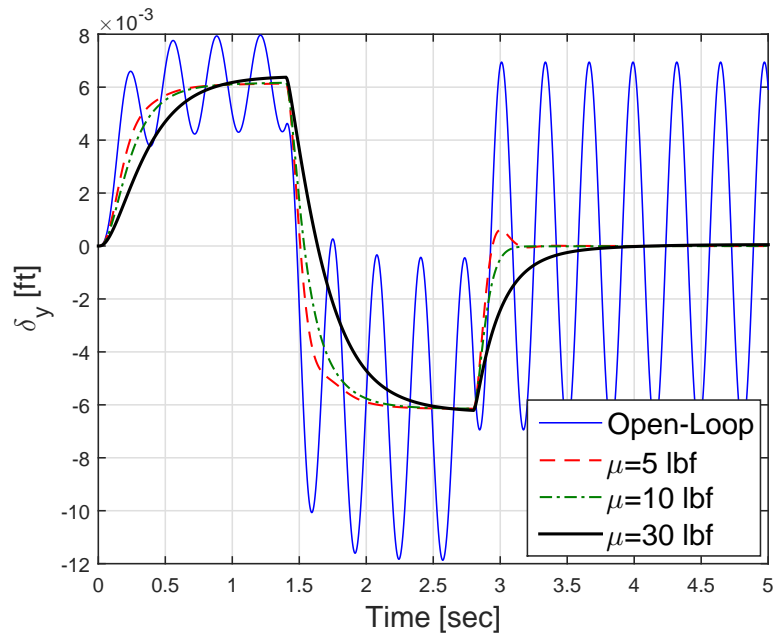


Fig. 4.1: Elastic displacement of the antenna in the y direction for different input control upper bounds, μ .

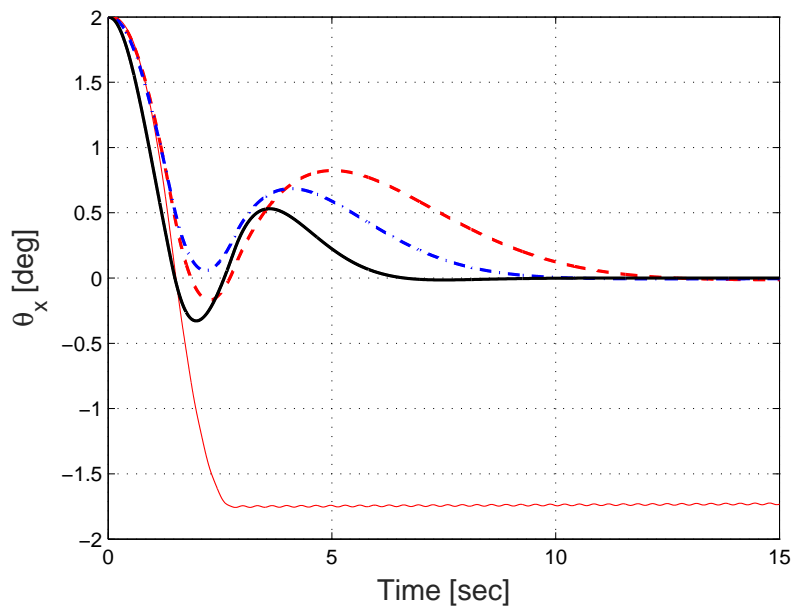


Fig. 4.2: Angular position of the rigid platform for different input control upper bound, μ .

attitude stabilizes after about 20 seconds.

To check the boundedness of the input controls, we plot the time history of the actuator

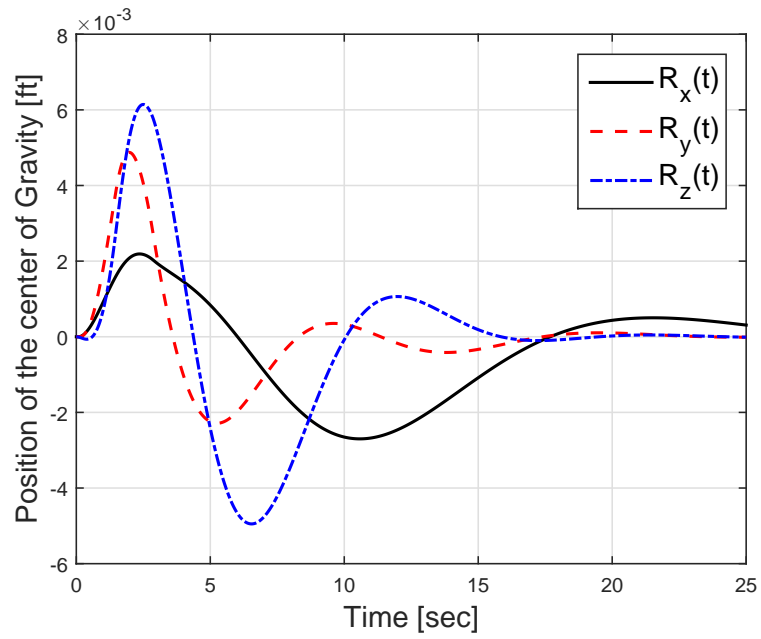


Fig. 4.3: Position of the platform center of gravity in the inertial frame with input constraint upper bound of $\mu = 5$ lbf.

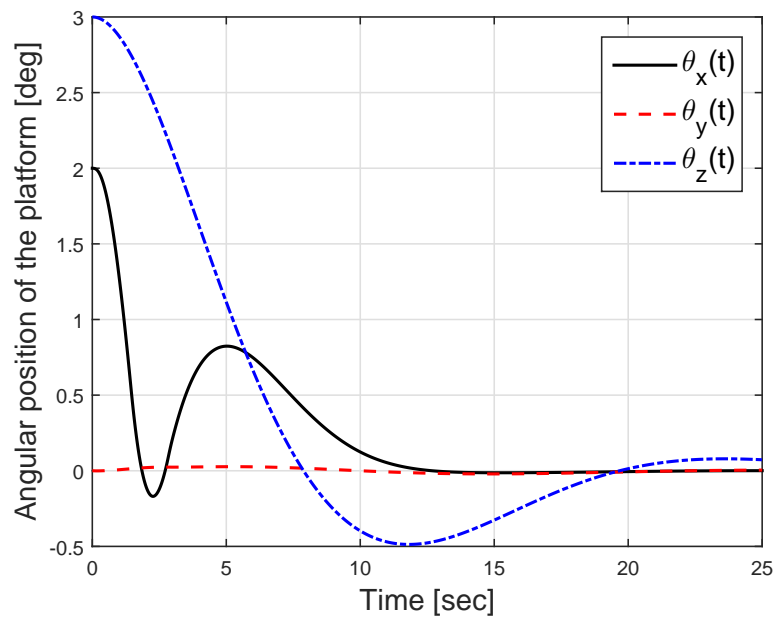


Fig. 4.4: Angular position of the rigid platform with input constraint upper bound of $\mu = 5$ lbf.

forces, and moments on the platform for $\mu = 5\text{ lbf}$. The results are shown in Figs. (4.5,4.6), respectively.

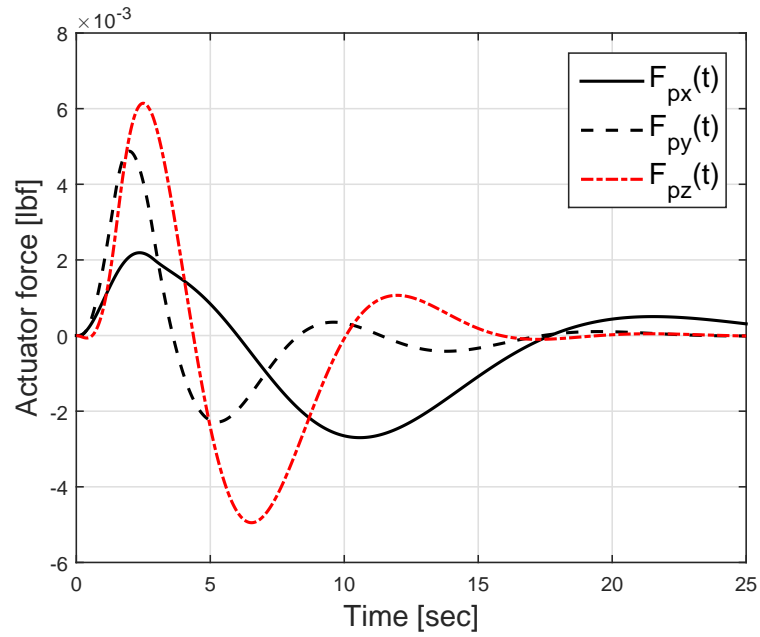


Fig. 4.5: Actuator forces on the platform with input constraint upper bound of $\mu = 5$ lbf.

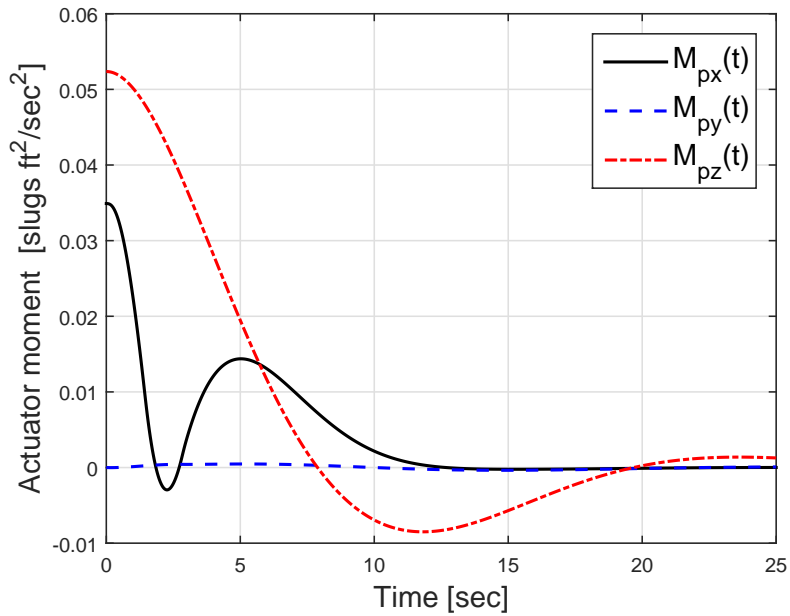


Fig. 4.6: Actuator moments on the platform with input constraint upper bound of $\mu = 5$ lbf.

It can be seen that the control inputs generated by the proposed PDC controller are bounded. In addition, the actuator forces at the tip and in the lateral directions of the appendage are shown in the Fig. (4.7). The control forces are bounded as well.

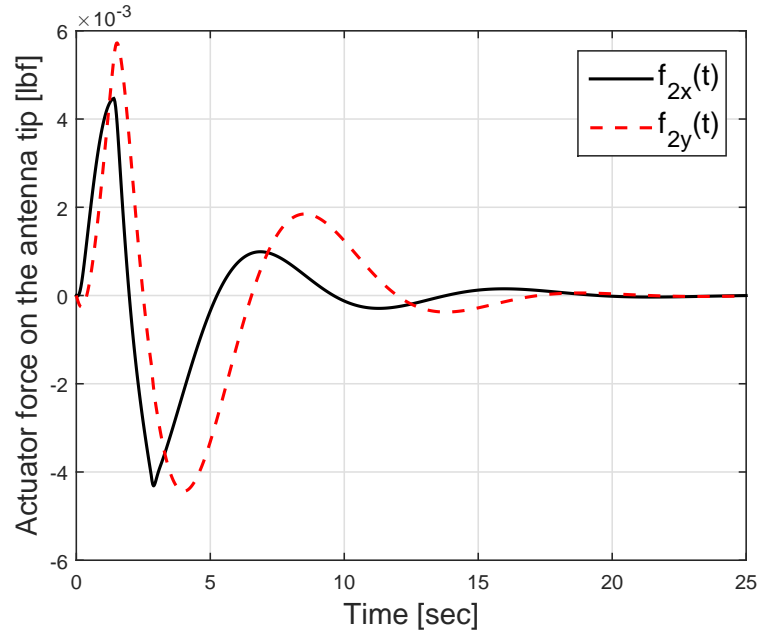


Fig. 4.7: Actuator forces on the tip of antenna in the x and y directions with input constraint upper bound of $\mu = 5$ lbf.

CHAPTER 5

Robust-Optimal Fuzzy Control With Individual Actuator Constraint

5.1 Introduction

In most applications, real systems are vulnerable to external disturbances, uncertainty and measurement noise. Furthermore there are always differences between mathematical models used for design and the actual system. Hence, a control engineer is required to design a controller which will stabilize a plant and satisfy certain performance levels in the presence of disturbance signals, noise interference, unmodelled plant dynamics and plant parameter variations. Those design objectives are best realized via the feedback control mechanism. Therefore, robustness is of crucial importance in control system design.

In this chapter, we present a robust-optimal fuzzy controller for position and attitude stabilization, and vibration suppression of the flexible spacecraft during an antenna retargeting maneuver. The fuzzy controller is based on the Takagi-Sugeno (T-S) fuzzy model and uses the parallel distributed compensator (PDC) technique to stabilize quadratically the closed-loop system. The proposed controller is robust to parameter and unstructured uncertainties of the model. We improve the performance and the efficiency of the controller by minimizing the upper bound of the actuator's amplitude and maximizing the uncertain terms included in the T-S fuzzy model. In addition to actuator amplitude constraints, a fuzzy model-based observer is considered for estimating unmeasurable states. Using Lyapunov stability theory and linear matrix inequalities (LMIs), we formulate the problem of designing an optimal-robust fuzzy

controller/observer with actuator amplitude constraint as a convex optimization problem. Numerical simulation is provided to demonstrate and compare the stability, performance, and robustness of the proposed fuzzy controller with a baseline nonlinear controller.

5.2 Takagi-Sugeno (T-S) Fuzzy Model for Uncertain Systems with Disturbance

The fuzzy model proposed by Takagi and Sugeno [44] can be modified to accommodate disturbances and uncertainties [49]. The i^{th} rule of the T-S fuzzy models for a dynamic system with uncertainty is of the following forms.

Model Rule i :

IF $z_1(t)$ is about $\mu_{i1}[z_1(t)]$, and \dots , $z_p(t)$ is about $\mu_{ip}[z_p(t)]$ THEN

$$\dot{x}(t) = [A_i + \Delta A_i]x(t) + [B_i + \Delta B_i]u(t) + \varphi(t), \quad (i = 1, 2, \dots, r) \quad (5.1)$$

where $A_i \in \mathbb{R}^{n \times n}$ is the nominal system matrix, $B_i \in \mathbb{R}^{n \times m}$ is the nominal control matrix, $x(t) \in \mathbb{R}^{n \times 1}$ is the state vector, $u(t) \in \mathbb{R}^{m \times 1}$ is the control input, and $\varphi(t) \in \mathbb{R}^{n \times 1}$ represents the disturbance due to the reconfiguration of the spacecraft during the maneuver.

The parameter uncertainties in the system and control matrices are defined as $\Delta A_i = D_{ai}\Delta_{ai}(t)E_{ai}$, and $\Delta B_i = D_{bi}\Delta_{bi}(t)E_{bi}$, respectively. The $\Delta_{ai}(t)$ and $\Delta_{bi}(t)$ blocks satisfy the following conditions [50][51]

$$\|\Delta_{ai}(t)\| \leq \frac{1}{\gamma_{ai}}, \quad \|\Delta_{bi}(t)\| \leq \frac{1}{\gamma_{bi}} \quad (5.2)$$

and

$$\Delta_{ai}(t) = \Delta_{ai}^T(t), \quad \Delta_{bi}(t) = \Delta_{bi}^T(t) \quad (5.3)$$

and $D_{ai} \in \mathbb{R}^{n \times p}$, $E_{ai} \in \mathbb{R}^{p \times n}$, $D_{bi} \in \mathbb{R}^{n \times q}$ and $E_{bi} \in \mathbb{R}^{q \times m}$ are constant row vectors which

characterize the structure of the uncertainty.

The firing strength of each rule can be determined using a T – norm product as in Eq. (3.2)

$$w_i[z(t)] = \prod_{j=1}^p \mu_{ij}[z(t)], \quad 0 \leq \mu_{ij}[z(t)] \leq 1, \quad (i = 1, 2, \dots, r) \quad (5.4)$$

and the fuzzy basis functions are determined using Eq. (3.3)

$$h_i[z(t)] = \frac{w_i[z(t)]}{\sum_{i=1}^r w_i[z(t)]}, \quad \sum_{i=1}^p h_i[z(t)] = 1, \quad (i = 1, 2, \dots, r) \quad (5.5)$$

After combining the rules for the T-S models, the overall system can be approximated as

$$\Sigma_{TS} : \begin{cases} \dot{x}(t) = \sum_{i=1}^r h_i[z(t)] \{ [A_i + \Delta A_i]x(t) + [B_i + \Delta B_i]u(t) \} + \varphi(t) \\ y(t) = \sum_{i=1}^r h_i[z(t)] C_i x(t) \end{cases} \quad (5.6)$$

The Parallel Distributed Compensation (PDC) introduced by Wang et al. [39] uses the estimated state provided from the observer Eq. (3.7) as a feedback. The general structure of each control rule is as follows

Control Rule i:

IF $z_1(t)$ is about $\mu_{i1}[z_1(t)]$, and \dots , $z_p(t)$ is about $\mu_{ip}[z_p(t)]$, THEN

$$u(t) = -K_i \hat{x}(t), \quad (i = 1, 2, \dots, r) \quad (5.7)$$

where $K_i \in \mathbb{R}^{m \times n}$ represents the state feedback gain, $\hat{x}(t)$ denotes the state vector estimated by the fuzzy observer. The overall control law with fuzzy basis functions becomes

$$u(t) = - \sum_{i=1}^r h_i(z) K_i \hat{x}(t) \quad (5.8)$$

It should be noted that the actuator amplitude constraint is subject to the following constraints

$$|u_k| \leq \mu_k, \quad (k = 1, 2, \dots, m) \quad (5.9)$$

5.3 Robust Stability Condition

Substituting Eq. (3.6) into Eq. (5.6), yields

$$\dot{x}(t) = \sum_{i=1}^r \sum_{j=1}^r h_i[z(t)]h_j[z(t)] \left\{ A_i - B_i K_j + [D_{ai} \ D_{bi}] \begin{bmatrix} \Delta_{ai} & 0 \\ 0 & \Delta_{bi} \end{bmatrix} \begin{bmatrix} E_{ai} \\ -E_{bi} K_j \end{bmatrix} \right\} x(t) \quad (5.10)$$

The following theorem presents the robust stability conditions for the fuzzy model described by Eq. (5.6)

Theorem 5.3.1. *The fuzzy system Eq. (5.6) is stabilized via the PDC controller Eq. (3.6)*

$\exists P_1 > 0$ satisfying

$$\begin{cases} S_{ii} < 0 \\ T_{ij} < 0 \end{cases} \quad (i \neq j \mid h_i \cap h_j \neq \emptyset) \quad (5.11)$$

where

$$S_{ii} = \begin{bmatrix} (A_i - B_i K_i)^T P_1 + P_1 (A_i - B_i K_i) & * & * & * & * \\ D_{ai}^T P_1 & -I & * & * & * \\ D_{bi}^T P_1 & 0 & -I & * & * \\ E_{ai} & 0 & 0 & -\gamma_{ai}^2 I & * \\ -E_{bi} K_i & 0 & 0 & 0 & -\gamma_{bi}^2 I \end{bmatrix} \quad (5.12)$$

and

$$T_{ij} = \begin{bmatrix} T_{ij}(1, 1) & * & * & * & * & * & * & * & * \\ D_{ai}^T P_1 & -I & * & * & * & * & * & * & * \\ D_{bi}^T P_1 & 0 & -I & * & * & * & * & * & * \\ D_{aj}^T P_1 & 0 & 0 & -I & * & * & * & * & * \\ D_{bj}^T P_1 & 0 & 0 & 0 & -I & * & * & * & * \\ E_{ai} & 0 & 0 & 0 & 0 & -\gamma_{ai}^2 I & * & * & * \\ -E_{bi} K_j & 0 & 0 & 0 & 0 & 0 & -\gamma_{bi}^2 I & * & * \\ E_{aj} & 0 & 0 & 0 & 0 & 0 & 0 & -\gamma_{aj}^2 I & * \\ -E_{bj} K_i & 0 & 0 & 0 & 0 & 0 & 0 & 0 & -\gamma_{bj}^2 I \end{bmatrix} \quad (5.13)$$

where

$$T_{ij}(1, 1) = (A_i - B_i K_j)^T P_1 + P_1 (A_i - B_i K_j) + (A_j - B_j K_i)^T P_1 + P_1 (A_j - B_j K_i) \quad (5.14)$$

The (*) denotes the transposed elements for symmetric positions.

Proof. Equation (5.10) can be written as

$$\begin{aligned} \dot{x}(t) = & \sum_{i=1}^r h_i^2 [z(t)] \left\{ A_i - B_i K_i + [D_{ai} \ D_{bi}] \begin{bmatrix} \Delta_{ai} & 0 \\ 0 & \Delta_{bi} \end{bmatrix} \begin{bmatrix} E_{ai} \\ -E_{bi} K_i \end{bmatrix} \right\} x(t) \\ & + \sum_{i=1}^r \sum_{i < j} h_i [z(t)] h_j [z(t)] \left\{ A_i - B_i K_j + A_j - B_j K_i + [D_{ai} \ D_{bi}] \begin{bmatrix} \Delta_{ai} & 0 \\ 0 & \Delta_{bi} \end{bmatrix} \right. \\ & \left. \begin{bmatrix} E_{ai} \\ -E_{bi} K_j \end{bmatrix} + [D_{aj} \ D_{bj}] \begin{bmatrix} \Delta_{aj} & 0 \\ 0 & \Delta_{bj} \end{bmatrix} \begin{bmatrix} E_{aj} \\ -E_{bj} K_i \end{bmatrix} \right\} x(t) \end{aligned} \quad (5.15)$$

$$\begin{aligned}
& \begin{bmatrix} D_{ai}^T \\ D_{bi}^T \end{bmatrix} P_1 + [E_{ai}^T - (E_{bi}K_j)^T] \begin{bmatrix} \Delta_{ai} & 0 \\ 0 & \Delta_{bi} \end{bmatrix}^T \begin{bmatrix} \Delta_{ai} & 0 \\ 0 & \Delta_{bi} \end{bmatrix} \begin{bmatrix} E_{ai} \\ -E_{bi}K_j \end{bmatrix} \\
& - \left(\begin{bmatrix} D_{ai}^T \\ D_{bi}^T \end{bmatrix} P_1 - \begin{bmatrix} \Delta_{ai} & 0 \\ 0 & \Delta_{bi} \end{bmatrix} \begin{bmatrix} E_{ai} \\ -E_{bi}K_j \end{bmatrix} \right)^T \left(\begin{bmatrix} D_{ai}^T \\ D_{bi}^T \end{bmatrix} P_1 - \begin{bmatrix} \Delta_{ai} & 0 \\ 0 & \Delta_{bi} \end{bmatrix} \begin{bmatrix} E_{ai} \\ -E_{bi}K_j \end{bmatrix} \right) \\
& + (A_j - B_jK_i)^T P_1 + P_1(A_j - B_jK_i) + P_1[D_{aj} \ D_{bj}] \begin{bmatrix} D_{aj}^T \\ D_{bj}^T \end{bmatrix} P_1 \\
& + [E_{aj}^T - (E_{bj}K_i)^T] \begin{bmatrix} \Delta_{aj} & 0 \\ 0 & \Delta_{bj} \end{bmatrix}^T \begin{bmatrix} \Delta_{aj} & 0 \\ 0 & \Delta_{bj} \end{bmatrix} \begin{bmatrix} E_{aj} \\ -E_{bj}K_i \end{bmatrix} - \left(\begin{bmatrix} D_{aj}^T \\ D_{bj}^T \end{bmatrix} P_1 - \begin{bmatrix} \Delta_{aj} & 0 \\ 0 & \Delta_{bj} \end{bmatrix} \begin{bmatrix} E_{aj} \\ -E_{bj}K_i \end{bmatrix} \right)^T \\
& - \left(\begin{bmatrix} D_{aj}^T \\ D_{bj}^T \end{bmatrix} P_1 - \begin{bmatrix} \Delta_{aj} & 0 \\ 0 & \Delta_{bj} \end{bmatrix} \begin{bmatrix} E_{aj} \\ -E_{bj}K_i \end{bmatrix} \right) \left(\begin{bmatrix} D_{aj}^T \\ D_{bj}^T \end{bmatrix} P_1 - \begin{bmatrix} \Delta_{aj} & 0 \\ 0 & \Delta_{bj} \end{bmatrix} \begin{bmatrix} E_{aj} \\ -E_{bj}K_i \end{bmatrix} \right) \Big\} x(t)
\end{aligned}$$

if

$$\begin{aligned}
& (A_i - B_iK_j)^T P_1 + P_1(A_i - B_iK_j) + P_1[D_{ai} \ D_{bi}] \begin{bmatrix} D_{ai}^T \\ D_{bi}^T \end{bmatrix} P_1 + [E_{ai}^T - (E_{bi}K_j)^T] \\
& \begin{bmatrix} \frac{1}{\gamma_{ai}^2} I & 0 \\ 0 & \frac{1}{\gamma_{bi}^2} I \end{bmatrix} \begin{bmatrix} E_{ai} \\ -E_{bi}K_j \end{bmatrix} + (A_j - B_jK_i)^T P_1 + P_1(A_j - B_jK_i) + P_1[D_{aj} \ D_{bj}] \\
& \begin{bmatrix} D_{aj}^T \\ D_{bj}^T \end{bmatrix} P_1 + [E_{aj}^T - (E_{bj}K_i)^T] \begin{bmatrix} \frac{1}{\gamma_{aj}^2} I & 0 \\ 0 & \frac{1}{\gamma_{bj}^2} I \end{bmatrix} \begin{bmatrix} E_{aj} \\ -E_{bj}K_i \end{bmatrix} < 0 \tag{5.17}
\end{aligned}$$

then

$$\begin{aligned}
& \frac{d}{dt} x(t)^T P_1 x(t) < \sum_{i=1}^r h_i^2 [z(t)] x^T(t) \left\{ (A_i - B_iK_i)^T P_1 + P_1(A_i - B_iK_i) + P_1[D_{ai} \ D_{bi}] \right. \\
& \left. \begin{bmatrix} D_{ai}^T \\ D_{bi}^T \end{bmatrix} P_1 + [E_{ai}^T - (E_{bi}K_i)^T] \begin{bmatrix} \Delta_{ai} & 0 \\ 0 & \Delta_{bi} \end{bmatrix}^T \begin{bmatrix} \Delta_{ai} & 0 \\ 0 & \Delta_{bi} \end{bmatrix} \begin{bmatrix} E_{ai} \\ -E_{bi}K_i \end{bmatrix} - \left(\begin{bmatrix} D_{ai}^T \\ D_{bi}^T \end{bmatrix} P_1 - \begin{bmatrix} \Delta_{ai} & 0 \\ 0 & \Delta_{bi} \end{bmatrix} \begin{bmatrix} E_{ai} \\ -E_{bi}K_i \end{bmatrix} \right)^T \right. \\
& \left. \left(\begin{bmatrix} D_{ai}^T \\ D_{bi}^T \end{bmatrix} P_1 - \begin{bmatrix} \Delta_{ai} & 0 \\ 0 & \Delta_{bi} \end{bmatrix} \begin{bmatrix} E_{ai} \\ -E_{bi}K_i \end{bmatrix} \right) \right\}
\end{aligned}$$

$$\begin{aligned}
& - \begin{bmatrix} \Delta_{ai} & 0 \\ 0 & \Delta_{bi} \end{bmatrix} \begin{bmatrix} E_{ai} \\ -E_{bi}K_i \end{bmatrix} \Big)^T \left(\begin{bmatrix} D_{ai}^T \\ D_{bi}^T \end{bmatrix} P_1 - \begin{bmatrix} \Delta_{ai} & 0 \\ 0 & \Delta_{bi} \end{bmatrix} \begin{bmatrix} E_{ai} \\ -E_{bi}K_i \end{bmatrix} \right) \Big\} x(t) \\
& \leq \sum_{i=1}^r h_i^2 [z(t)] x^T(t) \left\{ (A_i - B_i K_i)^T P_1 + P_1 (A_i - B_i K_i) + P_1 [D_{ai} \ D_{bi}] \begin{bmatrix} D_{ai}^T \\ D_{bi}^T \end{bmatrix} P_1 \right. \\
& + [E_{ai}^T \ - (E_{bi} K_i)^T] \begin{bmatrix} \Delta_{ai} & 0 \\ 0 & \Delta_{bi} \end{bmatrix} \Big)^T \begin{bmatrix} \Delta_{ai} & 0 \\ 0 & \Delta_{bi} \end{bmatrix} \begin{bmatrix} E_{ai} \\ -E_{bi} K_i \end{bmatrix} - \left(\begin{bmatrix} D_{ai}^T \\ D_{bi}^T \end{bmatrix} P_1 \right. \\
& \left. - \begin{bmatrix} \Delta_{ai} & 0 \\ 0 & \Delta_{bi} \end{bmatrix} \begin{bmatrix} E_{ai} \\ -E_{bi} K_i \end{bmatrix} \right)^T \left(\begin{bmatrix} D_{ai}^T \\ D_{bi}^T \end{bmatrix} P_1 - \begin{bmatrix} \Delta_{ai} & 0 \\ 0 & \Delta_{bi} \end{bmatrix} \begin{bmatrix} E_{ai} \\ -E_{bi} K_i \end{bmatrix} \right) \Big\} x(t) \\
& = \sum_{i=1}^r h_i^2 [z(t)] x^T(t) \left\{ (A_i - B_i K_i)^T P_1 + P_1 (A_i - B_i K_i) + P_1 [D_{ai} \ D_{bi}] \begin{bmatrix} D_{ai}^T \\ D_{bi}^T \end{bmatrix} P_1 \right. \\
& + [E_{ai}^T \ - (E_{bi} K_i)^T] \begin{bmatrix} \Delta_{ai} & 0 \\ 0 & \Delta_{bi} \end{bmatrix} \Big)^T \begin{bmatrix} \Delta_{ai} & 0 \\ 0 & \Delta_{bi} \end{bmatrix} \begin{bmatrix} E_{ai} \\ -E_{bi} K_i \end{bmatrix} - \left(\begin{bmatrix} D_{ai}^T \\ D_{bi}^T \end{bmatrix} P_1 \right. \\
& \left. - \begin{bmatrix} \Delta_{ai} & 0 \\ 0 & \Delta_{bi} \end{bmatrix} \begin{bmatrix} E_{ai} \\ -E_{bi} K_i \end{bmatrix} \right)^T \left(\begin{bmatrix} D_{ai}^T \\ D_{bi}^T \end{bmatrix} P_1 - \begin{bmatrix} \Delta_{ai} & 0 \\ 0 & \Delta_{bi} \end{bmatrix} \begin{bmatrix} E_{ai} \\ -E_{bi} K_i \end{bmatrix} \right) \Big\} x(t)
\end{aligned}$$

if

$$\begin{aligned}
& (A_i - B_i K_i)^T P_1 + P_1 (A_i - B_i K_i) + P_1 [D_{ai} \ D_{bi}] \begin{bmatrix} D_{ai}^T \\ D_{bi}^T \end{bmatrix} P_1 + [E_{ai}^T \ - (E_{bi} K_i)^T] \\
& \begin{bmatrix} \frac{1}{\gamma_{ai}^2} I & 0 \\ 0 & \frac{1}{\gamma_{bi}^2} I \end{bmatrix} \begin{bmatrix} E_{ai} \\ -E_{bi} K_i \end{bmatrix} < 0 \tag{5.18}
\end{aligned}$$

then

$$\frac{d}{dt} x^T(t) P_1 x(t) < 0$$

since

$$\|\Delta_{ai}(t)\| \leq \frac{1}{\gamma_{ai}}, \quad \|\Delta_{bi}(t)\| \leq \frac{1}{\gamma_{bi}}$$

using the Schur complement, Eq. (5.17) and Eq. (5.18) can be written as Eq. (5.11) \square

5.4 Optimal Fuzzy Control

The control objective of optimal fuzzy control is to minimize certain performance functions. The fuzzy controller proposed by Tanaka et al. [49] minimizes the upper bound of the following cost function

$$J = \int_0^{\infty} [y^T(t)W y(t) + u^T(t)R u(t)] dt \quad (5.19)$$

where

$$y(t) = \sum_{i=1}^r h_i[z(t)] C_i x(t) \quad (5.20)$$

and $W = W^T > 0$ and $R = R^T > 0$ are weighting coefficient matrices. The following theorem presents a basis for the optimal control problem

Theorem 5.4.1. *The fuzzy system Eq. (3.4) is stabilized via the PDC controller Eq. (3.6)*

$\exists P_1 > 0$ satisfying

$$\begin{cases} U_{ii} < 0 \\ V_{ij} < 0 \end{cases} \quad (i \neq j \mid h_i \cap h_j \neq \emptyset) \quad (5.21)$$

where

$$U_{ii} = \begin{bmatrix} (A_i - B_i K_i)^T P_1 + P_1 (A_i - B_i K_i) & * & * \\ C_i & -W^{-1} & * \\ -K_i & 0 & -R^{-1} \end{bmatrix} \quad (5.22)$$

and

$$V_{ij} = \begin{bmatrix} V_{ij}(1,1) & * & * & * & * \\ C_i & -W^{-1} & * & * & * \\ -K_j & 0 & -R^{-1} & * & * \\ C_j & 0 & 0 & -W^{-1} & * \\ -K_i & 0 & 0 & 0 & -R^{-1} \end{bmatrix} \quad (5.23)$$

and

$$V_{ij}(1,1) = (A_i - B_i K_j)^T P_1 + P_1 (A_i - B_i K_j) + (A_j - B_j K_i)^T P_1 + P_1 (A_j - B_j K_i) \quad (5.24)$$

Proof.

Corollary 5.4.1.1. $\forall W > 0$, we have

$$-C_i^T W C_i - C_j^T W C_j \leq -C_i^T W C_j - C_j^T W C_i \quad (5.25)$$

Corollary 5.4.1.2. $\forall W > 0$ and $R > 0$, we have

$$\begin{aligned} & -[C_i^T \quad -K_j^T] \begin{bmatrix} W & 0 \\ 0 & R \end{bmatrix} \begin{bmatrix} C_i \\ -K_j \end{bmatrix} - [C_j^T \quad -K_i^T] \begin{bmatrix} W & 0 \\ 0 & R \end{bmatrix} \begin{bmatrix} C_j \\ -K_i \end{bmatrix} \\ & \leq -[C_i^T \quad -K_j^T] \begin{bmatrix} W & 0 \\ 0 & R \end{bmatrix} \begin{bmatrix} C_j \\ -K_i \end{bmatrix} - [C_j^T \quad -K_i^T] \begin{bmatrix} W & 0 \\ 0 & R \end{bmatrix} \begin{bmatrix} C_i \\ -K_j \end{bmatrix} \end{aligned} \quad (5.26)$$

from 5.4.1.1, we have

$$\begin{aligned}
& - [C_i^T \quad -K_j^T] \begin{bmatrix} W & 0 \\ 0 & R \end{bmatrix} \begin{bmatrix} C_i \\ -K_j \end{bmatrix} - [C_j^T \quad -K_i^T] \begin{bmatrix} W & 0 \\ 0 & R \end{bmatrix} \begin{bmatrix} C_j \\ -K_i \end{bmatrix} \\
& = -C_i^T W C_i - K_j^T R K_j - C_j^T W C_j - K_i^T R K_i \\
& \leq -C_i^T W C_j - K_j^T R K_i - C_j^T W C_i - K_i^T R K_j \\
& = [C_i^T \quad -K_j^T] \begin{bmatrix} W & 0 \\ 0 & R \end{bmatrix} \begin{bmatrix} C_j \\ -K_i \end{bmatrix} - [C_j^T \quad -K_i^T] \begin{bmatrix} W & 0 \\ 0 & R \end{bmatrix} \begin{bmatrix} C_i \\ -K_j \end{bmatrix}
\end{aligned} \tag{5.27}$$

now let's consider the new variable

$$\hat{y}(t) = \begin{bmatrix} y(t) \\ u(t) \end{bmatrix} = \sum_{i=1}^r h_i[z(t)] \begin{bmatrix} C_i \\ -K_i \end{bmatrix} x(t) \tag{5.28}$$

Equation (5.19) can be written as

$$J = \int_0^\infty \hat{y}^T(t) \begin{bmatrix} W & 0 \\ 0 & R \end{bmatrix} \hat{y}(t) dt \tag{5.29}$$

then from the Schur complement we can write

$$(A_i - B_i K_i)^T P_1 + P_1 (A_i - B_i K_i) + [C_i^T \quad -K_i^T] \begin{bmatrix} W & 0 \\ 0 & R \end{bmatrix} \begin{bmatrix} C_i \\ -K_i \end{bmatrix} < 0 \tag{5.30}$$

and

$$\begin{aligned}
& (A_i - B_i K_j)^T P_1 + P_1 (A_i - B_i K_j) + (A_j - B_j K_i)^T P_1 + P_1 (A_j - B_j K_i) + [C_i^T \quad -K_i^T] \\
& \begin{bmatrix} W & 0 \\ 0 & R \end{bmatrix} \begin{bmatrix} C_i \\ -K_j \end{bmatrix} + [C_i^T \quad -K_j^T] + [C_j^T \quad -K_i^T] \begin{bmatrix} W & 0 \\ 0 & R \end{bmatrix} \begin{bmatrix} C_j \\ -K_i \end{bmatrix} < 0.
\end{aligned} \tag{5.31}$$

From Eq. (5.30) and Eq. (5.31), we obtain

$$(A_i - B_i K_i)^T P_1 + P_1 (A_i - B_i K_i) < 0 \tag{5.32}$$

and

$$(A_i - B_i K_j)^T P_1 + P_1 (A_i - B_i K_j) + (A_j - B_j K_i)^T P_1 + P_1 (A_j - B_j K_i) < 0. \tag{5.33}$$

Using theorem 4.2.2, we conclude that the fuzzy system is globally asymptotically stable.

Next we consider the Lyapunov function $V[x(t)] = x^T(t)P_1x(t)$, we would like to prove that

$$J < x^T(0)P_1x(0)$$

$$\begin{aligned}
& \frac{d}{dt} x^T(t)P_1x(t) = \dot{x}^T(t)P_1x(t) + x^T(t)P_1\dot{x}(t) \\
& = \sum_{i=1}^r \sum_{j=1}^r h_i[z(t)]h_j[z(t)]x^T(t) \left\{ (A_i - B_i K_j)^T P_1 + P_1 (A_i - B_i K_j) \right\} x(t) \\
& = \sum_{i=1}^r h_i^2[z(t)]x^T(t) \left\{ (A_i - B_i K_i)^T P_1 + P_1 (A_i - B_i K_i) \right\} x(t) \\
& + \sum_{i=1}^r \sum_{i \neq j} h_i[z(t)]h_j[z(t)]x^T(t) \left\{ (A_i - B_i K_j)^T P_1 + P_1 (A_i - B_i K_j) \right\} x(t) \\
& < \sum_{i=1}^r h_i^2[z(t)]x^T(t) \left\{ (A_i - B_i K_i)^T P_1 + P_1 (A_i - B_i K_i) \right\} x(t) \\
& - x^T(t) \left\{ \sum_{i=1}^r \sum_{i < j} h_i[z(t)]h_j[z(t)] [C_i^T \quad -K_j^T] \begin{bmatrix} W & 0 \\ 0 & R \end{bmatrix} \begin{bmatrix} C_i \\ -K_j \end{bmatrix} + \right.
\end{aligned}$$

$$\begin{aligned}
& \sum_{i=1}^r \sum_{i < j} h_i[z(t)]h_j[z(t)][C_j^T - K_i^T] \begin{bmatrix} W & 0 \\ 0 & R \end{bmatrix} \begin{bmatrix} C_j \\ -K_i \end{bmatrix} \Big\} x(t) \\
& < -x^T(t) \left\{ \sum_{i=1}^r h_i^2[z(t)][C_i^T - K_j^T] \begin{bmatrix} W & 0 \\ 0 & R \end{bmatrix} \begin{bmatrix} C_i \\ -K_j \end{bmatrix} \right\} x(t) - \\
& x^T(t) \left\{ \sum_{i=1}^r \sum_{i < j} h_i[z(t)]h_j[z(t)][C_j^T - K_i^T] \begin{bmatrix} W & 0 \\ 0 & R \end{bmatrix} \begin{bmatrix} C_j \\ -K_i \end{bmatrix} \right\} + \\
& \sum_{i=1}^r \sum_{i < j} h_i[z(t)]h_j[z(t)][C_j^T - K_i^T] \begin{bmatrix} W & 0 \\ 0 & R \end{bmatrix} \begin{bmatrix} C_j \\ -K_i \end{bmatrix} \Big\} x(t) \\
& \leq -x^T(t) \left\{ \sum_{i=1}^r h_i^2[z(t)][C_i^T - K_i^T] \begin{bmatrix} W & 0 \\ 0 & R \end{bmatrix} \begin{bmatrix} C_i \\ -K_i \end{bmatrix} \right\} x(t) \\
& - x^T(t) \left\{ \sum_{i=1}^r \sum_{i < j} h_i[z(t)]h_j[z(t)][C_i^T - K_j^T] \begin{bmatrix} W & 0 \\ 0 & R \end{bmatrix} \begin{bmatrix} C_j \\ -K_i \end{bmatrix} \right\} + \\
& \sum_{i=1}^r \sum_{i < j} h_i[z(t)]h_j[z(t)][C_j^T - K_i^T] \begin{bmatrix} W & 0 \\ 0 & R \end{bmatrix} \begin{bmatrix} C_i \\ -K_j \end{bmatrix} \Big\} x(t) \\
& = -x^T(t) \left\{ \sum_{i=1}^r \sum_{j=1}^r h_i[z(t)]h_j[z(t)][C_i^T - K_i^T] \begin{bmatrix} W & 0 \\ 0 & R \end{bmatrix} \begin{bmatrix} C_j \\ -K_j \end{bmatrix} \right\} x(t) \\
& = -x^T(t) \left\{ \left(\sum_{i=1}^r h_i[z(t)][C_i^T - K_i^T] \begin{bmatrix} W & 0 \\ 0 & R \end{bmatrix} \right) \left(\sum_{i=1}^r h_i[z(t)] \begin{bmatrix} C_i \\ -K_i \end{bmatrix} \right) \right\} x(t) \\
& = -y^T(t) \begin{bmatrix} W & 0 \\ 0 & R \end{bmatrix} y(t)
\end{aligned}$$

therefore

$$\frac{d}{dt} x^T(t) P_1 x(t) < -\hat{y}^T(t) \begin{bmatrix} W & 0 \\ 0 & R \end{bmatrix} \hat{y}(t) \quad (5.34)$$

Integrating both sides, we get

$$J = \int_0^\infty \hat{y}^T(t) \begin{bmatrix} W & 0 \\ 0 & R \end{bmatrix} \hat{y}(t) dt < -x^T(t)P_1x(t) \Big|_0^\infty \quad (5.35)$$

since the fuzzy control system is stable,

$$J = \int_0^\infty \hat{y}^T(t) \begin{bmatrix} W & 0 \\ 0 & R \end{bmatrix} \hat{y}(t) dt < x^T(0)P_1x(0) \quad (5.36)$$

□

5.5 Fuzzy Controller Design

The fuzzy controller needs to address the problem of actuator amplitude constraint described by Eq. (5.9). The problem of actuator amplitude constraint has been addressed in the literature as a bounded norm problem on the magnitude of the control input, i.e., $\|u(t)\| \leq \mu$. See for instance Tanaka and Wang [49]. This condition gives a conservative control gain. In this section, we derive an individual actuator amplitude constraint in terms of LMI. Then, we cast the fuzzy controller design as an optimization problem. It should be noted that the actuator amplitude constraint is subject to the following constraints:

$$|u_k| \leq \mu_k, \quad (k = 1, 2, \dots, m). \quad (5.37)$$

The following theorem gives the conditions that need to be satisfied for the robust–optimal fuzzy control with amplitude saturation.

Theorem 5.5.1. *if $\exists P_1 > 0, P_2 > 0, \forall i, j = 1, 2, \dots, r, i < j \leq r, i \neq j \mid h_i \cap h_j \neq \emptyset$, the robust-optimal fuzzy PDC controller Eq. (5.8) which quadratically stabilizes Eq. (5.6) and satisfies the following constraints*

$$\|x(0)\| \leq \phi^2 \quad (5.38)$$

and

$$|u_k| \leq \mu_k, \quad (k = 1, 2, \dots, m) \quad (5.39)$$

can be found by minimizing the following augmented cost function

$$\min_{(\mu_1, \dots, \mu_k, \gamma_{a1}, \dots, \gamma_{ar}, \gamma_{b1}, \dots, \gamma_{br}, \phi)} J_a = \Lambda^T \Psi \Lambda \quad (5.40)$$

subject to :

$$S_{ii} < 0 \quad (5.41)$$

$$T_{ij} < 0 \quad (5.42)$$

$$U_{ii} < 0 \quad (5.43)$$

$$V_{ij} < 0 \quad (5.44)$$

$$A_i^T P_2 - C_i^T N_i^T + P_2 A_i - N_i C_i < 0 \quad (5.45)$$

$$A_i^T P_2 - C_j^T N_i^T + P_2 A_i - N_i C_j + A_j^T P_2 - C_i^T N_j^T + P_2 A_j - N_j C_i < 0 \quad (5.46)$$

$$\frac{1}{\mu_k^2} M_i^T D_k^T D_k M_i - X \leq 0 \quad (5.47)$$

$$X - \phi^2 I \geq 0 \quad (5.48)$$

where D_k is a $(1 \times m)$ zero row matrix in which the k^{th} element is 1, and Ψ is a weighting matrix. It should be noted that since $X = P^{-1}$ and $M_i = K_i P^{-1}$, then the matrices Λ , S_{ii} , T_{ij} , U_{ii} , and V_{ij} become [42]

$$\Lambda = [\mu_1, \dots, \mu_m, \gamma_{a1}, \dots, \gamma_{ar}, \gamma_{b1}, \dots, \gamma_{br}, \phi]^T, \quad (5.49)$$

$$S_{ii} = \begin{bmatrix} XA_i^T + A_iX - B_iM_i - M_i^T B_i^T & * & * & * & * \\ D_{ai}^T & -I & * & * & * \\ D_{bi}^T & 0 & -I & * & * \\ E_{ai}X & 0 & 0 & -\gamma_{ai}^2 I & * \\ -E_{bi}M_i & 0 & 0 & 0 & -\gamma_{bi}^2 I \end{bmatrix} \quad (5.50)$$

and

$$U_{ii} = \begin{bmatrix} XA_i^T + A_iX - B_iM_i - M_i^T B_i^T & * & * \\ C_iX & -W^{-1} & * \\ -M_i & 0 & -R^{-1} \end{bmatrix} \quad (5.51)$$

and

$$T_{ij} = \begin{bmatrix} T_{ij}(1,1) & * & * & * & * & * & * & * & * \\ D_{ai}^T & -I & * & * & * & * & * & * & * \\ D_{bi}^T & 0 & -I & * & * & * & * & * & * \\ D_{aj}^T & 0 & 0 & -I & * & * & * & * & * \\ D_{bj}^T & 0 & 0 & 0 & -I & * & * & * & * \\ E_{ai}X & 0 & 0 & 0 & 0 & -\gamma_{ai}^2 I & * & * & * \\ -E_{bi}M_j & 0 & 0 & 0 & 0 & 0 & -\gamma_{bi}^2 I & * & * \\ E_{aj}X & 0 & 0 & 0 & 0 & 0 & 0 & -\gamma_{aj}^2 I & * \\ -E_{bj}M_i & 0 & 0 & 0 & 0 & 0 & 0 & 0 & -\gamma_{bj}^2 I \end{bmatrix} \quad (5.52)$$

and

$$V_{ij} = \begin{bmatrix} V_{ij}(1,1) & * & * & * & * \\ C_i X & -W^{-1} & * & * & * \\ -M_j & 0 & -R^{-1} & * & * \\ C_j X & 0 & 0 & -W^{-1} & * \\ -M_i & 0 & 0 & 0 & -R^{-1} \end{bmatrix} \quad (5.53)$$

where

$$T_{ij}(1,1) = V_{ij}(1,1) = XA_i^T + A_iX - B_iM_j - M_j^T B_i^T + XA_j^T + A_jX - B_jM_i - M_i^T B_j^T \quad (5.54)$$

where $X = P_1^{-1}$, $M_i = K_i P_1^{-1}$, and $N_i = P_2 L_i$, then the feedback gains and the observer

gains can be obtained from the following equations, respectively.

$$K_i = M_i P_1^{-1}, \quad L_i = P_2^{-1} N_i, \quad (i = 1, 2, \dots, r). \quad (5.55)$$

Proof. To show the proof of Eqs. (5.47) and (5.48), let us start with Eq. (5.9), the individual actuator amplitude constraint, and rewrite it in the following form:

$$u_k^2(t) = u^T(t) D_k^T D_k u(t) \leq \mu_k^2, \quad (k = 1, 2, \dots, m) \quad (5.56)$$

Using Eq. (4.2), we get

$$u_k^2(t) = \sum_{i=1}^r \sum_{j=1}^r h_i[z(t)] h_j[z(t)] x^T(t) K_i^T D_k^T D_k K_j x(t) \leq \mu_k^2 \quad (5.57)$$

\Rightarrow

$$\frac{1}{\mu_k^2} \sum_{i=1}^r \sum_{j=1}^r h_i[z(t)] h_j[z(t)] x^T(t) K_i^T D_k^T D_k K_j x(t) \leq 1. \quad (5.58)$$

Using a quadratic Lyapunov function $V(x) = x(t)^T P_1 x(t)$, let us assume that

$$x^T(0) P_1 x(0) \leq 1; \quad \forall t > 0 \quad (5.59)$$

and

$$\frac{1}{\mu_k^2} \sum_{i=1}^r \sum_{j=1}^r h_i[z(t)] h_j[z(t)] x^T(t) K_i^T D_k^T D_k K_j x(t) \leq x^T(t) P_1 x(t) \quad (5.60)$$

therefore Eq. (5.58) will be satisfied. Let us rewrite Eq. (5.58) as

$$\sum_{i=1}^r \sum_{j=1}^r h_i[z(t)] h_j[z(t)] x^T(t) \left[\frac{1}{\mu_k^2} K_i^T D_k^T D_k K_j - P_1 \right] x(t) \leq 0. \quad (5.61)$$

Following a similar procedure in [49] and after some algebraic manipulation, we can show that

$$\frac{1}{\mu_k^2} K_i^T D_k^T D_k K_i - P_1 \leq 0 \quad (5.62)$$

or

$$\frac{1}{\mu_k^2} M_i^T D_k^T D_k M_i - X \leq 0 \quad (5.63)$$

which proves Eq. (5.47). Using Eq. (4.2.6), Eq. (5.9) can be written as

$$x^T(0) \left(P_1 - \frac{1}{\phi^2} I \right) x(0) \leq 0 \quad (5.64)$$

or

$$X - \phi^2 I \geq 0 \quad (5.65)$$

which completes the proof of Eq. (5.48). \square

The schematic diagram of the system is shown in Fig. (5.1). From the nonlinear model we obtain the matrices A_i , B_i , ΔA_i , ΔB_i , h_i , and y . The controller and observer gains are obtained from the LMI solver. Using the estimated states and the controller gains, the fuzzy control law u is used to stabilize the flexible spacecraft.

5.6 Numerical Simulation

We will use Matlab toolbox YALMIP [52] to solve Eqs. (5.40). YALMIP is a modeling language for solving convex optimization problems. To examine the performance of the closed-loop system, we use the same maneuver as in Fig. (2.2) which consists of a 45-degree antenna retargeting maneuver. We use the nominal values of the spacecraft parameters which are listed

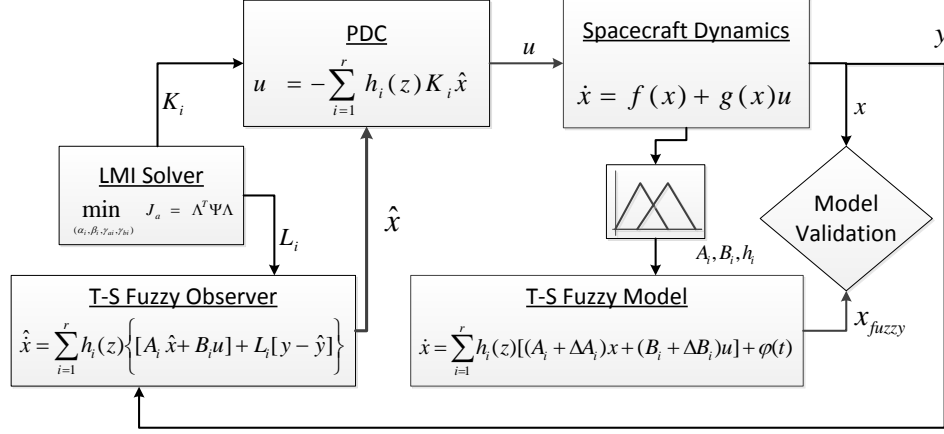


Fig. 5.1: Schematic diagram of the system.

in table 2.1.

The matrices in Eq. (5.19) are $W = 80 I_{16 \times 16}$, and $R = 0.01 I_{12 \times 12}$. The spacecraft has ten actuators; six on the platform for controlling the position and attitude along three body-axes, and four actuators in the middle and tip of the antenna in the x_a and y_a directions.

5.6.1 Sliding Mode Control Law

We compare the effectiveness of the T-S fuzzy controller with a sliding mode controller which we call a baseline controller. The baseline controller is designed based on Eqs. (2.30–2.33) which can be written as

$$\Sigma_{OL} : \begin{cases} \dot{x}_1 = x_2 \\ \dot{x}_2 = -M^{-1}(t)K(t)x_1 - M^{-1}(t)G(t)x_2 - M^{-1}(t)B^*(t)u(t) - M^{-1}(t)d(t) \end{cases} \quad (5.66)$$

where $x_1 = [R_0^T \theta^T q^T]^T$ and $x_2 = [V_0^T G \omega B^T \dot{q}^T]^T$. The equations of motion that describe the dynamic system in Eq. (5.66) are known as the regular form[53], the nonlinear feedback

control law that stabilizes the origin and constrains the motion of the system to the manifold

$$s = x_2 + \lambda x_1 \quad (5.67)$$

can be determined as

$$u_{SM} = (M^{-1}(t)B^*(t))^\dagger [-M^{-1}(t)K(t)x_1 - (M^{-1}(t)G(t) - \lambda)x_2] - \gamma(x) \text{sat}\left(\frac{s}{\epsilon}\right) \quad (5.68)$$

where λ and ϵ are real positive numbers and $\gamma(x)$ satisfies the following condition

$$\gamma(x) \geq \frac{\rho(x)}{1 - k_0} + \gamma_0 \quad \gamma_0 > 0, \quad k_0 \in [0 \ 1]. \quad (5.69)$$

It should be noted that a height slope saturation function $\text{sat}\left(\frac{s}{\epsilon}\right)$ is used in Eq. (5.68) to avoid issues associated with discontinuity and chattering.

5.6.2 Simulation for Nominal System

Figure (5.2) shows the displacement of the antenna tip in the y -direction for the open-loop and closed-loop systems without uncertainties.

It can be seen that the closed-loop of the system with T-S fuzzy controller and sliding mode controller are very close. Both controllers can stabilize the system and suppress the vibration in the antenna.

The time history of the Euler angle θ_x for the T-S fuzzy controller, sliding mode controller along with the estimated $\hat{\theta}$ are shown in Fig. (5.3). It can be seen that the sliding mode controller has faster response and slightly better performance than the T-S fuzzy controller.

In addition, we notice that the observed maximum relative error is on the order of 10^{-3} . The closed loop response of the position vector of the platform center-of-gravity is shown in Fig.

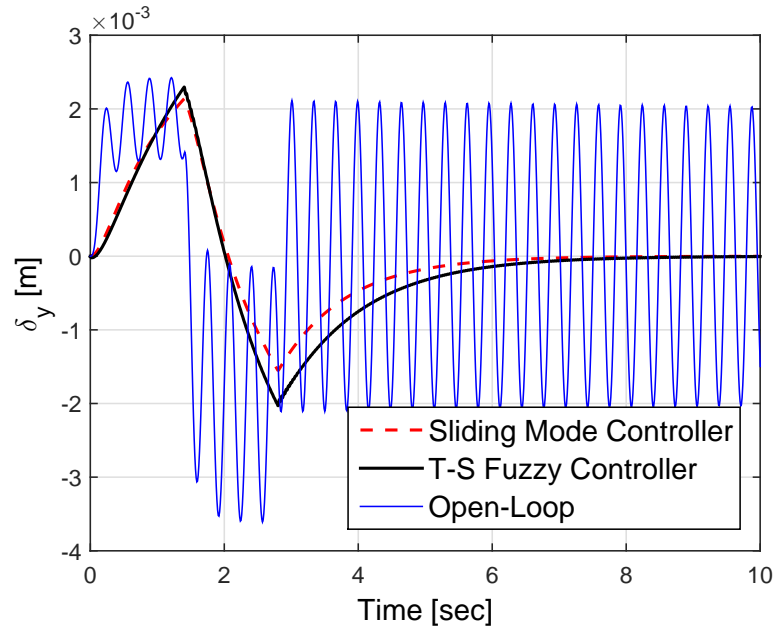


Fig. 5.2: Elastic displacement δ_y of the antenna in the y direction.

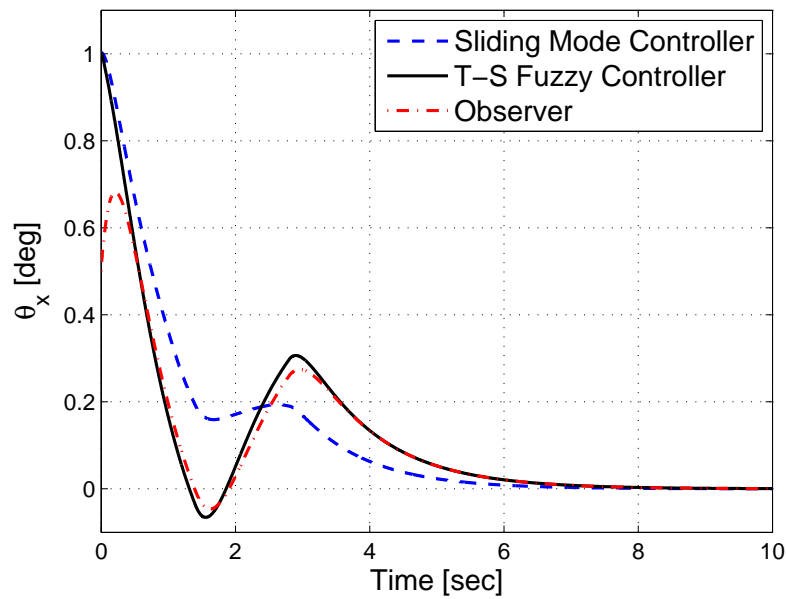


Fig. 5.3: Angular position of the rigid platform θ_x .

(5.4). It is clear that both controllers have very similar performance.

Figures (5.5) and (5.6) show the time history of the actuator amplitude $u_y = M_y \leq |\mu_5| =$

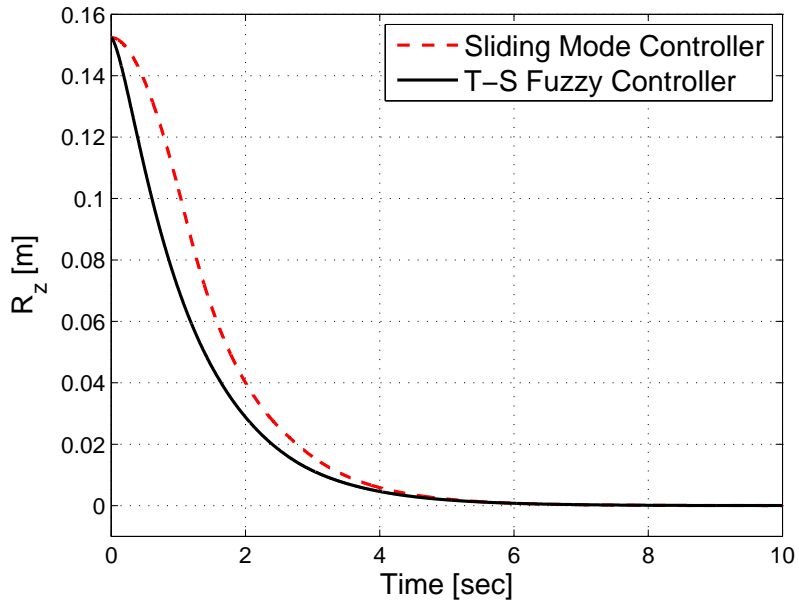


Fig. 5.4: Position of the platform center-of-gravity R_z .

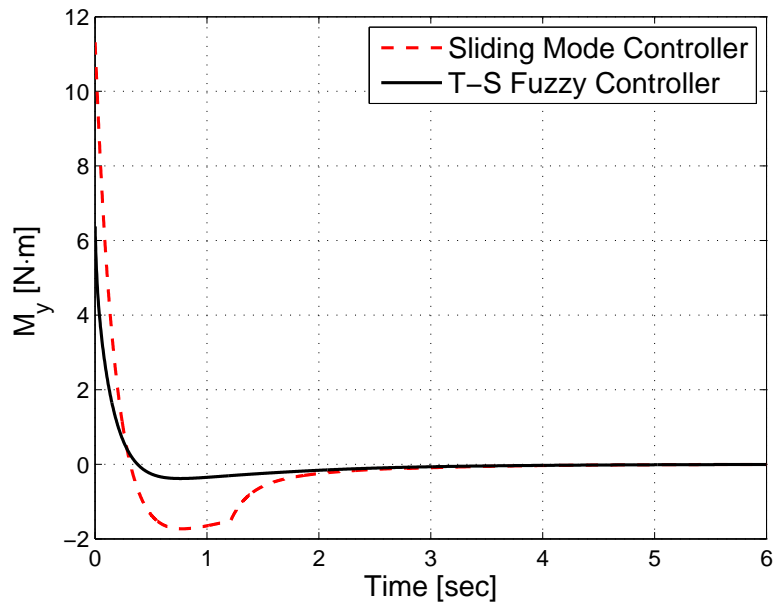


Fig. 5.5: Actuator moment M_y on the rigid platform.

$3.1029N.m$ and actuator force on the tip of the antenna $f_{2y} \leq |\mu_{11}| = 11.2303N$, where μ_5 and μ_{11} represent the upper bounds on the actuator amplitudes.

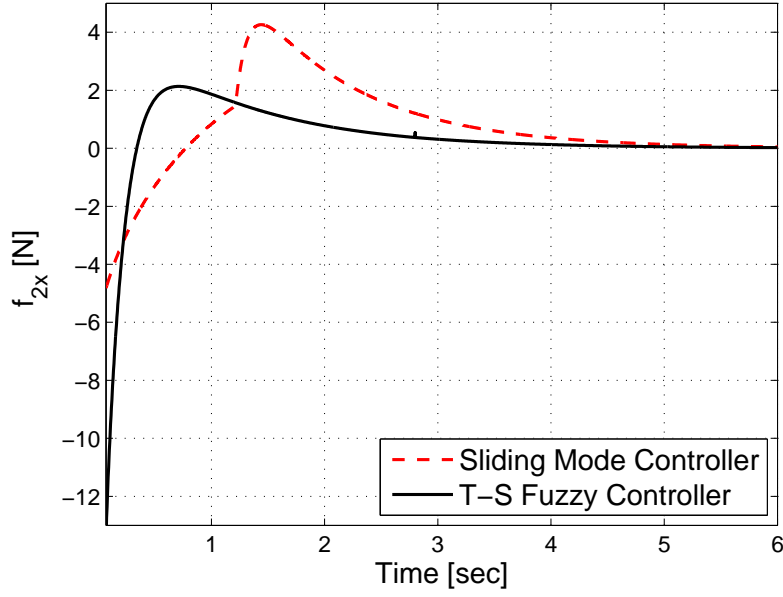


Fig. 5.6: Actuator force f_{2x} on the antenna tip in the x -direction.

5.6.3 Simulation for System With Uncertainty

As mentioned before, one of the advantages of a fuzzy controller is to cope with systems and actuators uncertainties. To examine the robustness of the proposed fuzzy controller-observer, we investigate the effect of uncertainties on the geometry, mass, and mass moment-of-inertia of the spacecraft. We simulate the closed-loop system with $l = 1.5 l^*$, $m = 0.9 m^*$, $m_p = 1.5 m_p^*$, $\mathbb{I}_p = 1.5 \mathbb{I}_p^*$, and $\mathbb{I} = 0.9 \mathbb{I}^*$ where superscript $*$ denotes the nominal values listed in 2.1.

To compare the results with a nominal case, the time history of U_y , θ_x , and R_z are shown in Figs. (5.7–5.9), respectively. The results shows the superiority of the T-S fuzzy over the sliding mode controller in the presence of uncertainties and disturbance in the system. It can be seen clearly in Fig. (5.8) that the baseline nonlinear controller fails to stabilize the system.

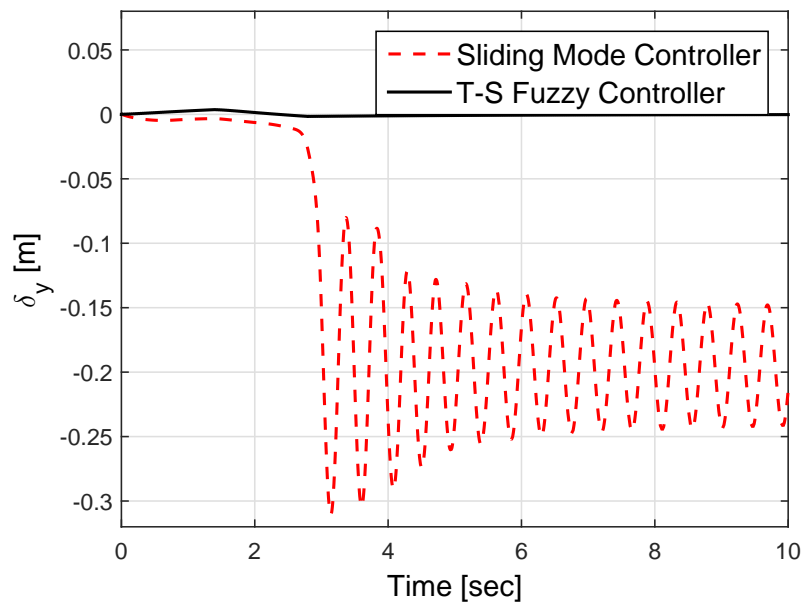


Fig. 5.7: Elastic displacement of the antenna δ_y in the y -direction for a system with uncertainties.

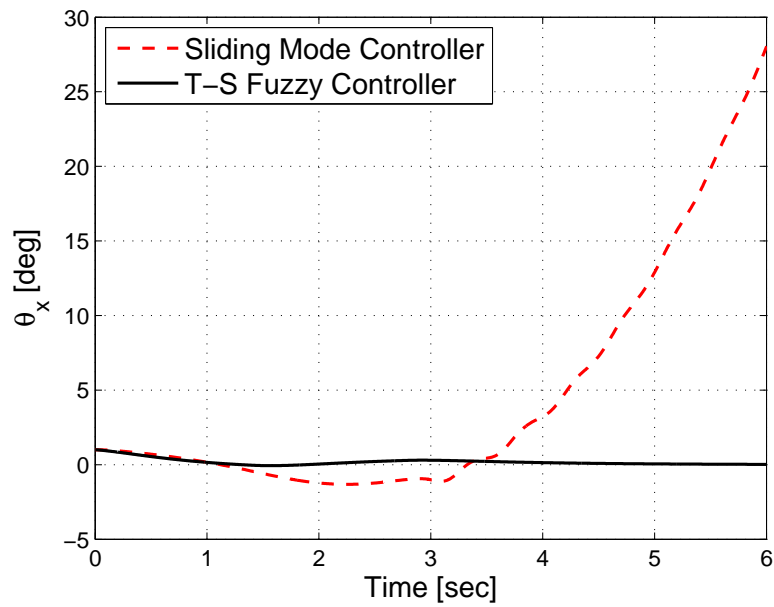


Fig. 5.8: Angular position of the rigid platform θ_x for a system with uncertainties.

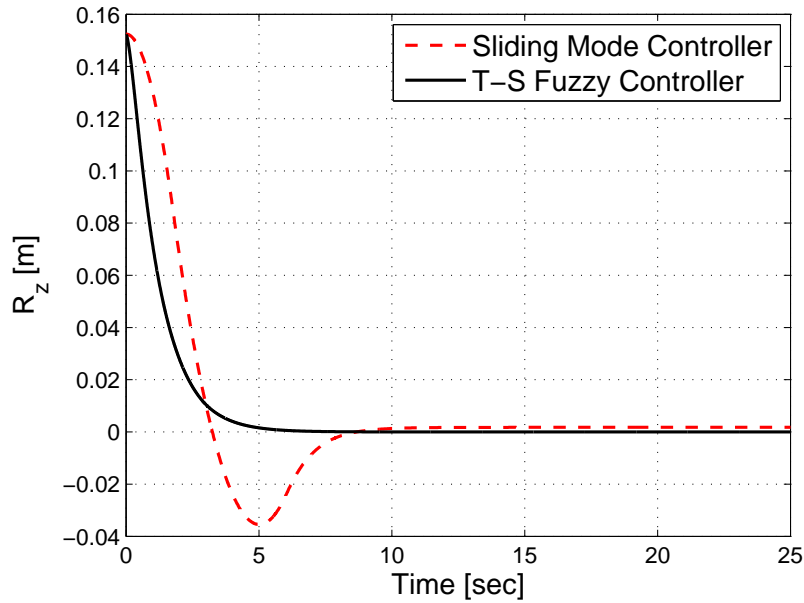


Fig. 5.9: Position of the platform center-of-gravity R_z for a system with uncertainties.

5.6.4 Higher Frequency Modes and Controller Performance

Theoretically, the mathematical model used to describe the dynamics of the flexible spacecraft has an infinite number of modes. To control the system completely, each mode would need to be considered in the feedback control scheme. Because it is not practical to include an infinite number of mode, the controller is designed based on the reduced model. The truncated model when used for control system design results in what is commonly referred to as controller spillover. It was demonstrated by Balas et al. [36], that even for a simple loop flexible beam, control spillover can cause closed-loop instability and increase the response time due to unmodeled higher frequencies. To check the performance of the fuzzy controller developed in the previous section, we used the same controller gains and modified the parameters of the spacecraft such as the flexure rigidity $EI = 1.5 EI^*$ and the length of the antenna $l = 0.8 l^*$ such that we excite higher mode frequency. Then we compare the results with the sliding mode controller. The simulation results are shown in Figs. (5.10–5.13)

It should be noted that we expected that the sliding mode controller will perform better since

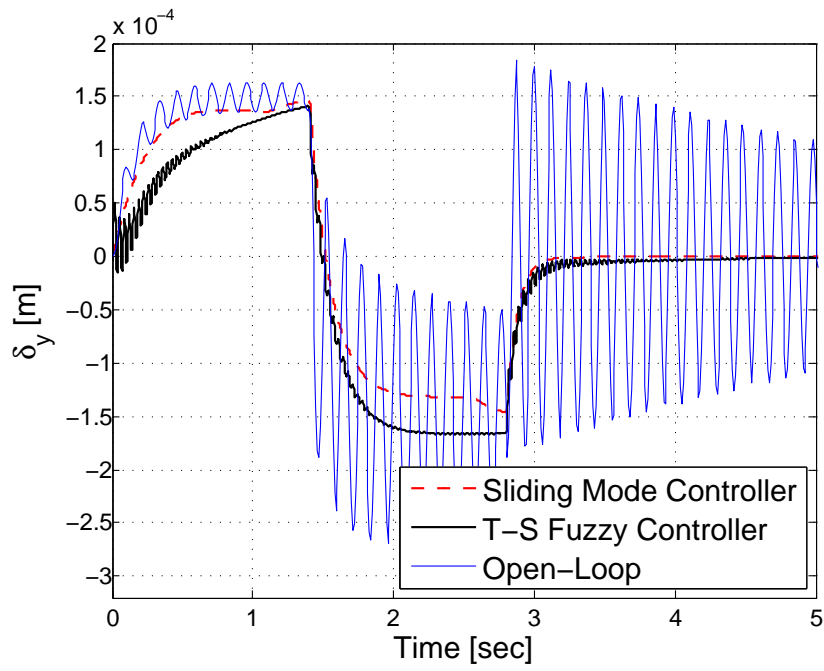


Fig. 5.10: Elastic displacement of the antenna δ_y in the y -direction for higher frequency mode.

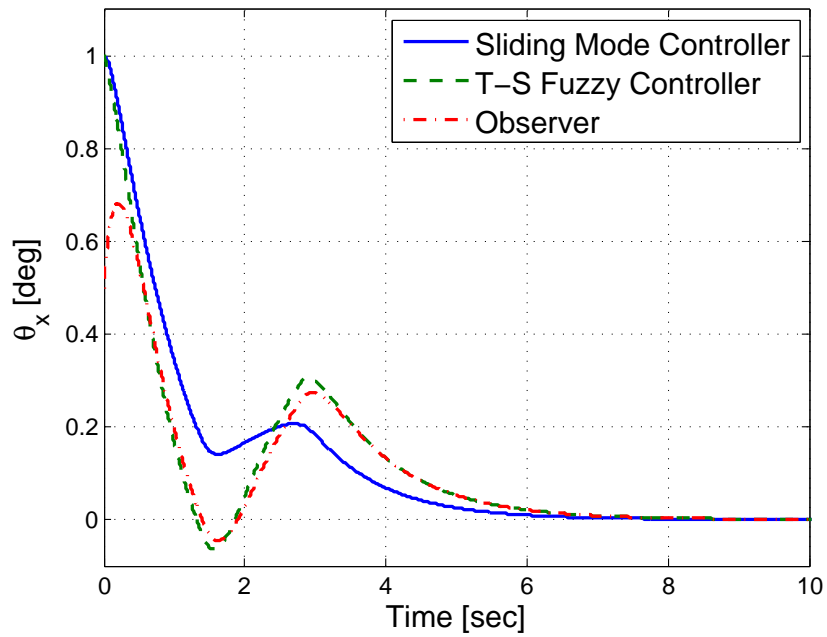


Fig. 5.11: Angular position of the rigid platform θ_x for a system with higher frequency mode.

the gains of the sliding mode controller are calculated in real time based on the modified model.

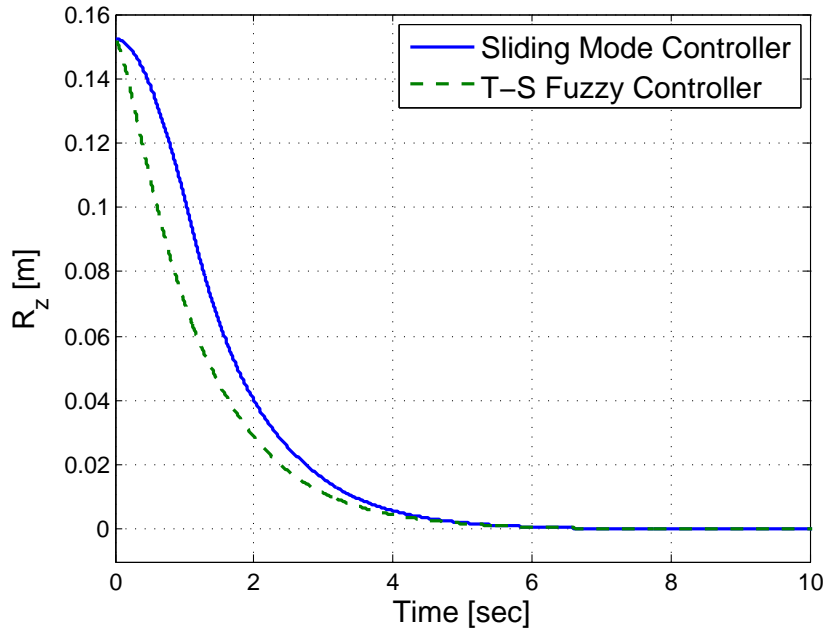


Fig. 5.12: Position of the platform center-of-gravity R_z for a system with higher frequency mode.

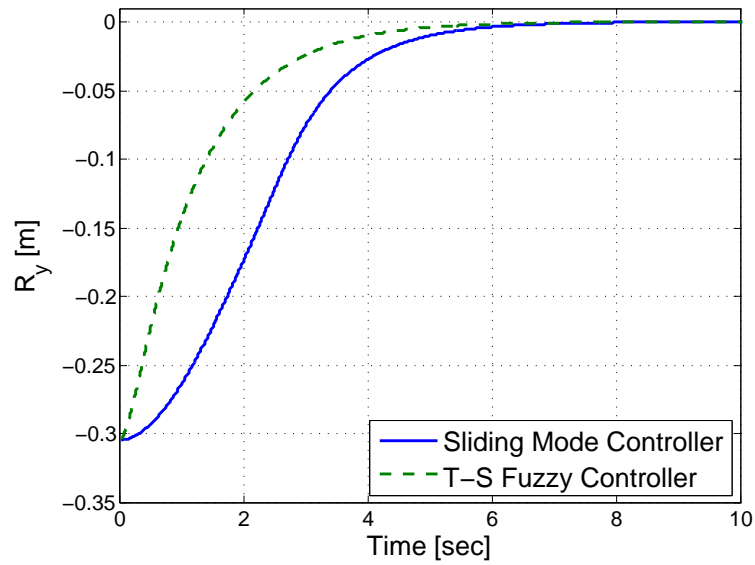


Fig. 5.13: Position of the platform center-of-gravity R_z for a system with higher frequency mode.

We notice that despite the higher modes being excited, the fuzzy controller was able to stabilize the platform and eliminate the vibration in the antenna. This shows that the fuzzy controller being used has a good performance and can cope with unmodeled dynamics, dis-

turbances and uncertainties.

CHAPTER 6

Robust Model-Reference Fuzzy Control

6.1 Introduction

In this chapter, a novel application of a robust fuzzy controller for the position and attitude stabilization of a flexible spacecraft is presented. The proposed controller follows a reference model to stabilize the position and the attitude, and to suppress the vibration in the flexible antenna during a retargeting antenna maneuver. The fuzzy controller is designed based on the Takagi-Sugeno (T-S) fuzzy model of the system. We use a full-order fuzzy observer to estimate the unavailable states and apply the parallel distributed compensation (PDC) control technique to stabilize quadratically the closed-loop system while the actuator amplitude constraints are enforced. The controller is robust to model uncertainties and disturbance. The fuzzy controller design process is cast into a convex optimization problem in the form of linear matrix inequalities (LMIs). Numerical simulations and comparison results with a non-linear baseline controller are provided to demonstrate the performance and the robustness of the proposed fuzzy controller.

6.2 Takagi-Sugeno (T-S) Fuzzy Modeling

Takagi-Sugeno fuzzy models allow describing nonlinear dynamical models by a set of linear time invariant (LTI) models interconnected by nonlinear functions. Each rule associates a LTI model as a concluding part to a weight function obtained from the premises. In this chapter,

we focused on the class of uncertain and disturbed T \check{A} SS fuzzy models described by Eq. (5.6). The bounded uncertainties and external disturbances are added, in a classical way, to each nominal LTI models.

$$\Sigma_{TS} : \begin{cases} \dot{x}(t) = \sum_{i=1}^r h_i[z(t)] \{ [A_i + \Delta A_i]x(t) + [B_i + \Delta B_i]u(t) \} + \varphi(t) \\ y(t) = \sum_{i=1}^r h_i[z(t)]C_i x(t) \end{cases} \quad (6.1)$$

where $A_i \in \mathbb{R}^{n \times n}$ is the nominal system matrix, $B_i \in \mathbb{R}^{n \times m}$ is the nominal control matrix, $x(t) \in \mathbb{R}^{n \times 1}$ is the state vector, $u(t) \in \mathbb{R}^{m \times 1}$ is the control input, and $\varphi(t) \in \mathbb{R}^{n \times 1}$ represents a disturbance term with a finite energy. The modeling of parameter uncertainty blocks satisfies the conditions stated in Eq. (5.2), and $\Delta A_i = H_i \Delta_a(t) E_{ai}$, and $\Delta B_i = H_i \Delta_b(t) E_{bi}$, respectively. In addition, we use a fuzzy observer to estimate the unavailable states. The fuzzy observer is based on the model without uncertainties as seen in Eq. (4.9).

$$\Sigma_{obs} : \begin{cases} \dot{\hat{x}}(t) = \sum_{i=1}^r h_i(z) \{ A_i \hat{x}(t) + B_i u(t) + L_i [y(t) - \hat{y}(t)] \} \\ \hat{y}(t) = \sum_{i=1}^r h_i(z) C_i \hat{x}(t) \end{cases} \quad (6.2)$$

where $L_i \in \mathbb{R}^{n \times s}$ is the observer gain, $y(t) \in \mathbb{R}^{s \times 1}$ is the measurable output, and $\hat{y}(t)$ is the estimated output vector.

6.3 Parallel Distributed Compensation (PDC) Control and H_∞ Performance

Consider the desired trajectory

$$\dot{x}_r(t) = A_r x_r(t) \quad (6.3)$$

where $x_r(t) \in \mathbb{R}^{n \times 1}$ is the reference state and $A_r \in \mathbb{R}^{n \times n}$ is a Hurwitz matrix. The attenuation of external disturbances is guaranteed using the H_∞ performance [54], and it is expressed as follows

$$\int_0^{t_f} [x_r(t) - x(t)]^T Q [x_r(t) - x(t)] dt \leq \eta^2 \int_0^{t_f} \varphi^T(t) \varphi(t) dt \quad (6.4)$$

where t_f is the final time, $Q = Q^T > 0$ is a positive definite matrix, and η is an attenuation level. The feedback control law is based on the Parallel Distributed Compensation (PDC) technique as

$$u_i(t) = -K_i[x_r(t) - \hat{x}(t)] \quad (i = 1, 2, \dots, r) \quad (6.5)$$

where $K_i \in \mathbb{R}^{m \times n}$ represents the feedback gain and $\hat{x}(t)$ denotes the state vector estimated by the fuzzy observer.

6.4 Output Feedback LMI Tracking Control

Let $\tilde{x}(t) = [e_0(t) \ e_p(t) \ x_r]^T$, where $e_0(t) = x(t) - \hat{x}(t)$ is the error between the states and the estimated states, and $e_p(t) = x(t) - x_r(t)$ is the error between the states and the reference model. Substituting Eq. (6.5) into Eq. (6.1), we obtain

$$\dot{\tilde{x}}(t) = \sum_{i=1}^r \sum_{j=1}^r h_i[z(t)] h_j[z(t)] \tilde{A}_{ij} \tilde{x}(t) + \tilde{S} \tilde{\Phi}(t) \quad (6.6)$$

where

$$\tilde{A}_{ij} = \begin{bmatrix} A_i - L_i C_j & \Delta A_i + \Delta B_i K_j & \Delta A_i \\ -B_i K_j - \Delta B_i K_j & A_i + B_i K_j + \Delta A_i + \Delta B_i K_j & A_j - A_r + \Delta A_i \\ 0 & 0 & A_r \end{bmatrix} \quad (6.7)$$

and

$$\tilde{S} = \begin{bmatrix} I & 0 \\ I & -I \\ 0 & I \end{bmatrix} \quad (6.8)$$

and

$$\tilde{\Phi}(t) = \begin{bmatrix} \varphi(t) \\ 0 \end{bmatrix} \quad (6.9)$$

with $\tilde{Q} = \text{diag}[0 \ Q \ 0]$, Eq. (6.4) can be transformed into the following

$$\int_0^{t_f} \tilde{x}^T(t) \tilde{Q} \tilde{x}(t) dt \leq \eta^2 \int_0^{t_f} \tilde{\Phi}^T(t) \tilde{\Phi}(t) dt \quad (6.10)$$

the stability condition of the closed-loop system described by Eq. (6.6) with H_∞ performance is stated in the following theorem:

Theorem 6.4.1 ([55]). $\forall t > 0$ and $h_i[z(t)]h_j[z(t)] \neq 0$, if \exists a matrix $\tilde{P} = \tilde{P}^T > 0$ and a constant $\eta > 0$ such that the following inequality are satisfied $\forall i, j = 1, 2, \dots, r$

$$\begin{cases} \Upsilon_{ii} < 0 \\ \frac{2}{r-1} \Upsilon_{ii} + \Upsilon_{ij} + \Upsilon_{ji} \leq 0 \end{cases} \quad i \neq j \quad (6.11)$$

where

$$\Upsilon_{ii} = \begin{bmatrix} \tilde{A}_{ij}^T \tilde{P} + \tilde{P} \tilde{A}_{ij} + \tilde{Q} & \tilde{P} \tilde{S} \\ \tilde{S}^T \tilde{P} & -\eta^2 I \end{bmatrix} \quad (6.12)$$

then, the asymptotic stability of the system Eq. (6.6) is guaranteed with H_∞ tracking control performance with an attenuation η

Proof. Using the Lyapunov function:

$$V[\tilde{x}(t)] = \tilde{x}^T(t) \tilde{P} \tilde{x}(t) \quad (6.13)$$

then

$$\dot{V}[\tilde{x}(t)] = \tilde{x}^T(t)\tilde{Q}\tilde{x}(t) - \eta^2\tilde{\Phi}^T(t)\tilde{\Phi}(t) \leq 0 \quad (6.14)$$

Equation (6.14) can be written as

$$\begin{aligned} \tilde{x}^T(t) \left[\sum_{i=1}^r \sum_{j=1}^r h_i[z(t)]h_j[z(t)](\tilde{A}_{ij}^T\tilde{P} + \tilde{P}\tilde{A}_{ij} + \tilde{Q}) \right] \tilde{x}(t) + \\ + \Phi^T(t)\tilde{S}^T\tilde{P}\tilde{x}(t) + \tilde{x}^T(t)\tilde{P}\tilde{S}\tilde{\Phi}(t) - \eta^2\tilde{\Phi}^T(t)\tilde{\Phi}(t) \leq 0. \end{aligned} \quad (6.15)$$

or

$$\begin{bmatrix} \tilde{x}(t) \\ \tilde{\Phi}(t) \end{bmatrix}^T \sum_{i=1}^r \sum_{j=1}^r h_i[z(t)]h_j[z(t)] \begin{bmatrix} \tilde{A}_{ij}^T\tilde{P} + \tilde{P}\tilde{A}_{ij} + \tilde{Q} & \tilde{P}\tilde{S} \\ \tilde{S}^T\tilde{P} & -\eta^2I \end{bmatrix} \begin{bmatrix} \tilde{x}(t) \\ \tilde{\Phi}(t) \end{bmatrix} \leq 0. \quad (6.16)$$

□

It was shown in [55] that Eq. (6.16) is satisfied if condition in Eq. (6.11) holds. To derive the LMI conditions, the following lemmas are needed

Lemma 6.4.2. [50] *for real matrices X, Y and $S = S^T > 0$ with appropriate dimensions and a positive constant γ , the following inequalities must hold:*

$$X^TY + Y^TX \leq \gamma X^TX + \gamma^{-1}Y^TY \quad (6.17)$$

and

$$X^TY + Y^TX \leq X^TS^{-1}X + Y^TSY. \quad (6.18)$$

Lemma 6.4.3. *For real matrices A, B, W, Y, Z and Q with appropriate dimensions then*

$$\begin{bmatrix} Y + B^TQ^{-1}b & W^T \\ W & Z + AQA^T \end{bmatrix} < 0 \Rightarrow \begin{bmatrix} Y & W^T + B^TA^T \\ W + AB & Z \end{bmatrix} < 0. \quad (6.19)$$

Proof. the proof of lemma (6.4.3) is as follows:

$$\begin{bmatrix} Y & W^T + B^T A^T \\ W + AB & Z \end{bmatrix} = \begin{bmatrix} Y & W^T \\ W & Z \end{bmatrix} \begin{bmatrix} 0 & B^T A^T \\ AB & 0 \end{bmatrix} < 0 \quad (6.20)$$

from inequality (6.18), $\exists Q$ such that

$$\begin{bmatrix} 0 \\ A \end{bmatrix} [B \ 0] + \begin{bmatrix} B^T \\ 0 \end{bmatrix} [0 \ A^T] \leq \begin{bmatrix} 0 \\ A \end{bmatrix} Q [0 \ A^T] + \begin{bmatrix} B^T \\ 0 \end{bmatrix} Q^{-1} [B \ 0] \quad (6.21)$$

□

Lemma 6.4.4. [56] let a matrix $\Omega < 0$, a matrix X with appropriate dimension such that $X^T \Omega X \leq 0$, and a scalar α , the following inequality holds:

$$X^T \Omega X \leq -\alpha(X^T + X) - \alpha^2 \Omega^{-1} \quad (6.22)$$

Proof. Since Ω is negative definite matrix, then if $X^T \Omega X \leq 0$, hence $\exists \alpha \in \mathbb{R}$ such that:

$$(X + \alpha \Omega^{-1})^T \Omega (X + \alpha \Omega^{-1}) \leq 0 \quad (6.23)$$

$$X^T \Omega X + \alpha(X^T + X) + \alpha^2 \Omega^{-1} \leq 0 \quad (6.24)$$

□

Theorem 6.4.5. $\forall i, j = 1, 2, \dots, r, i < j \leq r$, and $h_i[z(t)]h_j[z(t)] \neq 0$, if there $\exists P_1 = P_1^T > 0, P_2 = P_2^T > 0, P_3 = P_3^T > 0, Y_i, Z_i$, positive constants μ_n ; ($n = 1, \dots, 8$), and η ,

such that the following conditions are satisfied:

$$\begin{cases} \Upsilon_{ii} < 0 \\ \frac{2}{r-1}\Upsilon_{ii} + \Upsilon_{ij} + \Upsilon_{ji} \leq 0 \end{cases} \quad i \neq j \quad (6.25)$$

where

$$\Upsilon_{ij} = \left[\begin{array}{c|c} \Gamma_{ij} & (*) \\ \hline \begin{array}{c|c} -B_i Y_j & N \\ \hline 0_{8 \times 2} & 0_{8 \times 8} \end{array} & \Psi_{ij} \end{array} \right] \quad (6.26)$$

where

$$\Gamma_{ij} = \begin{bmatrix} -2\alpha N & 0 & (*) & (*) & (*) & 0 & 0 & 0 \\ 0 & -2\alpha N & 0 & 0 & 0 & 0 & 0 & (*) \\ E_{bi} Y_j & 0 & -\mu_1^{-1} I & 0 & 0 & 0 & 0 & 0 \\ E_{bi} Y_j & 0 & 0 & -\mu_5^{-1} I & 0 & 0 & 0 & 0 \\ \alpha I & 0 & 0 & 0 & \Gamma_{ij}(5,5) & (*) & (*) & P_1 \\ 0 & 0 & 0 & 0 & H_i^T P_1 & \Gamma_{ij}(6,6) & 0 & 0 \\ 0 & 0 & 0 & 0 & H_i^T P_1 & 0 & -\mu_4 I & 0 \\ 0 & \alpha I & 0 & 0 & P_1 & 0 & 0 & -\eta^2 I \end{bmatrix} \quad (6.27)$$

where

$$\Gamma_{ij}(5,5) = P_1 A_i - Z_i C_j + A_i^T P_1 - C_j^T Z_i$$

and

$$\Gamma_{ij}(6,6) = -(\mu_1^{-1} + \mu_2^{-1} + \mu_3^{-1})^{-1} I$$

and

$$\Psi_{ij} = \begin{bmatrix} \Psi_{ij}(1, 1) & (*) & (*) & (*) & (*) & (*) & (*) & 0 & (*) \\ N & -Q^{-1} & 0 & 0 & 0 & 0 & 0 & 0 & 0 \\ E_{bi}Y_j & 0 & -\mu_2^{-1}I & 0 & 0 & 0 & 0 & 0 & 0 \\ E_{bi}Y_j & 0 & 0 & -\mu_7^{-1}I & 0 & 0 & 0 & 0 & 0 \\ E_{ai}N & 0 & 0 & 0 & -\mu_3^{-1}I & 0 & 0 & 0 & 0 \\ E_{ai}N & 0 & 0 & 0 & 0 & -\mu_6^{-1}I & 0 & 0 & 0 \\ A_i^T - A_r^T & 0 & 0 & 0 & 0 & 0 & \Psi_{ij}(7, 7) & (*) & (*) \\ 0 & 0 & 0 & 0 & 0 & 0 & E_{ai} & -\mu_8^{-1} & 0 \\ -I & 0 & 0 & 0 & 0 & 0 & P_3 & 0 & -\eta^2 I \end{bmatrix} \quad (6.28)$$

where

$$\Psi_{ij}(1, 1) = A_i N + B_i Y_j + N^T A_i + Y_j B_i^T + (\mu_5^{-1} + \mu_6^{-1} + \mu_7^{-1} + \mu_8^{-1}) H_i H_i^T$$

and

$$\Psi_{ij}(7, 7) = A_r^T P_3 + P_3 A_r + \mu_4 E_{ai}^T E_{ai}$$

where $(*)$ in the LMI formulation indicates a transpose quantity in a symmetric matrix.

Proof. For a convenient design, we consider the following matrix $\tilde{P} = \text{diag}[P_1 \ P_2 \ P_3]$, then

Eq. (6.16) can be written as:

$$\sum_{i=1}^r \sum_{j=1}^r h_i[z(t)] h_j[z(t)] \left(\tilde{\Pi}_{ij} + \Delta \tilde{\Pi}_{ij} \right) \leq 0 \quad (6.29)$$

where

$$\tilde{\Pi}_{ij} = \begin{bmatrix} \begin{pmatrix} P_1(A_i - L_i C_i) \\ +(A_i - L_i C_i)^T P_1 \end{pmatrix} & * & 0 & * & 0 \\ -P_2 B_i & \begin{pmatrix} P_2(A_i + B_i K_j) \\ +(A_i + B_i K_j)^T P_2 + Q \end{pmatrix} & * & * & * \\ 0 & (A_i^T - A_r^T) P_2 & A_r^T P_3 + P_3 A_r & 0 & * \\ P_1 & P_2 & 0 & -\eta^2 I & 0 \\ 0 & -P_2 & P_3 & 0 & -\eta^2 I \end{bmatrix}$$

and

$$\Delta \tilde{\Pi}_{ij} = \begin{bmatrix} -P_1 \Delta B_i K_j - K_j^T \Delta B_i^T P_1 & * & * & 0 & 0 \\ \begin{pmatrix} -P_2 \Delta B_i K_j + K_j^T \Delta B_i^T P_1 \\ +\Delta A_i^T P_1 \end{pmatrix} & \begin{pmatrix} P_2(\Delta A_i + \Delta B_i K_j) \\ +(\Delta A_i + \Delta B_i K_j)^T P_2 + Q \end{pmatrix} & * & 0 & 0 \\ \Delta A_i^T P_1 & \Delta A_i^T P_2 & 0 & 0 & 0 \\ 0 & 0 & 0 & 0 & 0 \\ 0 & 0 & 0 & 0 & 0 \end{bmatrix}$$

Then using lemma 6.4.3 we get

$$\sum_{i=1}^r \sum_{j=1}^r h_i[z(t)] h_j[z(t)] \Delta \tilde{\Pi}_{ij} \leq \sum_{i=1}^r \sum_{j=1}^r h_i[z(t)] h_j[z(t)] \text{diag} \left[d_{1ij} \quad d_{2ij} \quad d_{3i} \quad 0 \quad 0 \right]$$

where

$$d_{1ij} = (\mu_1 + \mu_5) K_j^T E_{bi}^T E_{bi} K_j + (\mu_1^{-1} + \mu_2^{-1} + \mu_3^{-1} + \mu_4^{-1}) P_1 H_i H_i^T P_1$$

$$d_{2ij} = (\mu_2 + \mu_7) K_j^T E_{bi}^T E_{bi} K_j + (\mu_5^{-1} + \mu_6^{-1} + \mu_7^{-1} + \mu_8^{-1}) P_2 H_i H_i^T P_2 + (\mu_3 + \mu_6) E_{ai}^T E_{ai}$$

$$d_{3ij} = (\mu_4 + \mu_8) E_{ai}^T E_{ai}.$$

Then the inequality Eq. (6.29) will hold if:

$$\sum_{i=1}^r \sum_{j=1}^r h_i[z(t)]h_j[z(t)] \begin{bmatrix} \Theta_{ij}(1,1) & * & 0 & * & 0 \\ -P_2 B_i K_j & \Theta_{ij}(2,2) & * & * & * \\ 0 & (A_i^T - A_r^T)P_2 & \Theta_{ij}(3,3) & 0 & * \\ P_1 & P_2 & 0 & -\eta^2 I & 0 \\ 0 & -P_2 & P_3 & 0 & -\eta^2 I \end{bmatrix} \leq 0 \quad (6.30)$$

where

$$\Theta_{ij}(1,1) = P_1(A_i - L_i C_i) + (A_i - L_i C_i)^T P_1 + d_{1ij}$$

$$\Theta_{ij}(2,2) = P_2(A_i + B_i K_j) + (A_i + B_i K_j)^T P_2 + Q + d_{2ij}$$

$$\Theta_{ij}(3,3) = A_r^T P_3 + P_3 A_r + d_{3i}$$

Inequality Eq. (6.30) can rearranged as:

$$\sum_{i=1}^r \sum_{j=1}^r h_i[z(t)]h_j[z(t)] \begin{bmatrix} \Theta_{ij}(1,1) & * & 0 & * & 0 \\ P_1 & -\eta^2 I & * & 0 & 0 \\ -P_2 B_i K_j & P_2 & \Theta_{ij}(2,2) & * & * \\ 0 & 0 & (A_i^T - A_r^T)P_2 & \Theta_{ij}(3,3) & * \\ 0 & 0 & -P_2 & P_3 & -\eta^2 I \end{bmatrix} \leq 0 \quad (6.31)$$

Pre-post multiplying of the inequality Eq. (6.31) by $\text{diag} \begin{bmatrix} N & N & N & I & I \end{bmatrix}$, and let $N = P_2^{-1}$, $Y_i = K_i N$ and $Z_i = P_1 L_i$, we obtain:

$$\sum_{i=1}^r \sum_{j=1}^r h_i[z(t)]h_j[z(t)] \left[\begin{array}{c|c} \Sigma(1,1) & * \\ \hline \Sigma(2,1) & \Sigma(2,2) \end{array} \right] \leq 0 \quad (6.32)$$

where

$$\Sigma(1, 1) = \begin{bmatrix} N & 0 \\ 0 & N \end{bmatrix} \Omega_{1ij} \begin{bmatrix} N & 0 \\ 0 & N \end{bmatrix} + \begin{bmatrix} (\mu_1 + \mu_5)Y_j^T E_{bi}^T E_{bi} Y_j & 0 \\ 0 & 0 \end{bmatrix} \quad (6.33)$$

$$\Sigma(2, 1) = \begin{bmatrix} -B_i Y_j & N \\ 0 & 0 \\ 0 & 0 \end{bmatrix}$$

$$\Sigma(2, 2) = \begin{bmatrix} \Omega_{2ij} & * & * \\ A_i^T - A_r^T & A_r^T P_3 + P_3 A_r + d_{3i} & * \\ -I & P_3 & -\eta^2 I \end{bmatrix}$$

and

$$\Omega_{1ij} = \begin{bmatrix} P_1 A_i - Z_i C_j + A_i^T P_1 - C_j^T Z_i^T + (\mu_1^{-1} + \mu_2^{-1} + \mu_3^{-1} + \mu_4^{-1}) P_1 H_i H_i^T P_1 & P_1 \\ & P_1 \\ & & -\eta^2 I \end{bmatrix}$$

and

$$\begin{aligned} \Omega_{2ij} = & N A_i + B_i Y_j + A_i^T N + Y_j^T B_i^T + N Q N + (\mu_2 + \mu_7) Y_j^T E_{bi}^T E_{bi} Y_j \\ & + (\mu_5^{-1} + \mu_6^{-1} + \mu_7^{-1} + \mu_8^{-1}) H_i H_i^T P_2 + (\mu_3 + \mu_6) N E_{ai}^T E_{ai} \end{aligned}$$

Applying lemma 6.4.4 to Eq. (6.33) and using the Schur complement we obtain:

$$\begin{bmatrix} -2\alpha N + (\mu_1 + \mu_5)Y_j^T E_{bi}^T E_{bi} Y_i & 0 & * & 0 \\ 0 & -2\alpha N & 0 & * \\ \alpha I & 0 & \Xi_{ij}(3, 3) & * \\ 0 & \alpha I & P_1 & -\eta^2 I \end{bmatrix} \quad (6.34)$$

where

$$\Xi_{ij}(3, 3) = P_1 A_i - Z_i C_j + A_i^T P_1 - C_j^T Z_i^T + (\mu_1^{-1} + \mu_2^{-1} + \mu_3^{-1} + \mu_4^{-1}) P_1 H_i H_i^T P_1$$

substituting Eq. (6.34) into Eq. (6.32) we obtain the following:

$$\left[\begin{array}{cccc|ccc} H_{ij}(1, 1) & 0 & \alpha I & 0 & * & 0 & 0 \\ 0 & -2\alpha N & 0 & \alpha I & * & 0 & 0 \\ \alpha I & 0 & H_{ij}(3, 3) & P_1 & 0 & 0 & 0 \\ 0 & \alpha I & P_1 & -\eta^2 I & 0 & 0 & 0 \\ \hline -B_i Y_j & N & 0 & 0 & H_{ij}(5, 5) & * & * \\ 0 & 0 & 0 & 0 & A_i^T - A_r^T & H_{ij}(6, 6) & * \\ 0 & 0 & 0 & 0 & -I & P_3 & -\eta^2 I \end{array} \right] \quad (6.35)$$

Applying the Schur complement to the diagonal blocks, the conditions of theorem 6.4.5 hold

□

The design of a model-reference robust fuzzy controller that follows a reference input (6.3), satisfies H_∞ norm for a given attenuation level η , satisfies the actuators amplitude constraints [22] given by $|u_k| \leq \alpha_k$, ($k = 1, 2, \dots, m$) for an arbitrary bounded initial conditions $\|x(0)\| \leq \delta^2$, can be formulated in terms of linear matrix inequalities and cast as an optimization problem in the following form:

$$\min_{(\alpha_k, \eta)} J = \Lambda^T \Omega \Lambda. \quad (6.36)$$

Subject to :

$$\begin{cases} \Upsilon_{ii} < 0 \\ \frac{2}{r-1}\Upsilon_{ii} + \Upsilon_{ij} + \Upsilon_{ji} \leq 0 \\ \frac{1}{\alpha_k^2}Y_i^T D_k^T D_k Y_i - N \leq 0 \\ N - \delta^2 I \geq 0 \end{cases} \quad i \neq j. \quad (6.37)$$

The controller gains and observer gains are obtained as follows:

$$K_i = Y_i N^{-1} \quad (6.38)$$

$$L_i = P_1^{-1} Z_i \quad (6.39)$$

The design process of the fuzzy controller consists of the following steps:

1. Model the parameters of uncertainty Δa and Δb in Eq. (5.2), and generate the matrices H_i , E_{ai} and E_{bi} .
2. Choose a weighting matrix Ω in the cost function J Eq. (5.40) and the matrix Q in Eq. (6.4)
3. The values of μ_1 , μ_2 and μ_3 will be chosen arbitrarily [57] but they will be balanced by the computed values of μ_4 , μ_5 , μ_6 , μ_7 and μ_8 .
4. If a feasible solution exists, the matrices P_1 , Y_i , N , and Z_i can be computed by an optimization algorithm.
5. The controller and observer gains are computed using Eq. (6.38) and Eq. (6.39).

The schematic diagram of this process is shown in Fig. (6.1).

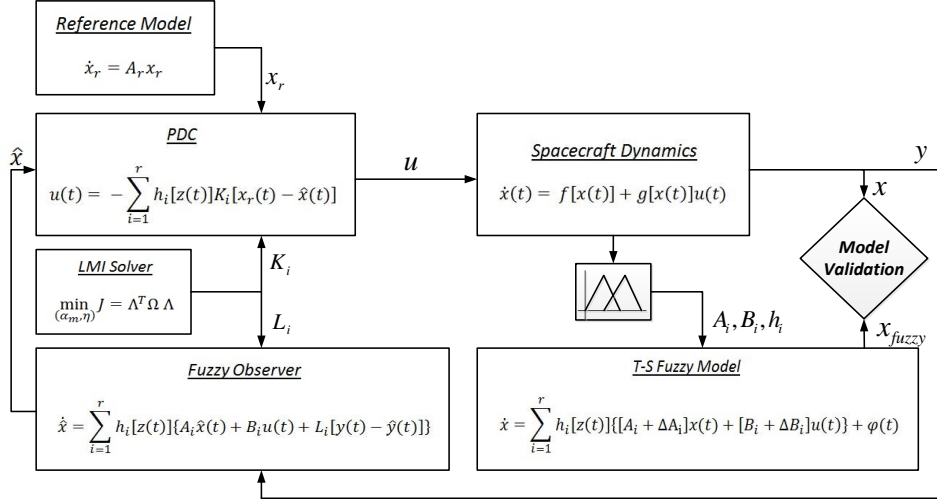


Fig. 6.1: Schematic diagram of the system.

6.5 Numerical Simulation

In this section, we present and compare the stability, performance and robustness of the proposed controller with the baseline controller. We use the Matlab toolbox YALMIP [52] to solve Eqs. (6.36). YALMIP is a modeling language for solving convex and non convex optimization problems. To examine the performance of the closed-loop system, we use a 45° antenna retargeting maneuver. The nominal values of the spacecraft parameters are listed in Table. 2.1.

The matrices in Eqs. (6.4,6.36) are $Q = 10^{-2}I_{16 \times 16}$ and $\Omega = \text{diag}[10^2 I_{6 \times 6} \ 10^{-2} I_{6 \times 6}]$, where I is the identity matrix. The spacecraft has ten actuators; six on the platform for controlling the position and attitude along three body-axes, and four actuators in the middle and tip of the antenna in the x_e and y_e directions.

6.5.1 Adaptive Control Law

To compare the performance of the T-S fuzzy controller, we choose the model-reference adaptive controller (MRAC) with σ modification as a baseline. σ modification is perhaps the simplest modification method that demonstrates the potential for improved robustness [58]. The σ modification is quite effective and yet simple to implement. Therefore, it is frequently used in adaptive control to ensure robustness.

The adaptive control law is designed based on Eqs. (2.30 – 2.33) which can be written as:

$$\dot{x}(t) = A(t)x(t) + B(t)[u(t) + \Theta^{*T}(t)\Phi(x)] \quad (6.40)$$

where $x(t) \in \mathbb{R}^{16 \times 1}$ is the state vector, $u(t) \in \mathbb{R}^{12 \times 1}$ is the control vector, $A(t) \in \mathbb{R}^{16 \times 16}$ is known, $B(t) \in \mathbb{R}^{16 \times 12}$ is also known, $\Theta^* \in \mathbb{R}^{16 \times 12}$ is the unknown parameter and $\Phi(x) = D(t)d(t)$ is a known, bounded function. The adaptive control law can be formulated as:

$$u(t) = K_x(t)x(t) - \Theta^T(t)\Phi(x) \quad (6.41)$$

where

$$\dot{\Theta}(t) = -\Gamma_{\Theta}[\Phi(x)e^T P B(t) + \sigma\Theta(t)] \quad (6.42)$$

and

$$K_x(t) = B^\dagger(t)[A_r(t) - A(t)] \quad (6.43)$$

where $e(t) = x_r(t) - x(t)$ is the tracking error, $\Gamma_{\Theta} = \Gamma_{\Theta}^T > 0 \in \mathbb{R}^{16 \times 16}$ is an adaptation rate matrix and $P = P^T > 0 \in \mathbb{R}^{16 \times 16}$ solves the Lyapunov equation $PA_r + A_r^T P = -Q$ where $Q = Q^T > 0$ is a positive definite matrix.

6.5.2 Simulation for Nominal System

We simulate the adaptive closed loop response with $Q = 0.1I_{16 \times 16}$, $\Gamma_{\Theta} = 10I_{16 \times 16}$ and $\sigma = 0.1$. Figure (6.2) shows the displacement of the antenna tip in the y_e -direction for the open-loop and closed-loop systems without uncertainties.

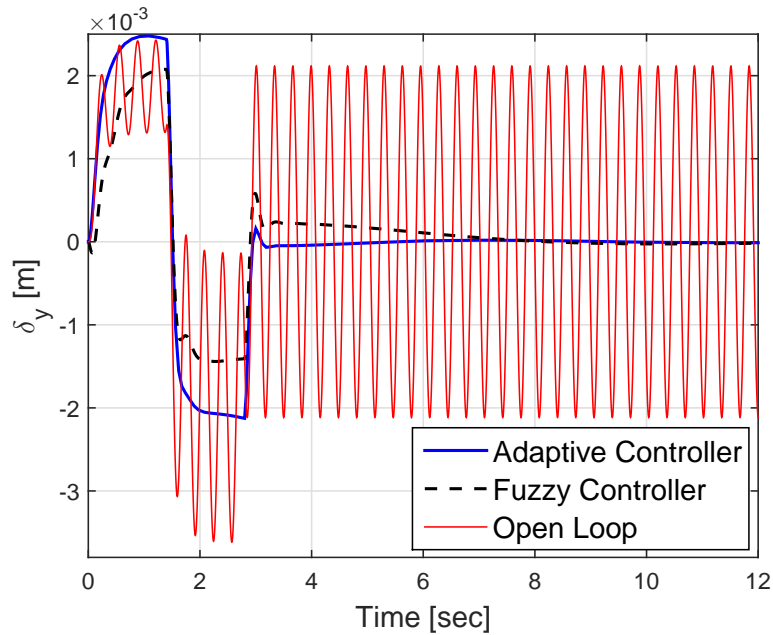


Fig. 6.2: Elastic displacement δ_y of the antenna tip in the y direction.

It can be seen that the settling time for the adaptive controller is slightly better than the fuzzy controller. However both controllers can stabilize the system and suppress the vibration in the antenna.

The time history of the Euler angles θ_x , θ_y , and θ_z , for the T-S fuzzy controller, adaptive controller, reference model along with the estimated $\hat{\theta}$ are shown in Figs. (6.3),(6.4) and (6.5)

It can be seen that the fuzzy controller has slightly better performance, it tracks closely the reference input, but the adaptive controller has faster response than the T-S fuzzy controller. In addition, we notice that the observer maximum relative error is on the order of 10^{-3} .

The closed loop response of the position vector of the platform center-of-gravity is shown

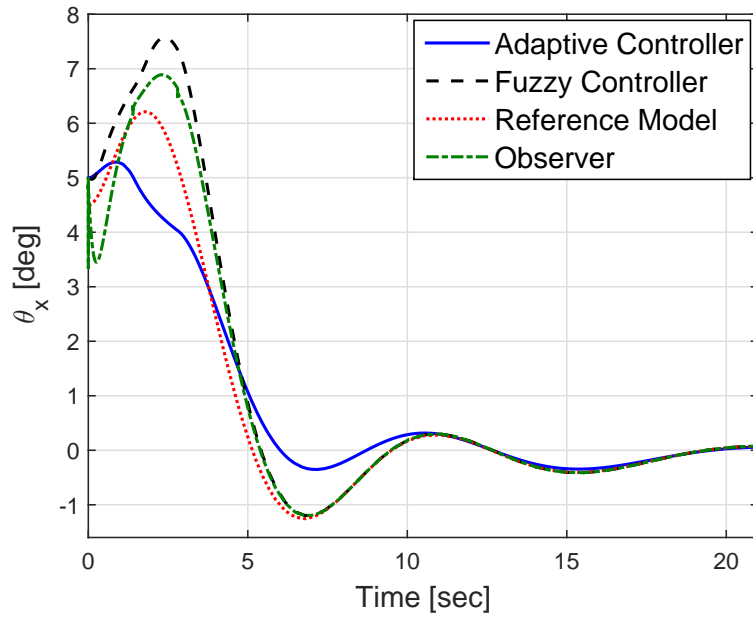


Fig. 6.3: Angular position of the rigid platform θ_x .

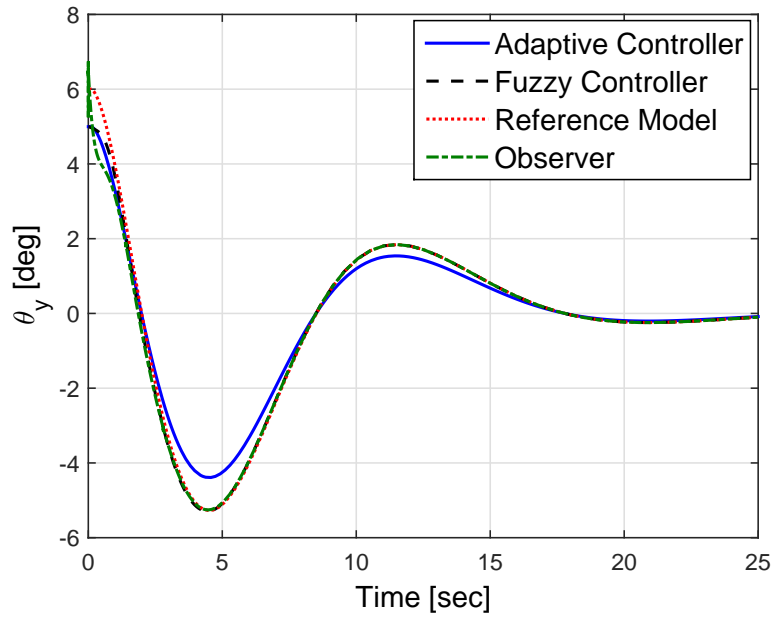


Fig. 6.4: Angular position of the rigid platform θ_y .

in Figs. (6.6), (6.7) and (6.8). It is clear that the fuzzy controller performs better than the adaptive controller.

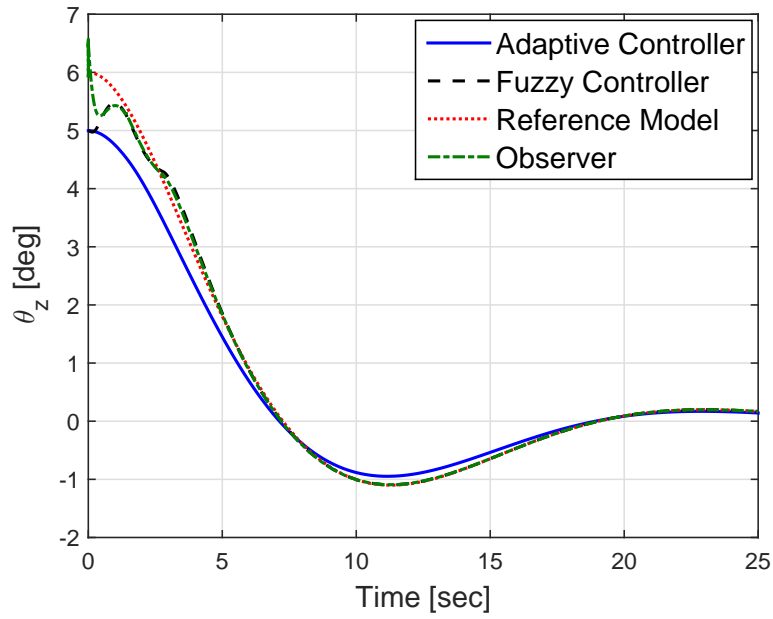


Fig. 6.5: Angular position of the rigid platform θ_z .

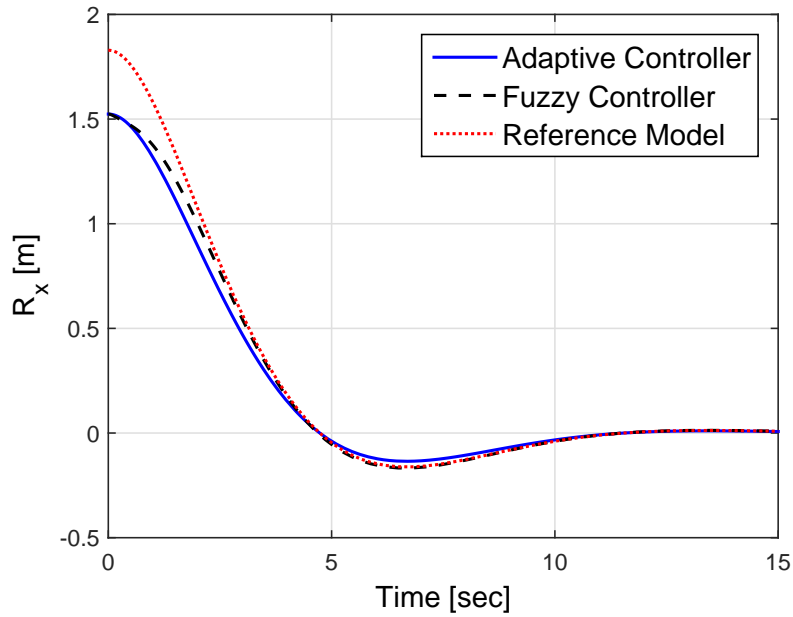


Fig. 6.6: Position of the rigid platform center-of-gravity R_x .

The forces and moments acting on the platform and the elastic antenna are shown in Figs. (6.9–6.12)

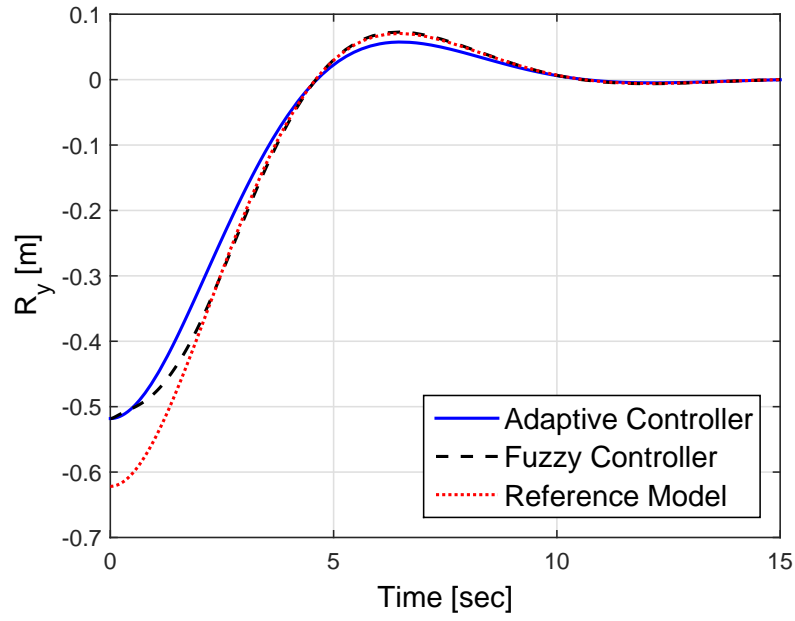


Fig. 6.7: Position of the rigid platform center-of-gravity R_y .

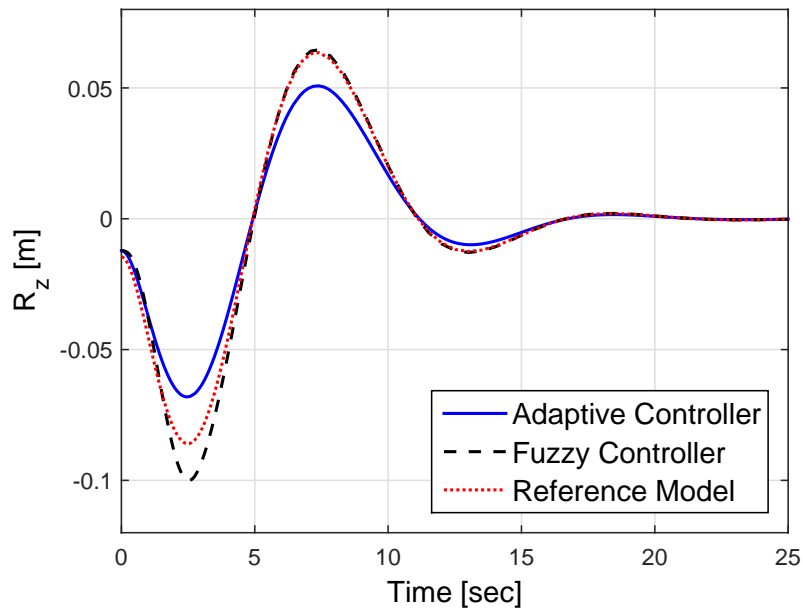


Fig. 6.8: Position of the rigid platform center-of-gravity R_z .

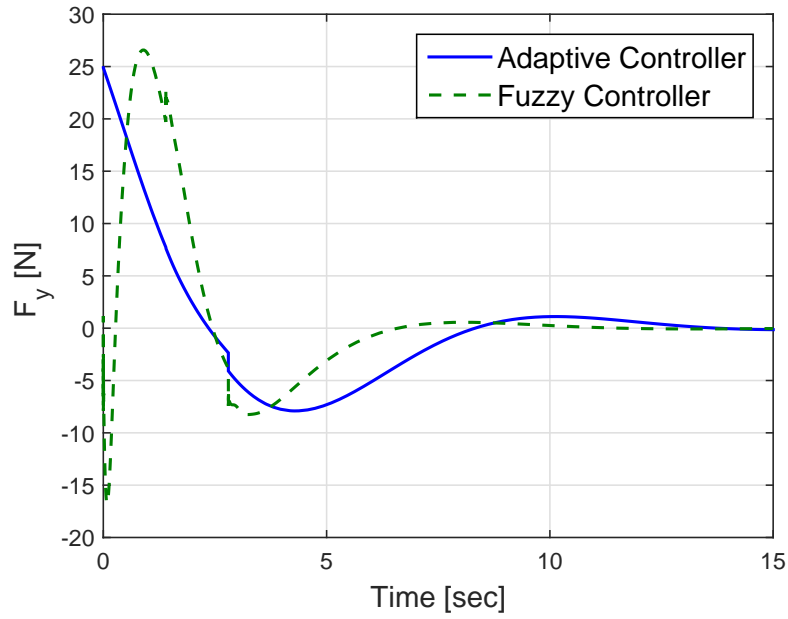


Fig. 6.9: Actuator force F_y on the rigid platform center-of-gravity.

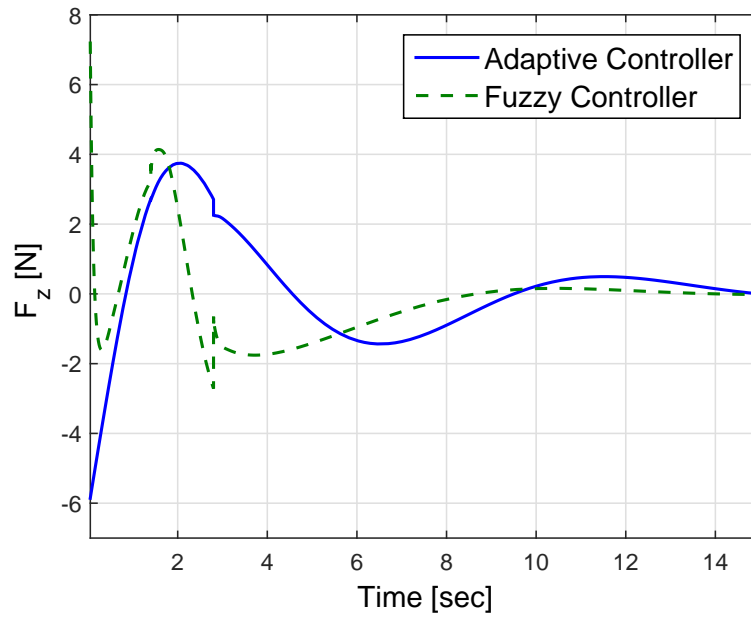


Fig. 6.10: Actuator force F_z on the rigid platform center-of-gravity.

6.5.3 Simulation for System With Uncertainty

As mentioned before, one of the advantages of a fuzzy controller is that it is able to cope with system and actuator uncertainties. To examine the robustness of the proposed fuzzy

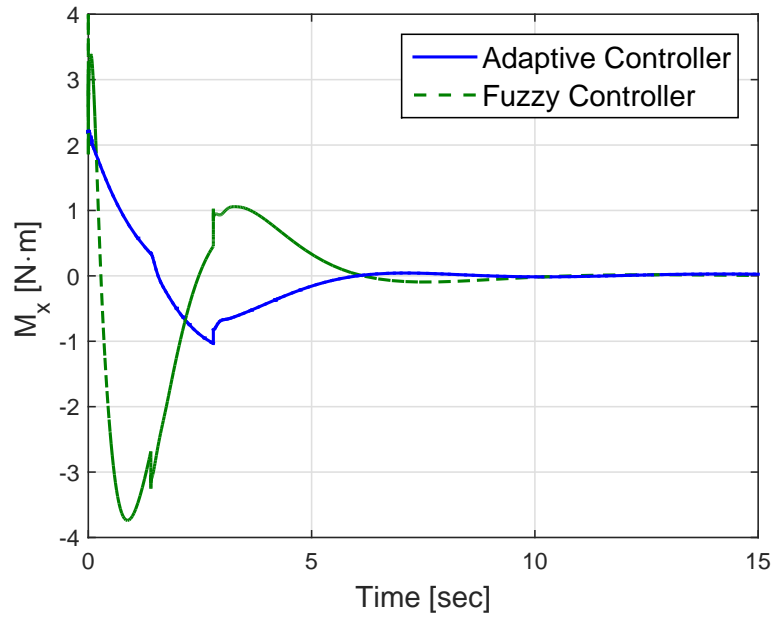


Fig. 6.11: Actuator moment M_x on the rigid platform center-of-gravity.

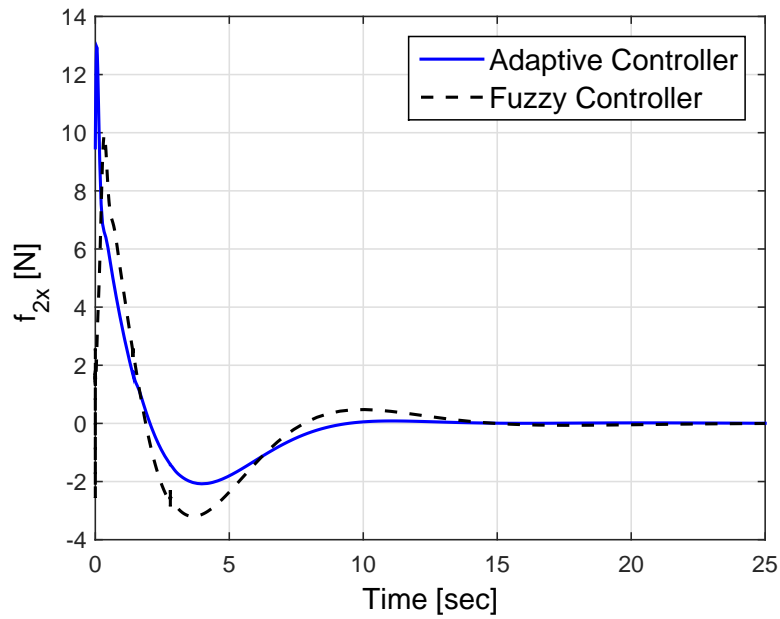


Fig. 6.12: Actuator force on the tip of the elastic antenna in the x direction.

controller-observer, we investigate the effect of uncertainties in the geometry, mass, and mass moment-of-inertia of the spacecraft. The parameters of the spacecraft with uncertainties are

listed in Table 2 where (*) indicate the nominal values of parameters as listed in Table. 6.1.

Table 6.1: Parameter of the Flexible Spacecraft with uncertainties

Parameters	Values
l	$1.35 l^*$
m	$0.65 m^*$
m_p	$1.35 m_p^*$
I_p	$1.35 I_p^*$
I	$0.65 I^*$

To compare the results with a nominal case, the time history of U_y , θ_x , and R_z are shown in Figs. (6.13 – 6.15) respectively.

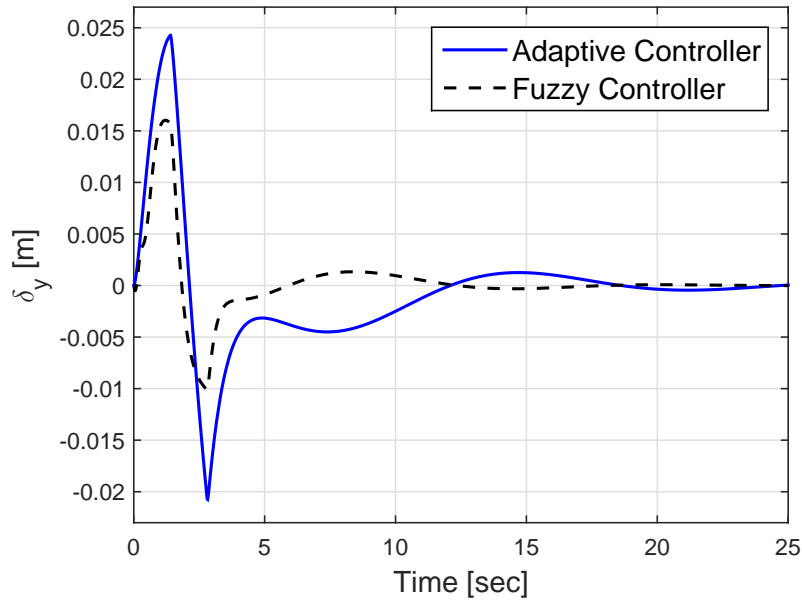


Fig. 6.13: Elastic displacement δ_y of the antenna tip in the y -direction for a system with uncertainties .

The results show the superiority of the T-S fuzzy controller over the adaptive controller in the presence of uncertainties and disturbance in the system. It can be seen clearly that the adaptive controller fails to track closely the reference input of the system.

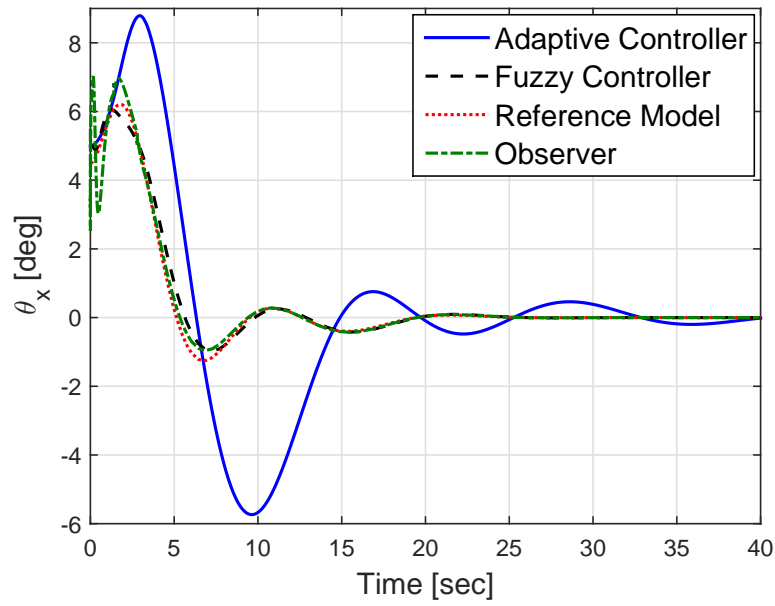


Fig. 6.14: Angular position θ_x of the rigid platform for a system with uncertainties.

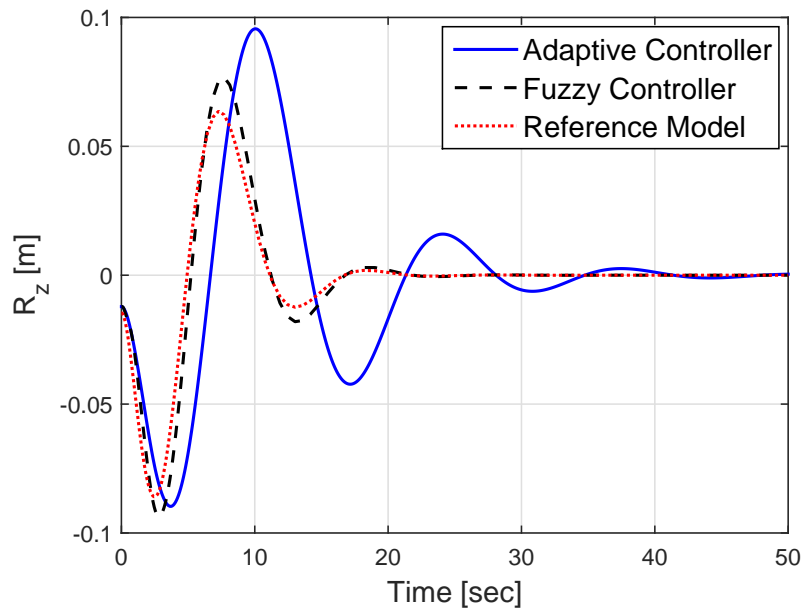


Fig. 6.15: Position of the platform center-of-gravity R_z for a system with uncertainties.

CHAPTER 7

Conclusions and Future Work

7.1 Conclusions

In this dissertation, we have studied the dynamics and control problems for a multibody flexible spacecraft made of a rigid platform and flexible appendages. The first objective was the development of a fuzzy control law for attitude stability and vibration suppression. The second objective was to demonstrate the superiority of the Takagi-Sugeno (T-S) fuzzy control over other nonlinear controller.

In Chapter 2, the equations of motion of multibody flexible spacecraft were developed based on a Lagrange technique in term of quasi-coordinate. The method of assumed mode was used, and it was shown that with five admissible functions, a good approximation can be reached to capture a higher order mode of vibration. Moreover it was shown that the dynamics of the system can be written in state space form for control purposes.

In Chapter 3, we introduced the Takagi-Sugeno (T-S) fuzzy modeling and control algorithm. Using a certain number of rules, the (T-S) fuzzy system can uniformly approximate any real continuous function and its derivatives to any degree of accuracy. Once the fuzzy model is validated, the parallel distributed compensator (PDC) approach provides a procedure to design a fuzzy controller from a given T-S fuzzy model. The general structure of the (PDC) is very simple and this simplicity gives the PDC a superiority for practical implementation. The feedback gains are obtained by mean of a linear matrix inequality (LMI) and the stability can be shown using the Lyapunov theories.

In Chapter 4, a (T-S) fuzzy model for a spacecraft with a flexible appendage such as a communication antenna was presented. The model is based on the weighted sum of local linear models. We use the full state-feedback stabilization combined with the H_∞ control techniques and design a nonlinear controller which is asymptotically stable. The input control constraint is considered in this design. The simulation results demonstrate the efficacy of the proposed PDC and the T-S fuzzy control model for attitude control and vibration suppression of the flexible spacecraft. The main advantage of PDC is its simple structure and consequently, ease of implementation.

In Chapter 5, we presented a robust-optimal T-S fuzzy model-based controller for position/attitude stabilization and vibration suppression of flexible spacecraft during a retargeting antenna maneuver. The proposed fuzzy controller is designed based on the Takagi-Sugeno fuzzy model of a spacecraft. The stability of the closed-loop system is guaranteed based on the Lyapunov stability theorem. The nonlinear optimal controller is robust to model uncertainties and has a disturbance rejection property. Furthermore, it satisfies the actuator amplitude constraint. Comparison of the T-S fuzzy control law with the sliding mode nonlinear control law, shows that the proposed controller is simple and therefore easier to implement. Numerical simulations and results demonstrate the stability, performance, robustness and the advantage of the proposed T-S fuzzy controller over the baseline sliding mode controller.

In Chapter 6, we presented a novel application of a robust model-reference fuzzy controller, to control the position and attitude of a flexible spacecraft consisting of a rigid platform and a flexible antenna during a minimum time retargeting antenna maneuver. The controller is designed based on the T-S fuzzy model of the flexible spacecraft and derived based on the parallel distributed compensator (PDC) technique. The main objective is its ability to track a reference input and to suppress the vibration while the actuator amplitudes are constrained and the H_∞ robustness criteria is guaranteed. A full-order fuzzy model-based observer was utilized to estimate the unavailable states. The proposed T-S fuzzy controller is simple, and

hence easy to implement. Numerical simulation shows the superiority of the proposed fuzzy controller in dealing with uncertainty and disturbances.

7.2 Future Work

Although it is beyond the scope of this dissertation project, several directions for future research to the work appear promising. These are:

- Actuator amplitude constraint on lower bounds: Due to fuel limitations and geometric design constraints, it is evident that all thrusters have finite upper bounds on the amount of force that they can provide. There is also a minimum nonzero force or impulse that imposes a lower bound on deliverable thrust. This means that arbitrarily small forces cannot be applied using thrusters. This limits the control precision that can be achieved, which can be critical during mission phases as docking or proximity operations.
- When implementing active control in large space structure, care must be taken to avoid spillover. to do so, a complete dynamic model of the flexible structure that includes the actuator dynamics and multiple appendages need to be developed. a) extending this work for control of multiple flexible appendage or antenna
- Building a physical experiment for validating the mathematical model and testing the performance, robustness, and stability of the developed controller on a physical system.
- extending the model and developing a new controller for large amplitude vibrations and highly flexible components
- extending this work for control of multiple flexible appendage or antenna with different physical characteristics.

APPENDIX A

A.1 Nomenclature

A_i	Nominal system matrix of the i^{th} fuzzy rule
B_i	Nominal control matrix of the i^{th} fuzzy rule
${}^A C^B$	Rotation matrix from the B -frame to the A -frame.
${}^G C^B$	Rotation matrix from the B -frame to the G -frame.
EI	Flexural rigidity of the antenna.
f_1	Actuator force components on the middle of the appendage
f_2	Actuator force vector on the tip of the appendage
F_p	Actuator force vector on the spacecraft platform.
I	Identity matrix.
\mathbb{I}	Moment of inertia of the antenna.
\mathbb{I}_p	Moment of inertia of the platform.
K_i	State-feedback gain of the i^{th} fuzzy rule
K	Stiffness matrix.
l	Antenna length.
L_i	Observer gain of the i^{th} fuzzy rule
$\hat{\mathcal{L}}_a$	Lagrangian density of the antenna.
m	Mass of the antenna.
M	Mass matrix.
m_p	Mass of the platform.

M_p	Actuator moment vector on the platform.
$OXYZ$	Cartesian coordinate system attached to the G -frame
xyz	Cartesian coordinate system attached to the B -frame
q	Generalized coordinate vector.
R	Position vector of a point on the appendage with respect to point O
R_o	Position vector of the the origin of the B -frame with respect to point O
R_Q	Position vector of an arbitrary point on the B -frame with respect to point O
r_Q	Position vector of a point in the spacecraft with respect to point O
r	Position vector of a point in the undeformed appendage with respect to its hinge point
r_o	Position vector of the appendage hinge point with respect to point O
$\hat{\mathcal{T}}_a$	Kinetic energy density of the antenna.
\hat{U}	Nonconservative force density.
V	Velocity vector of a point on the antenna.
V_Q	Velocity vector of an arbitrary point on the B -frame with respect to G -frame
V_o	Velocity vector of the the origin of the B -frame.
β	Input angular position command to the antenna.
δ	Deflection of the flexible antenna.
$\theta_x, \theta_y, \theta_z$	Euler angles.
Φ	Matrix of admissible functions.
$\omega_x, \omega_y, \omega_z$	Spacecraft angular velocity.
${}^G\omega^B$	Angular velocity of the platform.
${}^G\tilde{\omega}^B$	Skew-symmetric angular velocity matrix.
$\varphi(t)$	Disturbance vector
μ_i	Fuzzy membership function

A.2 Fuzzy Model Parameters, Controller and Observer gains

A.2.1 Fuzzy Model Parameters:

$$A_1 = \left[\begin{array}{c|cc|c} 0_{8 \times 6} & & 0_{8 \times 2} & I_{8 \times 8} \\ \hline & 2.46 & 0 & \\ & 0 & 2.42 & \\ & 0 & 0 & \\ 0_{8 \times 6} & 0 & -12.07 & \\ & 3.26 & 0 & \\ & 0 & 0 & \\ & -341.87 & 0 & \\ & 0 & -369.67 & \\ \hline & & & 0_{8 \times 8} \end{array} \right]$$

$$A_2 = \left[\begin{array}{c|cc|c} 0_{8 \times 6} & & 0_{8 \times 2} & I_{8 \times 8} \\ \hline & 2.46 & 0 & \\ & 0 & 1.85 & \\ & 0 & 1.57 & \\ 0_{8 \times 6} & 0 & -11.76 & \\ & 2.58 & 0 & \\ & 1.52 & 0 & \\ & -340.81 & 0 & \\ & 0 & -367.87 & \\ \hline & & & 0_{8 \times 8} \end{array} \right]$$

$$B_1 = \left[\begin{array}{c|cccccccccccc} & & & & & & & & & & & & & \\ \hline & & & & & & 0_{8 \times 12} & & & & & & & \\ 0.06 & 0 & 0 & 0 & 0 & 0 & 0.03 & 0 & 0 & 0.04 & 0 & 0 & & \\ 0 & 0.06 & 0 & 0 & 0 & 0 & 0 & 0.03 & 0 & 0 & 0.03 & 0 & & \\ 0 & 0 & 0.06 & 0 & 0 & 0 & 0 & 0 & 0.06 & 0 & 0 & 0.06 & & \\ 0 & 0 & 0 & 0.08 & 0 & 0 & 0 & 0.12 & 0 & 0 & 0.43 & 0 & & \\ 0 & 0 & 0 & 0 & 0.02 & 0 & 0.03 & 0 & 0 & 0.12 & 0 & 0 & & \\ 0 & 0 & 0 & 0 & 0 & 0.02 & 0 & 0 & 0 & 0 & 0 & 0 & & \\ 0.05 & 0 & 0 & 0 & 0.07 & 0 & 4.61 & 0 & 0 & 13.72 & 0 & 0 & & \\ 0 & 0.05 & 0 & 0.24 & 0 & 0 & 0 & 4.88 & 0 & 0 & 14.71 & 0 & & \\ \hline & & & & & & & & & & & & & \end{array} \right]$$

$$B_2 = \left[\begin{array}{c|cccccccccccc} & & & & & & & & & & & & & \\ \hline & & & & & & 0_{8 \times 12} & & & & & & & \\ 0.06 & 0 & 0 & 0 & 0 & 0 & 0.03 & 0 & 0 & 0.04 & 0 & 0 & & \\ 0 & 0.06 & 0 & 0 & 0 & 0 & 0 & 0.02 & 0.04 & 0 & 0.03 & 0.04 & & \\ 0 & 0 & 0.06 & 0 & 0 & 0 & 0 & 0.02 & 0.05 & 0 & 0.02 & 0.05 & & \\ 0 & 0 & 0 & 0.08 & 0 & 0 & 0 & 0.12 & 0.02 & 0 & 0.42 & 0.02 & & \\ 0 & 0 & 0 & 0 & 0.02 & 0 & 0.02 & 0 & 0 & 0.09 & 0 & 0 & & \\ 0 & 0 & 0 & 0 & 0 & 0.02 & 0.02 & 0 & 0 & 0.06 & 0 & 0 & & \\ 0.05 & 0 & 0 & 0 & 0.05 & 0.03 & 4.60 & 0 & 0 & 13.69 & 0 & 0 & & \\ 0 & 0.04 & 0.03 & 0.24 & 0 & 0 & 0 & 4.88 & 0.06 & 0 & 14.66 & 0.06 & & \\ \hline & & & & & & & & & & & & & \end{array} \right]$$

$$E_1 = \begin{bmatrix} 0.063865 & 0 & 0 & 0 & -0.000085 & 0 & -0.049738 & 0 \\ 0 & 0.063866 & 0 & 0.000312 & 0 & 0 & 0 & -0.049019 \\ 0 & 0 & 0.063492 & 0 & 0 & 0 & 0 & 0 \\ 0 & 0.000312 & 0 & 0.076467 & 0 & 0 & 0 & 0.24125 \\ -0.000085 & 0 & 0 & 0 & 0.0208 & 0 & -0.065623 & 0 \\ 0 & 0 & 0 & 0 & 0 & 0.016949 & 0 & 0 \\ -0.049738 & 0 & 0 & 0 & -0.065623 & 0 & 6.9129 & 0 \\ 0 & -0.049019 & 0 & 0.24125 & 0 & 0 & 0 & 7.467 \end{bmatrix}$$

$$E_2 = \begin{bmatrix} 0.0638 & 0 & 0 & 0 & -0.0001 & 0 & -0.0497 & 0 \\ 0 & 0.0637 & 0.0002 & 0.0003 & 0 & 0 & 0 & -0.0375 \\ 0 & 0.0002 & 0.0636 & 0 & 0 & 0 & 0 & -0.0317 \\ 0 & 0.000339 & 0.000039 & 0.076476 & 0 & 0 & 0 & 0.23581 \\ -0.00007 & 0 & 0 & 0 & 0.020809 & -0.000009 & -0.052077 & 0 \\ -0.00003 & 0 & 0 & 0 & -0.000009 & 0.016945 & -0.030665 & 0 \\ -0.04977 & 0 & 0 & 0 & -0.052077 & -0.030665 & 6.8917 & 0 \\ 0 & -0.037499 & -0.031734 & 0.23581 & 0 & 0 & 0 & 7.4329 \end{bmatrix}$$

A.2.2 Full State Feedback Fuzzy Controller Gains:

$$K_1^T = \begin{bmatrix} 3.72 & 0 & 0 & 0 & -0.15 & 0.02 & 2.27 & 0 & 0 & -0.42 & 0 & 0 \\ 0 & 3.39 & 0.48 & 1.07 & 0 & 0 & 0 & 1.48 & -1.52 & 0 & -0.49 & -1.52 \\ 0 & 0.58 & 2.81 & -0.44 & 0 & 0 & 0 & 1.43 & 1.68 & 0 & -0.48 & 1.68 \\ 0 & 0.49 & 0.06 & 2.92 & 0 & 0 & 0 & -0.47 & 0.48 & 0 & 0.11 & 0.48 \\ -0.91 & 0 & 0 & 0 & 5.53 & 0.12 & 1.20 & 0 & 0 & 0.19 & 0 & 0 \\ -0.15 & 0 & 0 & 0 & 0.21 & 5.57 & -0.05 & 0 & 0 & -0.73 & 0 & 0 \\ 0.81 & 0 & 0 & 0 & 0.47 & -0.07 & 0.37 & 0 & 0 & -0.90 & 0 & 0 \\ 0 & 1.53 & 1.19 & -24.69 & 0 & 0 & 0 & 7.25 & -6.35 & 0 & -1.90 & -6.35 \\ 7.70 & 0 & 0 & 0 & -0.72 & -0.02 & 4.57 & 0 & 0 & -0.85 & 0 & 0 \\ 0 & 7.00 & 1.13 & 2.09 & 0 & 0 & 0 & 3.13 & -3.05 & 0 & -1.04 & -3.05 \\ 0 & 1.27 & 5.36 & -0.97 & 0 & 0 & 0 & 2.84 & 3.07 & 0 & -0.94 & 3.07 \\ 0 & 1.16 & 0.05 & 9.05 & 0 & 0 & 0 & -1.67 & 1.60 & 0 & 0.41 & 1.60 \\ -3.17 & 0 & 0 & 0 & 17.42 & 0.74 & 3.61 & 0 & 0 & 0.61 & 0 & 0 \\ -0.60 & 0 & 0 & 0 & 1.04 & 18.16 & -0.12 & 0 & 0 & -2.33 & 0 & 0 \\ -0.03 & 0 & 0 & 0 & 0.04 & 0.17 & 0.51 & 0 & 0 & 1.50 & 0 & 0 \\ 0 & 0 & 0.01 & -0.21 & 0 & 0 & 0 & 0.53 & -0.04 & 0 & 1.39 & -0.04 \end{bmatrix}$$

$$K_2^T = \begin{bmatrix} 3.72 & 0 & 0 & 0 & -0.14 & -0.01 & 2.28 & 0 & 0 & -0.39 & 0 & 0 \\ 0 & 3.72 & 0.15 & 0.60 & 0 & 0 & 0 & 2.03 & 0.15 & 0 & -0.67 & 0.15 \\ 0 & 0.07 & 2.42 & 0.18 & 0 & 0 & 0 & -0.01 & 2.42 & 0 & 0 & 2.42 \\ 0 & 0.53 & -0.03 & 2.96 & 0 & 0 & 0 & -0.58 & -0.03 & 0 & 0.15 & -0.03 \\ -0.93 & 0 & 0 & 0 & 5.53 & 0.12 & 1.09 & 0 & 0 & -0.32 & 0 & 0 \\ -0.11 & 0 & 0 & 0 & 0.19 & 5.57 & 0.26 & 0 & 0 & 0.81 & 0 & 0 \\ 0.82 & 0 & 0 & 0 & 0.37 & 0.23 & 0.35 & 0 & 0 & -0.91 & 0 & 0 \\ 0 & 1.52 & 1.43 & -25.71 & 0 & 0 & 0 & 8.63 & 1.43 & 0 & -2.38 & 1.43 \\ 7.70 & 0 & 0 & 0 & -0.70 & -0.08 & 4.59 & 0 & 0 & -0.77 & 0 & 0 \\ 0 & 7.64 & 0.45 & 1.17 & 0 & 0 & 0 & 4.19 & 0.45 & 0 & -1.39 & 0.45 \\ 0 & 0.34 & 4.62 & 0.19 & 0 & 0 & 0 & 0.14 & 4.62 & 0 & -0.05 & 4.62 \\ 0 & 1.26 & -0.20 & 9.23 & 0 & 0 & 0 & -2.03 & -0.20 & 0 & 0.53 & -0.20 \\ -3.22 & 0 & 0 & 0 & 17.42 & 0.76 & 3.29 & 0 & 0 & -0.89 & 0 & 0 \\ -0.47 & 0 & 0 & 0 & 1.00 & 18.15 & 0.90 & 0 & 0 & 2.60 & 0 & 0 \\ -0.05 & 0 & 0 & 0 & 0.13 & -0.10 & 0.52 & 0 & 0 & 1.50 & 0 & 0 \\ 0 & -0.01 & 0.02 & -0.22 & 0 & 0 & 0 & 0.54 & 0.02 & 0 & 1.38 & 0.02 \end{bmatrix}$$

A.2.3 Robust-Optimal Fuzzy Controller and Observer Gains:

$$K_1^T = \begin{bmatrix} 784.17 & 0.23 & -0.05 & 0.02 & -26.28 & 2.19 & 458.01 & 0.11 & -0.07 & -151.55 & -0.07 & -0.07 & -90.89 & -154.05 & -90.89 \\ 0.25 & 802.25 & 87.72 & 54.83 & 0.02 & -0.01 & 0.15 & 470.96 & -90.89 & -0.06 & -154.05 & -90.89 & -90.89 & -154.05 & -90.89 \\ -0.12 & 90.10 & 649.63 & -32.99 & -0.01 & 0.00 & -0.07 & 175.37 & 437.70 & 0.03 & 47.00 & 437.70 & 437.70 & 47.00 & 437.70 \\ -0.01 & 62.88 & -32.46 & 890.99 & -0.00 & -0.00 & -0.01 & -215.61 & 34.30 & 0.00 & 128.35 & 34.30 & 34.30 & 128.35 & 34.30 \\ -93.24 & 0.01 & -0.00 & -0.00 & 866.83 & -77.43 & 184.72 & 0.01 & -0.01 & -87.12 & -0.00 & -0.01 & -0.01 & -87.12 & -0.00 \\ 2.82 & -0.01 & -0.00 & -0.00 & -96.32 & 1090.53 & 18.34 & -0.00 & -0.00 & 66.73 & 0.00 & -0.00 & -0.00 & 66.73 & 0.00 \\ 12.53 & -0.00 & 0.00 & 0.00 & -13.64 & 75.39 & 168.25 & 0.00 & 0.00 & 397.39 & 0.01 & 0.00 & 0.00 & 397.39 & 0.01 \\ -0.00 & 17.68 & -77.34 & 6.57 & 0.00 & 0.00 & -0.00 & 679.00 & -77.74 & 0.00 & 2304.22 & -77.74 & -77.74 & 2304.22 & -77.74 \\ 884.83 & 0.02 & 0.00 & 0.00 & -33.56 & 3.77 & 515.90 & 0.01 & -0.00 & -170.13 & -0.00 & -0.00 & -0.00 & -170.13 & -0.00 \\ 0.02 & 906.24 & 104.56 & 63.54 & 0.00 & -0.00 & 0.01 & 532.53 & -104.82 & -0.00 & -168.20 & -104.82 & -104.82 & -168.20 & -104.82 \\ 0.00 & 107.05 & 728.87 & -39.13 & 0.00 & -0.00 & 0.00 & 205.68 & 489.86 & -0.00 & 50.14 & 489.86 & 489.86 & 50.14 & 489.86 \\ 0.00 & 72.29 & -38.59 & 1006.82 & 0.00 & -0.00 & 0.00 & -242.71 & 39.40 & -0.00 & 144.48 & 39.40 & 39.40 & 144.48 & 39.40 \\ -119.26 & 0.00 & 0.00 & 0.00 & 1078.42 & -125.32 & 226.46 & 0.00 & 0.00 & -110.07 & 0.00 & 0.00 & 0.00 & -110.07 & 0.00 \\ 7.19 & -0.00 & -0.00 & -0.00 & -156.21 & 1490.66 & 22.95 & -0.00 & -0.00 & 101.37 & 0.00 & -0.00 & -0.00 & 101.37 & 0.00 \\ -7.46 & 0.00 & 0.00 & 0.00 & -36.22 & 94.59 & 174.27 & 0.00 & -0.00 & 467.48 & 0.00 & -0.00 & -0.00 & 467.48 & 0.00 \\ 0.00 & -4.68 & -102.17 & 28.99 & 0.00 & -0.00 & 0.00 & 760.85 & -88.46 & -0.00 & 2663.85 & -88.46 & -88.46 & 2663.85 & -88.46 \end{bmatrix}$$

$$K_1^T =$$

$$K_2^T = \begin{bmatrix} 784.20 & 0.23 & -0.05 & 0.02 & -26.07 & 2.09 & 457.58 & 0.10 & -0.11 & -152.88 & -0.05 & -0.11 & -204.68 & -95.51 & -204.68 \\ 0.25 & 829.64 & 55.49 & 43.51 & 0.02 & -0.02 & 0.15 & 468.21 & -204.68 & -0.05 & -95.51 & -204.68 & -204.68 & -95.51 & -204.68 \\ -0.12 & 51.02 & 618.48 & -20.15 & -0.01 & 0.00 & -0.07 & 186.49 & 397.26 & 0.02 & -125.36 & 397.26 & 397.26 & -125.36 & 397.26 \\ -0.01 & 47.50 & -10.13 & 896.93 & -0.00 & -0.00 & -0.01 & -208.87 & 85.14 & 0.00 & 119.22 & 85.14 & 85.14 & 119.22 & 85.14 \\ -93.83 & 0.01 & -0.00 & -0.00 & 869.34 & -81.40 & 202.17 & 0.01 & -0.01 & -41.42 & -0.00 & -0.01 & -0.01 & -41.42 & -0.00 \\ 4.60 & -0.01 & -0.00 & -0.00 & -96.50 & 1088.46 & -28.86 & -0.00 & 0.00 & -61.37 & 0.00 & 0.00 & 0.00 & -61.37 & 0.00 \\ 7.01 & -0.00 & 0.00 & 0.00 & 37.63 & -74.73 & 176.83 & 0.00 & 0.00 & 393.92 & 0.01 & 0.00 & 0.00 & 393.92 & 0.01 \\ -0.00 & -37.09 & 71.12 & 1.71 & 0.00 & 0.00 & -0.00 & 667.23 & 81.12 & 0.00 & 2275.01 & 81.12 & 81.12 & 2275.01 & 81.12 \\ 884.87 & 0.02 & 0.00 & 0.00 & -33.36 & 3.80 & 515.25 & 0.01 & -0.00 & -172.09 & -0.00 & -0.00 & -0.00 & -172.09 & -0.00 \\ 0.01 & 940.13 & 64.10 & 49.49 & 0.00 & -0.00 & 0.01 & 533.63 & -226.42 & -0.00 & -105.56 & -226.42 & -226.42 & -105.56 & -226.42 \\ 0.01 & 59.34 & 690.47 & -23.42 & 0.00 & -0.00 & 0.00 & 206.59 & 446.90 & -0.00 & -134.49 & 446.90 & 446.90 & -134.49 & 446.90 \\ 0.00 & 53.85 & -12.11 & 1013.95 & 0.00 & 0.00 & 0.00 & -236.85 & 94.07 & -0.00 & 135.30 & 94.07 & 94.07 & 135.30 & 94.07 \\ -120.08 & 0.00 & 0.00 & 0.00 & 1081.73 & -130.45 & 250.72 & 0.00 & -0.00 & -46.33 & 0.00 & -0.00 & -0.00 & -46.33 & 0.00 \\ 9.75 & -0.00 & -0.00 & -0.00 & -156.57 & 1487.69 & -47.31 & -0.00 & 0.00 & -90.24 & 0.00 & 0.00 & 0.00 & -90.24 & 0.00 \\ -14.46 & 0.00 & 0.00 & 0.00 & 28.71 & -95.80 & 185.03 & 0.00 & -0.00 & 462.94 & 0.00 & -0.00 & -0.00 & 462.94 & 0.00 \\ 0.00 & -69.20 & 72.80 & 23.84 & 0.00 & 0.00 & 0.00 & 747.06 & 94.11 & -0.00 & 2630.05 & 94.11 & 94.11 & 2630.05 & 94.11 \end{bmatrix}$$

$$K_2^T =$$

53.75	1.32	1.00	-1.56	-3.58	-0.85	-1.65	8.06	50.00	5.14	0.35	-14.00	0.41	-3.13	49.21	-453.08
-2.40	53.89	-1.59	0.93	-5.17	7.53	-4.78	-4.24	-14.27	49.99	-1.47	76.36	-18.85	2.99	1539.36	2208.02
7.05	5.12	53.14	-1.49	-2.26	4.75	-1.51	1.14	6.85	3.28	50.90	2.74	-1.50	-0.41	31.11	77.83
-5.28	-1.35	-1.11	53.102.58	-1.15	-1.93	0.02	-1.99	-0.81	4.85	-0.75	49.99	-1.43	6.07	32.01	-421.14
-11.16	9.35	0.23	4.32	53.21.68	4.89	-4.12	2.78	-19.38	17.27	-0.41	-56.04	49.08	-1.15	1969.48	-1841.21
3.57	3.74	2.50	-3.32	9.65	53.56.57	0.27	-1.52	4.93	5.17	4.91	-8.63	4.28	49.9	-370.51	-312.35
48.83	-25.98	-52.07	27.53	55.13	295.81	53.94	873	12.29	-256	-1083	-337	16.05	133	-17.22	411
2617.93	-5.68	-162	-100	127	-741	-1380	53	220	12.11	1794	-59	-697	1651	400	-18.41
50.85	0.76	7.34	1.11	8.15	-0.73	12.29	-0.38	53.75	0.63	0.54	-26.38	71.48	5.40	-7296	-741
6.07	49.34	-0.98	2.74	4.75	-0.72	3.52	12.	-5.23	53.8.46	-3.29	461.51	2.17	-9.65	659	1452
0.61	-6.23	50.29	0.89	-0.97	3.26	-0.20	7.57	-2.03	-4.34	53.01	-28.08	3.63	3.01	-484.18	-856
2.52	5.69	1.90	49.77	-0.02	-0.83	-2.65	-59.84	-2.35	384.93	-0.63	53.69	-1.22	-5.19	481	-5946
14.26	-4.65	-1.75	-4.60	50.07	-0.66	16.55	-10.96	-116.18	-13.57	-3.43	34.67	53.18	6.11	1750	1139
-6.10	-0.86	-2.06	3.82	-2.55	49.86	3.26	6.73	11.09	-5.30	5.27	-6.57	14.69	53.41	-1405	-79.50
-0.75	1.92	-3.56	-0.83	9.70	2.09	-17.81	5.63	-273	7.87	-3.95	-25.54	-359	-3.71	53.77	-938
5.01	8.83	6.13	-9.34	-6.91	2.32	-2.23	-18.41	-10.90	-536	2.09	264	-9.40	4.13	126	53.72

$L_1 =$

$$L_2 =$$

53.4	1.08	-2.26	-0.75	-3.94	0.22	-0.75	8.64	50.34	4.95	2.28	-13.84	4.06	-3.49	53.88	-450
-2.64	53.67	1.70	1.44	-8.58	4.34	-5.09	-3.31	-12.44	49.87	-10.95	71.76	-16.76	-1.59	153	219
3.78	8.40	53.75.55	-3.54	-8.34	-0.25	2.96	-0.07	1.38	2.87	50.14	1.19	-5.92	1.20	32.91	75
-4.47	-0.84	-3.16	53.75.3	-4.10	0.39	0.26	0.49	-1.03	3.20	-0.03	49.96	1.47	-1.54	32.15	-420
-11.52	5.94	-5.85	1.37	53.75	-3.04	-4.52	3.47	-16.39	16.76	8.03	-55.72	49.99	-10.98	196	-183
4.64	0.55	-2.50	-1.00	1.72	53.35	3.58	-0.74	1.24	-0.09	4.44	-11.62	2.26	50.55	-370	-310
57.18	-36.89	-52.11	25.73	56.43	305.85	53.74	869	12.30	-257.34	-108	-331	12.86	75.74	-16.68	402
2605.99	-3.63	-159.68	-91.05	131.75	-736.20	-1375.97	53.74	221	92.14	78.66	-58.93	-691.63	164	402	-18.7
50.43	2.60	1.88	0.90	11.15	-4.41	12.30	0.27	53.75	5.34	2.69	-23.03	-751	921	-727	-738
6.59	49.54	-1.51	1.73	7.10	-5.50	1.25	92.77	0.63	53.89	-61.66	800	-0.61	-7.78	658.03	120
0.60	-6.31	50.86	-0.18	-0.37	1.47	-3.20	78.57.98	-3.02	-2.23	53.23	-918	4.35	4.70	-482	201
2.35	2.70	0.40	49.52	-1.04	-4.05	-2.16	-58.35	0.46	784	-890	53.92	-1.93	-5.08	476	-692
17.81	-5.59	-6.24	-1.76	50.09	-1.94	12.66	-9.78	-769	-15.88	-6.62	32.19	53.59	4541	465	113
-6.22	1.41	-0.31	-3.65	-3.62	49.47	75.92	6.56	918	-0.63	5.18	-4.28	462	53.99	-372	-82.03
4.08	2.68	-1.66	-0.60	9.20	0.68	-16.98	4.18	-273.11	6.50	0.22	-28.38	597	-527	53.28	-930
5.38	5.86	4.44	-10.61	-6.40	2.28	-2.23	-18.32	-10.81	-6.45	-630	158	-5.42	-4.42	126	53.46

A.2.4 Robust Model-Reference Fuzzy Controller and Observer Gains:

$$A_r = \begin{bmatrix}
 -0.32 & 0 & 0 & 0.029 & -0.01 & 2.36 & 0 & -0.65 & 0 & 0 & 0.11 & -0.04 & 0.04 & 0 \\
 0 & -0.27 & -0.09 & 0 & 0 & 0 & 2.04 & 0 & -0.57 & -0.19 & 0 & 0 & 0 & 0.03 \\
 0 & 0.1 & -0.39 & 0 & 0 & 0 & 0.73 & 0 & 0.31 & -0.73 & 0 & 0 & 0 & 0.004 \\
 0 & -0.05 & 0.06 & 0 & 0 & 0 & -10.2 & 0 & -0.09 & 0.13 & 0 & 0 & 0 & -0.63 \\
 0.02 & 0 & 0 & -0.05 & -0.08 & 3.15 & 0 & 0.065 & 0 & 0 & -0.17 & -0.29 & 0.18 & 0 \\
 0 & 0 & 0 & -0.002 & -0.09 & 0.001 & 0 & 0.0003 & -0 & -0 & -0.0126 & -0.30 & -0.002 & 0 \\
 -4.53 & 0 & 0 & -7.87 & 10.22 & -33.1 & 0 & -9.06 & 0 & 0 & -23.96 & 32.5866 & -22.9762 & 0 \\
 0 & -0.13 & 0.14 & 0 & 0 & 0 & -370 & 0 & -0.20 & 0.29 & 0 & 0 & 0 & -22.93
 \end{bmatrix}$$

$$K_1 = \begin{bmatrix}
 167.52 & 250.03 & 277.37 & 370.00 & 2727.27 & -4234.84 & 10484.97 & 341.51 & 184.37 & -14.96 & -1.32 & 29.30 & 556 & -23 & 31 & 11 \\
 10.73 & 77.97 & -26.20 & -147.82 & 12.27 & 6.06 & 54.58 & 841.03 & 4.64 & -381.04 & -48 & 63 & 6.3 & 1.2 & 1.3 & -0.6 \\
 30.04 & -132.09 & -52.83 & 43.74 & 14.53 & -2.35 & -10.63 & -52.94 & 15.07 & -149.65 & -65 & 66 & 19 & -2.2 & 0.6 & -1.9 \\
 -18.51 & -174.87 & -3.34 & -176.00 & -20.92 & -13.92 & -28.53 & -347.61 & -2.28 & 71.17 & 24.24 & -259 & -3.3 & -1.1 & -0.6 & 6.5 \\
 173.41 & 98.52 & 108.34 & 151.92 & 546.04 & -2125.40 & 5125.20 & 147.13 & 204.77 & -7.7 & -0.4 & 13.8 & -478 & -46 & 9.6 & 5.4 \\
 -11.31 & -20.86 & -20.75 & -18.61 & -2.79 & -788.50 & 56.60 & -30.42 & 7.45 & -1.48 & -0.7 & 1.4 & -21 & -677 & 0.2 & 0.1 \\
 -627.95 & -397.81 & -432.30 & -572.87 & -4146.52 & 6402.40 & -15929.72 & -545.73 & -659.40 & 22.56 & 2.08 & -44 & -848 & 35 & -48 & -16.7 \\
 -35.47 & -538.94 & 24.34 & 219.70 & -34.42 & -20.66 & -94.40 & -1333.53 & -7.30 & 201.01 & 75 & -92 & -10.3 & -2.1 & -2.1 & -0.1 \\
 -19.33 & 60.08 & -113.80 & -28.54 & -13.00 & -3.13 & 3.34 & 23.27 & -7.52 & 74.71 & -91 & -33 & -9.6 & 0.7 & -0.3 & 0.9 \\
 212.09 & 134.85 & 146.56 & 194.27 & 1403.86 & -2173.89 & 5409.50 & 184.90 & 222.91 & -7.6 & -0.7 & 15 & 284 & -12 & 15 & 5.6 \\
 12.06 & 182.02 & -8.13 & -70.55 & 11.79 & 7.09 & 31.73 & 452.85 & 2.48 & -69.15 & -25 & 35 & 3.5 & 0.7 & 0.7 & -1.1 \\
 -19.33 & 60.08 & -113.80 & -28.54 & -13.00 & -3.13 & 3.34 & 23.27 & -7.52 & 74 & -91 & -33 & -9.6 & 0.7 & -0.3 & 0.9
 \end{bmatrix}$$

$$K_2 = \begin{bmatrix} 272.96 & 247.43 & 304.98 & 360.25 & -519.81 & 2824.14 & 12088.14 & 401.97 & 100.04 & 7.96 & 2.42 & 45 & 410 & 28 & 42 & 10 \\ -14.66 & 108.91 & -99.22 & -161.34 & -4.72 & 2.56 & 50.70 & 713.38 & -5.60 & -262.53 & -187 & 10 & -6.6 & 3.1 & 0.8 & 0.8 \\ 33.56 & 46.59 & -89.01 & -24.52 & 20.97 & 4.94 & 21.21 & 469.27 & 13.00 & -175.75 & -143 & 80.1 & 17.3 & 0.8 & 1.2 & -1.6 \\ -8.07 & -185.44 & 23.11 & -170.80 & -14.04 & -12.17 & -26.20 & -279.59 & 1.89 & 21 & 86 & -237 & 1.8 & -1.6 & -0.4 & 5.9 \\ 216.63 & 93.79 & 115.27 & 139.71 & -1038.07 & 1312.05 & 5686.20 & 200.18 & 156.61 & 3.2 & 1 & 20 & -541 & -31 & 15 & 5.2 \\ 10.53 & -5.69 & -5.79 & -2.16 & -48.23 & -652.49 & 584.69 & 8.18 & 21.09 & 1.32 & 0.12 & 3.1 & -6.2 & -712 & -1.2 & 0.5 \\ -787.14 & -393.16 & -474.12 & -557.59 & 770.23 & -4287.22 & -18352.95 & -621.76 & -531 & -12 & -3.7 & -68 & -627 & -45 & -65 & -16 \\ -37.78 & -506.39 & -80.95 & 197.92 & -37.56 & -23.86 & -83.70 & -1315 & -6.3 & 186 & 119 & -86 & -9.6 & -4.3 & -2.2 & -0.4 \\ -16.98 & 100.79 & -101.88 & -45.60 & -10.84 & -2.03 & 4.86 & 43 & -6.7 & 63 & -100 & -27 & -8.7 & 0.4 & -0.2 & 0.8 \\ 266.13 & 133.27 & 160.73 & 189.06 & -264.64 & 1453.58 & 6232.08 & 210.83 & 179 & 4.1 & 1.2 & 23 & 210 & 13 & 21 & 5.6 \\ 12.83 & 171.17 & 26.95 & -63.28 & 12.83 & 8.16 & 28.11 & 446.66 & 2.14 & -63 & -41 & 32 & 3.2 & 1.4 & 0.7 & -1 \\ -16.98 & 100.79 & -101.88 & -45.60 & -10.84 & -2.03 & 4.86 & 43.49 & -6.7 & 63.4 & -100 & -27 & -8.7 & 0.4 & -0.2 & 0.8 \end{bmatrix}$$

$K_2 =$

$$L_1 = \begin{bmatrix} 318.98 & 674.25 & 579.93 & 709.66 & 479.49 & 221.71 & 618.27 & 718.23 & 587.33 & 492.30 & 0.45 & -2424.35 & 753.56 & -0.26 & -79361.12 & -75038.07 \\ 649.66 & 1459.73 & 1017.02 & 1361.22 & 863.39 & 402.96 & 1087.41 & 1597.64 & 1028.72 & 1123.20 & 0.77 & -5528.08 & 1312.63 & -0.45 & -138239.06 & -171105.68 \\ 678.78 & 1273.64 & 1599.85 & 1708.73 & 1273.92 & 581.11 & 1697.46 & 1263.03 & 1618.36 & 807.18 & 1.81 & -3976.47 & 2095.87 & -0.71 & -220729.34 & -123076.51 \\ 761.79 & 1527.98 & 1582.66 & 1806.14 & 1283.11 & 589.06 & 1683.74 & 1577.64 & 1601.98 & 1050.13 & 1.27 & -5171.67 & 2066.57 & -0.70 & -217642.58 & -160086.90 \\ 548.00 & 1047.24 & 1249.80 & 1357.76 & 1001.65 & 457.00 & 1327.80 & 1050.52 & 1265.29 & 679.44 & 1.02 & -3346.94 & 1637.56 & -0.55 & -172409.67 & -103592.37 \\ 251.17 & 483.22 & 565.88 & 618.59 & 453.62 & 208.78 & 601.30 & 486.75 & 572.88 & 316.15 & 0.46 & -1557.34 & 740.93 & 0.25 & -78031.86 & -48201.70 \\ 720.30 & 1354.14 & 1690.60 & 1810.24 & 1347.94 & 614.98 & 1796.81 & 1344.54 & 1712.89 & 860.38 & 1.39 & -4238.50 & 2218.09 & -0.75 & -233601.32 & -131186.86 \\ 641.35 & 1488.86 & 898.54 & 1287.42 & 779.16 & 366.30 & 963.01 & 1658.57 & 908.61 & 1181.55 & 0.66 & -5817.45 & 1153.26 & -0.39 & -121453.71 & -180062.56 \\ 0.48 & -0.06 & -0.02 & -0.04 & -0.02 & -0.01 & 1.21 & -0.07 & 1.40 & -0.00 & -0.00 & -0.00 & -0.00 & 0.00 & 0.00 & 0.00 \\ -0.06 & 0.31 & 0.01 & -0.07 & -0.01 & -0.01 & 0.01 & 0.99 & -0.00 & 1.40 & -0.00 & -0.00 & 0.00 & -0.00 & -0.00 & -0.01 \\ -0.02 & 0.01 & 0.35 & -0.10 & -0.11 & -0.05 & -0.16 & 0.04 & -0.00 & -0.00 & 1.40 & 0.00 & 0.00 & -0.00 & -0.00 & 0.00 \\ -0.04 & -0.07 & -0.10 & 0.40 & -0.08 & -0.04 & -0.11 & -6.03 & 0.00 & -0.00 & 0.00 & 1.40 & 0.00 & -0.00 & -0.00 & -0.00 \\ -0.02 & -0.01 & -0.11 & -0.08 & 0.42 & -0.04 & 1.51 & 0.01 & 0.00 & 0.00 & -0.00 & 0.00 & 1.40 & 0.00 & -0.01 & 0.00 \\ -0.01 & -0.01 & -0.05 & -0.04 & -0.04 & 0.48 & -0.05 & 0.00 & 0.00 & -0.00 & -0.00 & 0.00 & 0.00 & 1.40 & -0.00 & 0.00 \\ -0.02 & 0.01 & -0.16 & -0.11 & -0.11 & -0.05 & -170.58 & 0.04 & 0.00 & 0.00 & 0.00 & -0.00 & 0.00 & 0.00 & 1.40 & -0.01 \\ -0.07 & -0.22 & 0.04 & -0.06 & 0.01 & 0.00 & 0.04 & -184.39 & 0.00 & 0.00 & -0.00 & -0.00 & -0.00 & 0.00 & 0.00 & 1.38 \end{bmatrix}$$

$L_1 =$

267.37	475.90	666.53	690.96	527.10	239.71	707.75	462.68	587.62	376.06	319.87	-2369.53	597.55	352.33	-79118.12	-74695.61
538.98	1060.12	1148.02	1291.88	927.49	425.22	1221.67	1091.41	1029.19	858.15	729.09	-5403.09	1040.86	613.71	-137815.80	-170324.76
579.31	836.63	1882.79	1734.61	1446.21	650.48	1992.13	681.75	1619.23	616.50	525.75	-3886.53	1661.99	979.97	-220053.47	-122514.84
643.78	1045.21	1842.61	1796.41	1434.95	648.73	1953.57	945.92	1602.80	802.12	682.73	-5054.70	1638.74	966.26	-216976.17	-159356.31
466.47	695.90	1467.14	1371.19	1132.75	509.50	1553.97	585.22	1265.96	518.95	442.01	-3271.24	1298.66	765.44	-171881.75	-103119.61
213.59	322.45	663.60	623.47	512.35	232.25	702.96	274.17	573.18	241.47	205.65	-1522.11	587.54	346.94	-77792.93	-47981.72
614.58	890.61	1989.32	1836.67	1529.67	688.11	2107.88	728.25	1713.81	657.13	559.85	-4142.64	1758.91	1037.12	-232886.03	-130588.18
528.90	1098.19	999.11	1199.61	821.71	379.19	1065.17	1169.12	908.99	902.63	767.10	-5685.92	914.47	539.18	-121081.84	-179240.75
0.48	-0.06	-0.02	-0.04	-0.02	-0.01	1.21	-0.07	1.40	-0.00	-0.00	-0.00	0.00	0.00	0.00	0.00
-0.06	0.31	0.01	-0.07	-0.01	-0.01	0.01	0.70	-0.00	1.40	-0.00	-0.00	0.00	-0.00	-0.00	-0.01
-0.02	0.01	0.35	-0.10	-0.11	-0.05	-0.16	0.83	0.00	-0.00	1.40	0.00	0.00	0.00	-0.00	0.00
-0.04	-0.07	-0.10	0.40	-0.08	-0.04	-0.11	-5.89	0.00	-0.00	0.00	1.40	0.00	0.00	-0.00	-0.00
-0.02	-0.01	-0.11	-0.08	0.42	-0.04	1.17	0.01	0.00	-0.00	-0.00	0.00	1.40	0.00	-0.01	0.00
-0.01	-0.01	-0.05	-0.04	-0.04	0.48	0.71	0.00	0.00	-0.00	-0.00	0.00	0.00	1.40	-0.00	0.00
-0.02	0.01	-0.16	-0.11	-0.11	-0.05	-170.06	0.04	0.00	0.00	0.00	-0.00	0.00	0.00	1.40	-0.01
-0.07	-0.22	0.04	-0.06	0.01	0.00	0.04	-183.55	0.00	0.00	0.00	-0.00	-0.00	-0.00	0.00	1.38

$I_2 =$

Bibliography

- [1] Hughes, P. C., "Dynamics of a Chain of Flexible Bodies," *The Journal of Astronomical Sciences*, Vol. 27, No. 4, October–December 1979, pp. 359–380.
- [2] Modi, V. J. and Ibrahim, A. M., "A General Formulation for Librational Dynamics of Spacecraft with Deploying Appendages," *Journal of Guidance, Control and Dynamics*, Vol. 7, No. 5, September–October 1984, pp. 563–569.
- [3] Meirovitch, L. and Kwak, K. M., "Dynamics and Control of Spacecraft with Retargeting Flexible Antennas," *Journal of Guidance Control and Dynamics*, Vol. 13, No. 2, March–April 1990.
- [4] Meirovitch, L. and Kwak, K. M., "Control of Flexible Spacecraft with Time-Varying Configuration," *Journal of Guidance, Control and Dynamics*, Vol. 15, No. 2, March–April 1992.
- [5] Meirovitch, L. and Seungchul, L., "Maneuvering and Control of Flexible Space Robots," *Journal of Guidance Control and Dynamics*, Vol. 17, No. 3, May–June 1994.
- [6] Juang, N. N., Kyong, B. L., and L. L. Junkins, "Robust Eigensystem Assignment for Flexible Structures," *Journal of Guidance, Control and Dynamics*, Vol. 12, No. 3, May–June 1989.
- [7] Agrawal, B. N. and Bang, H., "Robust Closed-Loop Control Design for Spacecraft Slew Maneuver Using Thrusters," *Journal of Guidance, Control and Dynamics*, Vol. 18, No. 6, November–December 1995.

- [8] Turner, J. D. and Junkins, J. L., "Optimal Large Angle Maneuver with Simultaneous Shape Control Vibration Arrest," *Journal of Guidance, Control and Dynamics*, Vol. 18, No. 6, November–December 1985.
- [9] DI Gennaro, S., "Output Stabilization of Flexible Spacecraft with Active Vibration Suppression," *IEEE Transactions on Aerospace and Electronic Systems*, Vol. 39, No.3, July 2003.
- [10] Yurkovich, S., Oezguener, U., and Al-Abbass, F., "Model Reference Sliding Mode Adaptive Control for Flexible Structures," *Journal of the Astronautical Sciences*, Vol. 36, No. 3, July–September 1988, pp. 285–310.
- [11] Scarritt, S. "Nonlinear Model Reference Adaptive Control for Satellite Attitude Tracking," *AIAA Guidance Navigation and Control*, Honolulu, Hawaii, 18–21 August 2008, doi: 10.2514/6.2008-7165.
- [12] Park, Y., Kusong, Y., and Tahk, M. J., "Optimal Stabilization of Takagi-Sugeno Fuzzy Systems with Application of Spacecraft Control," *Journal of Guidance, Control, and Dynamics*, Vol. 24, No. 4, July–August 2001, pp. 767–777.
- [13] Park, Y., Tahk, M. J., and Bang, H., "Design and Analysis of Optimal Controller for Fuzzy Systems with Input Constraint," *IEEE Transactions on Fuzzy Systems*, Vol. 12, No. 6, December 2004, pp. 766–779.
- [14] Zhang, X., Zeng, M., and Xu, X., "Output Feedback Attitude Tracking Control of Rigid Spacecraft for Takagi-Sugeno Fuzzy Model," *Journal of Information and Computational Science*, Vol. 8, No. 13, pp. 2743–2750, December 2011.
- [15] Zhang, X., Zeng, M., and Yu, X., "Fuzzy Control of Rigid Spacecraft Attitude Maneuver with Decay Rate and Input Constraints," *International Journal of Uncertainty, Fuzziness and Knowledge-Based Systems*, Vol. 19, No. 6, December 2011, pp. 1033-1046.

- [16] Zhang, X., Zeng, M., and Li, Y., H_∞ "Control for Spacecraft Attitude Maneuver with Input Constraint," *Journal of Computational Information Systems*, Vol. 7, No. 9, September 2011, pp. 3077–3084.
- [17] Butler, E. J., Wanh, H. O., and Burken, J.J., "Takagi-Sugeno Fuzzy Model-Based Flight Control and Failure Stabilization," *Journal of Guidance, Control, and Dynamics*, Vol. 34, No. 5, , September–October 2011, pp. 1543–1555.
- [18] Hong, S. K. and Nam, Y., "Stable Fuzzy Control System Design with Pole Placement Constraint: An LMI Approach," *Computers in Industry*, Vol. 51, No. 1, May 2003, .pp. 1–11.
- [19] Park, J. and Young-do, I., "An Attitude Control of Flexible Spacecraft Using Fuzzy-PID Controller," *IEICE Transactions on Fundamentals of Electronics, Communications and Computer Sciences*, Vol. E92–A(4), 2009, pp.1237–1241.
- [20] Qu, Fa Yi, Zhu, Liang Kuan, Song, Wen Long, " Fuzzy Adaptive Variable Structure Active Attitude Control of Flexible Spacecraft," *Applied Mechanics and Materials*, Vol. 44-47, pp. 2070–2074.
- [21] Ayoubi, M. A. and Sendi, C., "Takagi-Sugeno Fuzzy Model-Based Control of Spacecraft with Flexible Appendage," *Journal of Astronautical Sciences*, Vol. 61, Issue 1, 2014, pp. 40–59.
- [22] Sendi, C. and Ayoubi, M. A., "Robust-Optimal Fuzzy Model-Based Control Of Flexible Spacecraft with Actuator Constraints," *Journal of Dynamic Systems, Measurement, and Control*, Vol. 138, Issue 9, 2015, doi: 10.1115/1.4033318.
- [23] Sendi, C. and Ayoubi, M. A., "Robust Fuzzy Logic-Based Tracking Control of a Flexible Spacecraft with H_∞ Performance Criteria," *AIAA Space Conference and Exposition*, San Diego, CA, 2013, doi: 10.2514/6.2014-4417.

- [24] Grote, P. B., McMunn, P. B., and Gluck, R., "Equations of Motion of Flexible Spacecraft," *Journal of Spacecraft and Rockets*, Vol. 8, 1971, pp. 561–567.
- [25] Gale, A. H. and Likins, P. W., "Influence of Flexible Appendages on Dual Spin Spacecraft Dynamics and Control," *Journal of Spacecraft and Rockets*, Vol. 7, 1970, pp. 1049–1056.
- [26] Hooker, W. W. and Margulies, G., "The Dynamical Attitude Equations for an N-Body Satellite," *Journal of Astronautical Science*, Vol. 12, 1965, pp. 123–128.
- [27] Arbel, A. and Gupta, N. K., "Robust Collocated Control for Large Flexible Space Structures," *Journal of Guidance, Control, and Dynamics*, Vol. 4, 1981, pp. 480–486.
- [28] Martin, G. and Bryson, A., "Attitude Control of Flexible Spacecraft," *Journal of Guidance, Control, and Dynamics*, Vol. 3, 1980, pp. 37–41.
- [29] Schaechter, D., "Optimal Local Control of Flexible Structures," *Journal of Guidance, Control, and Dynamics*, Vol. 4, 1981, pp. 22–26.
- [30] Singh, S. N., "Controller Design for Asymptotic Stability of Flexible Spacecraft," *In Proceeding IEEE Conference on Decision and Control*, San Diego, CA, 1981, pp. 961–966.
- [31] Meirovitch, L., "Stability of a Spinning Body Containing Elastic Parts," *AIAA Journal*, Vol. 8, 1970, pp. 1193–1200.
- [32] Meirovitch, L., "A Method of Liapunov Stability for Force Free Dynamical Systems," *AIAA Journal*, Vol. 9, 1971, pp. 1695–1701.
- [33] Ahmed, N. U. and Biswas, S. K., "Mathematical Modeling and Stabilization of Flexible Spacecraft," *SIAM Fall Meeting*, November 7–9, Norfolk, VA, 1983.

- [34] Biswas, S. K. and Ahmed, N. U., "Modeling of Flexible Spacecraft and Their Stabilization," *International Journal of Systems Science*, Vol. 16, 1985, pp. 535–551.
- [35] Biswas, S. K. and Ahmed, N. U., "Stabilization of a Class of Hybrid Systems Arising in Flexible Spacecraft," *Journal of Optimization Theory and Applications*, Vol. 1, 1986, pp. 83–108.
- [36] Balas, M. J., "Active Control of Flexible System," *Journal of Optimization Theory and Applications*, Vol. 25, No. 3, 1978, pp. 415–436.
- [37] Takagi, T. and Sugeno, M., "Fuzzy Identification of Systems and its Applications to Modeling and Control," *IEEE Transaction on Systems, Man, and Cybernetics*, Vol. 15, January–February 1985, pp. 116–132.
- [38] Tanaka, K. and Sugeno, M., "Stability Analysis and Design of Fuzzy Control Systems," *Fuzzy sets and Systems*, Vol. 45, Issue 2, January 1992, pp. 135–156.
- [39] Wang, H. O., Tanaka, K., and Griffin, M. F., "Parallel Distributed Compensation of Non-linear Systems by Takagi-Sugeno Fuzzy Model," *Proceeding of the Fuzzy-IEEE/IFES*, 1995, pp. 531–538.
- [40] Wang, H. O., Tanaka, K., and Griffin, M. F., "An Approach to Fuzzy Control of Non-linear Systems: Stability and Design Issue," *IEEE Transaction on Fuzzy Systems*, Vol. 4, Issue1, 1996, pp. 14–23.
- [41] Li, J., Wang, H. O., and Tanaka, K., "Stable Fuzzy Control of the Benchmark Nonlinear Control Problem: a System-Theoretic Approach," *Joint Conference of Information Science*, Triangle Park, NC 1997, pp. 263–266.
- [42] Tanaka, K., Ikeda, T., and Wang, H. O., "Robust Stabilization of a Class of Uncertain Nonlinear System Via Fuzzy Control: Quadratic Stabilizability, H_∞ Control Theory and

- Linear Matrix Inequalities," *IEEE Transaction on Fuzzy Systems* Vol. 4, Issue 1, 1996, pp. 1–13.
- [43] Zhao, J., Wertz, V., and Gorez, R., "Fuzzy Gain Scheduling Controllers Based on Fuzzy Models," *In Proceeding of the Fuzzy-IEEE*, New Orleans, LO 1996, pp. 1670–1676.
- [44] Takagi, T., and Sugeno, M., "Fuzzy Identification of Systems and its Applications to Modeling and Control," *IEEE Transaction on System, Man, and Cybernetics*, Vol. 15, Issue 1, 1985, pp. 116–132.
- [45] Yoneyama, J., Nishikawa, M., Katayama, H., and Ichikawa, A., "Output Stabilization of Takagi-Sugeno Fuzzy Systems," *Fuzzy Sets and Systems*, Vol. 111, Issue 2, 2000, pp. 253–266.
- [46] Xiao, J. M. , Zeng, Q. S., and Yan, H. Y., "Analysis and Design of Fuzzy Controller and Fuzzy Observer," *IEEE Transaction on Fuzzy System*, Vol. 6, Issue 1, 1998, pp. 41–51.
- [47] G. Zames. "Feedback and Optimal Sensitivity: Model Reference Transformations, Multiplicative Seminorms and Approximate Inverses", *IEEE Transactions on Automatic Control*, Vol. AC-26, No. 2, 1981, pp. 301–320.
- [48] G. Zames and B.A. Francis. Feedback, Minimax Sensitivity, and Optimal Robustness," *IEEE Transactions on Automatic Control*, Vol. AC-28, 1983, pp. 585–600.
- [49] Tanaka, K. and Wang, H. O., *Fuzzy Control Systems Design and Analysis: A Linear Matrix Inequality Approach*, John Wiley & Sons, New York, pp. 66–152.
- [50] Kemin, Z. and Pramod, K., "Robust Stabilization of Linear Systems With Norm-Bounded Time-Varying Uncertainty," *Systems and Control Letter*, Vol. 10, Issue 1, 1988, pp. 17–20.

- [51] Tanaka, K., Ikeda, T., and Wang, H. O., "Robust Stabilization of Class of Uncertain Nonlinear System via Fuzzy Control: Quadratic Stabilizability, H_∞ Control Theory, and Linear Matrix Inequalities," *IEEE Transaction on Fuzzy System*, Vol. 4, Issue 1, 1996, pp. 1–13.
- [52] Löfberg, J., "YALMIP: A Toolbox for Modeling and Optimization in MATLAB," *In Proceedings of the IEEE International Symposium on Computer Aided Control System Design*, Taipei, Taiwan, pp. 284–289.
- [53] Khalil, H. K., *Nonlinear Systems*, 3rd edition, Prentice Hall, Inc., Chp. 14.
- [54] Tseng, C.S., Chen, B. S., and Uang, H. J., "Fuzzy Tracking Control Design for Nonlinear Dynamic Systems via T-S Fuzzy Model," *IEEE Transaction on Fuzzy System*, Vol. 9, No. 3, June 2001.
- [55] Tuan, H. D., Apkarian, P., Narikiyo, T., and Yamamoto, Y. , "Parameterized Linear Matrix Inequality Techniques in Fuzzy Control System Design," *IEEE Transactions on Fuzzy Systems*, Vol. 9, Issue 2, 2001, pp. 324–332.
- [56] Guerra, T. M., Kruszewski, A., Vermeiren, L., and Tirmant, H., "Conditions of Output Stabilization for Nonlinear Models in the Takagi-Sugeno Form," *Fuzzy Sets and Systems*, Vol. 157, 2006, pp. 1248–1259.
- [57] Mansouri, B., Manamanni, N., Guelton, K., Kruszewski, A., and Guerra, T. M., "Output Feedback LMI Tracking Control Conditions with H_∞ Criterion for Uncertain and Disturbed T-S models," *Information Sciences*, Vol. 179, 2009, pp. 446–457.
- [58] Ioannou, P. A. and Kokotovic, P. V., "Instability Analysis and Improvement of Robustness of Adaptive Control," *Automatica*, Vol. 20, September 1984, pp. 583–594.

Vita

Chokri Sendi was born in Tunisia. After completing the high school and receiving his baccalaureate, he was accepted with a full scholarship at the Polytechnic University of Saint Petersburg, Russia. Chokri graduated with a Master of Science in mechanical engineering and a bachelor of art in mathematics. In 1998 he was hired as a chief engineer in the ministry of transportation in Tunisia. In 2003 Chokri moved to United State of America where he worked as Mathematics and Physics Instructor at the community college of Denver, in Colorado. In 2008, Chokri attended the University of Colorado and graduated in 2010 with a master in applied mathematics. In 2011 he started a PH.D program in the department of mechanical engineering at Santa Clara University, His main area of research is fuzzy control of multibody flexible spacecraft and structures.

Publications:

- 1 Ayoubi, M. A. and Sendi, C., "Takagi-Sugeno Fuzzy Model-Based Control of Spacecraft with Flexible Appendage," *Journal of Astronautical Sciences*, Vol. 61, Issue 1, 2014, pp. 40–59.
- 2 Sendi, C. and Ayoubi, M. A., "Robust-Optimal Fuzzy Model-Based Control Of Flexible Spacecraft with Actuator Constraints," *Journal of Dynamic Systems, Measurement, and Control*, Vol. 138, Issue 9, doi: 10.1115/1.4033318.
- 3 Ayoubi, M. A., Sendi, C., "Fuzzy-Logic Attitude Control of Spacecraft With Retargeting Flexible Antenna," *AIAA Guidance, Navigation, and Control Conference*, Boston, MA, August 19–22, 2013, doi: 10.2514/6.2013 – 4861.

- 4 Sendi, C. and Ayoubi, M. A., "Robust Fuzzy Logic-Based Tracking Control of a Flexible Spacecraft with H_∞ Performance Criteria," *AIAA Space Conference and Exposition*, San Diego, CA, 2015, doi: 10.2514/6.2014 – 4417.
- 5 Sendi, C. and Ayoubi, M. A., "Robust-Optimal Fuzzy Model-Based Control of Flexible Spacecraft With Actuator Amplitude and Rate Constraints, " *presented at the ASME Dynamic Systems and Control Conference*, Columbus, OH, October 28–30, 2015.